RF Electron Gun

Sakhorn Rimjaem

Department of Physics and Materials Science,
Faculty of Science, Chiang Mai University (CMU), Thailand

Lecture Outline

Lecture No. 1

- Introduction, types and benefits of electron guns
- Basic principle of RF structure

Lecture No. 2

- Design, simulations and construction of RF gun
- Low power tests and tuning of RF gun
- High power tests of RF gun

Lecture No. 3

- Operation of RF electron gun
- Generation and applications of ultra short electron bunches produced by RF gun

- **Introduction to electron sources**
  - Electron emission processes
- **Types of electron guns**
  - Conventional thermionic DC guns
  - Photocathode DC guns
  - Thermionic RF guns
  - Photocathode RF guns
- **Benefits of RF electron guns**
  (as compared to conventional guns)
- **Basic principle of RF structure**

Electron Accelerator and Sources

Electron source → **Accelerating and focusing section** → **Application**

Electron source:
- Thermionic
- Photoelectric
- Field emission
- Secondary emission

Accelerating and focusing section:

Acceleration by electric field:
- Electrostatic
- Pulsed DC
- Radio Frequency (RF) fields
- Wakefield

Focusing by magnetic fields

Application:
- Direct applications
- Radiation production

Characteristics of electron beams and reliability in operation of an accelerator facility strongly depend on properties of the source.

→ Development of high-brightness electron beams is a key and a critical issue in the success of most electron accelerator projects.

Electron Emission Processes

1. Thermionic emission

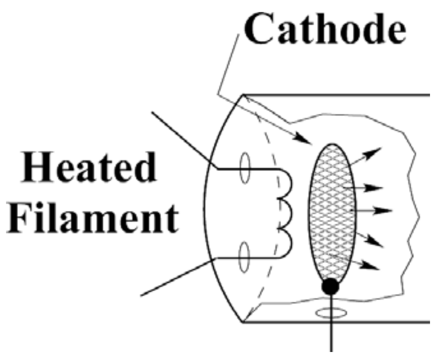

2. Photoelectric emission

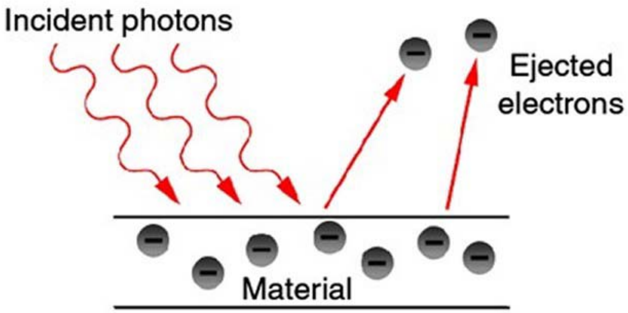

3. Field emission

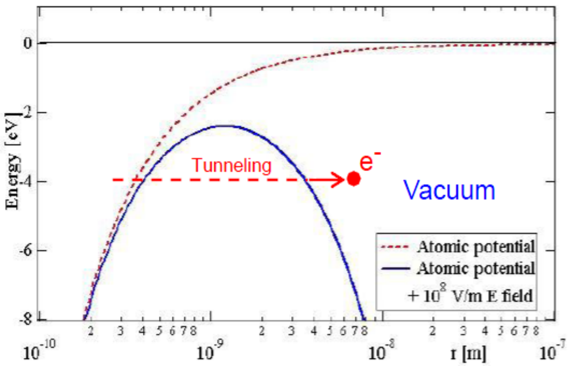

4. Secondary electron emission

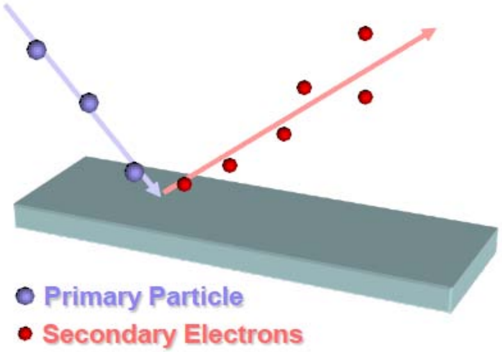

1. Thermionic Emission

• Thermionic emission was initially reported by F. Guthrie in 1873.

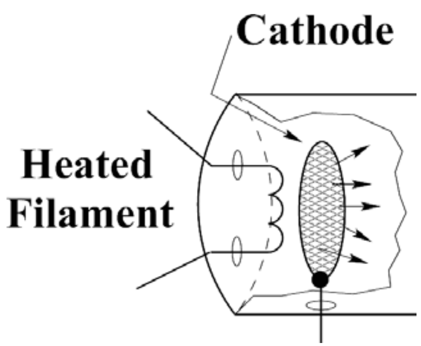

When the cathode is heated, electrons inside the cathode surface are moving with an average velocity controlled by the heating temperature.

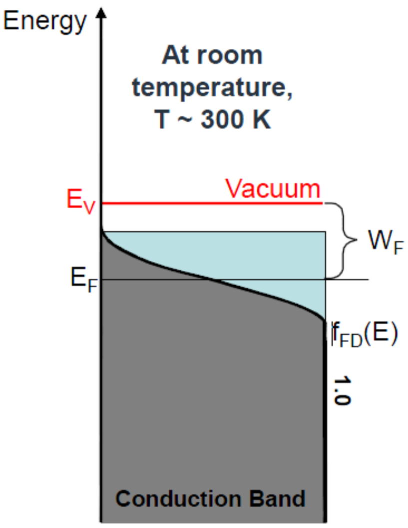

• Some electrons having kinetic energies higher than the cathode's work function can escape from the cathode surface with thermal energies depending on the cathode heating temperature (T),

$$E_k = \frac{3}{2}kT$$

where k is the Boltzmann's constant.

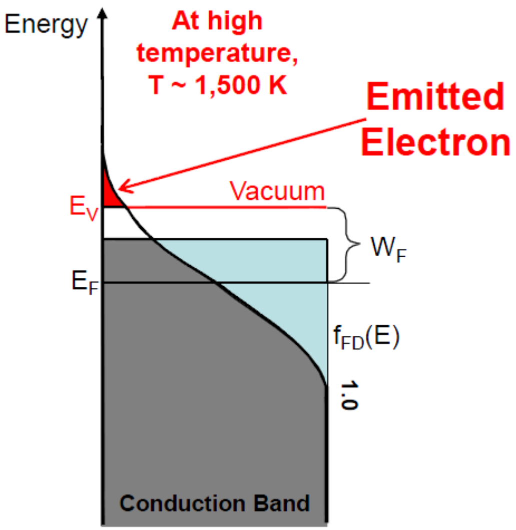

(F. Sannibale, Particle Sources, USPAS, UC Santa Cruz, January 2010)

Richardson's Law

- There is an important phenomenon affecting to the thermionic emission is called Richardson' s law.

  → Owen Richardson received a Nobel prize in 1928.

- Richardson' s law states that the current density of the thermionic emission is limited by the heating temperature as

$$j = AT^2 e^{-\frac{eW_F}{kT}}$$

A is the Richardson constant, $A = 4\pi emk^2 / h^3$

→ It practically depends on cathode materials.

T is the thermodynamics temperature of the cathode (K)

W_F is the work function of the emitter material (potential barrier)

k is the Boltzmann' s constant = 1.381×10^{-23} J/K

∴ Higher heating temperature (T) produces higher energy (E_k) electrons and more electrons boiling (J) off the cathode.

2. Photoelectric emission

- Photoelectric effect was discovered by Heinrich Hertz in 1887 and in 1921 Albert Einstein received a Nobel prize for his discovery of the law of photoelectric effect.

- In photoelectric emission, we illuminate a cathode surface with photons, which their energies (*E*) are expressed in term of the frequency (*f*), the wavelength (λ) of the incident light, the velocity of light (*c*) and the Plank's constant (*h*) as

$$E = hf = \frac{hc}{\lambda}$$

- If the photons have energies equal to or higher than the work function of the cathode material, electrons are emitted with kinetic energies given by

$$E_{kin} = hf - eW_F$$

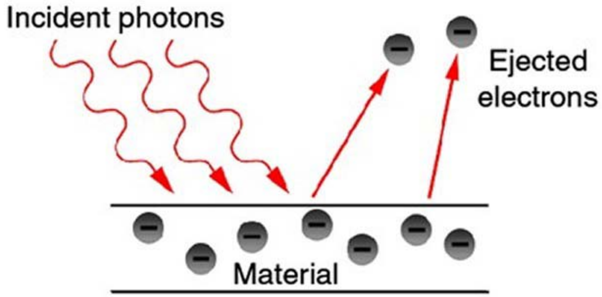

http://www.physicsoftheuniverse.com/topics_quantum_quanta.html

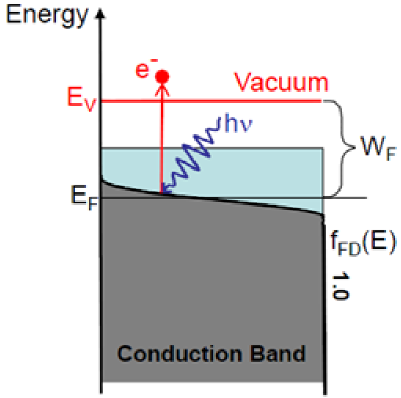

F. Sannibale, Particle Sources, USPAS, UC Santa Cruz, January 2010

3. Field emission

F. Sannibale, Particle Sources, USPAS, UC Santa Cruz, January 2010

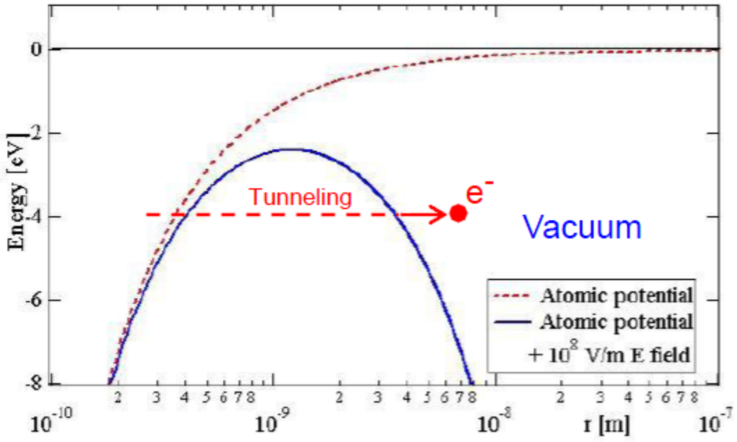

$$U_p = -\frac{1}{4\pi\varepsilon_0}\frac{e^2}{r} + e\left|\overline{E}\right| r$$

$$\left|\overline{E}\right| = \text{constant}$$

$$\left|\overline{E}\right| > 10^8 \div 10^9 \; V/m$$

Field emission is the emission of electrons induced by high electric field with gradients $\geq$ 1 GV/m from a solid surface into vacuum.

$\rightarrow$ It is a quantum tunneling effect of electron transitioning through a classically-forbidden energy state.

Electrons are emitted with a current density given by

$$j = (1.54 \times 10^{-10} \frac{E^2}{W_F}) \exp(-\frac{6.83 \times 10^9 \; W_F^{3/2} \; k}{E})$$

Fowler/Nordheim emission formula

$\rightarrow$ Field emission current density is strongly dependent on the electric field gradient and the work function of the cathode.

4. Secondary electron emission

Primary particles: photons, electrons, protons, neutrons, ions, ….

Physical processes: ionization, elastic scattering, bremsstrahlung and pair production, Thomson scattering, …

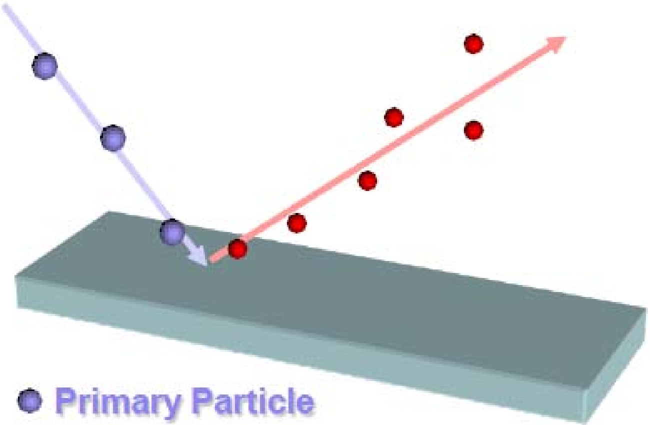

A Secondary Emission (SEM) Source

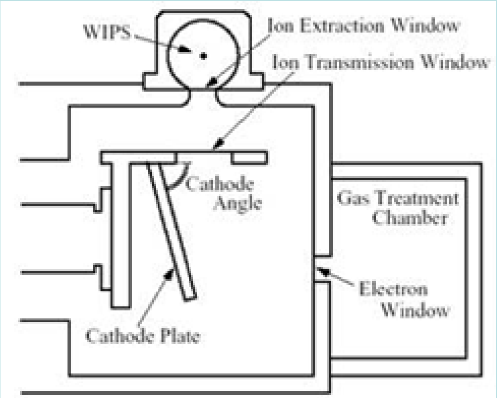

Fig. 1. Secondary emission electron gun.

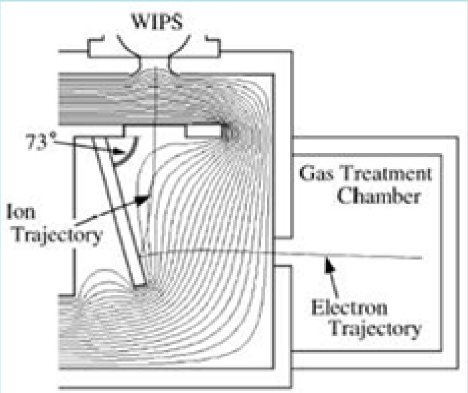

Fig. 4. Equipotential lines, ion and electron trajectories.

Electron energy = 40-80 kV
Current density: 6.4 mA/cm^2
Ion source energy = 10 kV
Large and uniform beam through the window
Application: pollutant gas treatment.

P.R Chalise et al., Jpn. J. Appl. Phys. 40, 1118 (2001)

(F. Sannibale, Particle Sources, USPAS, UC Santa Cruz, January 2010)

Limitations of Electron Sources

Field emission sources:

- There is a maximum electric field at the tip of the cathode, which limits the size of the cathode tip and therefore limits the current density of electron beams.
- It has lifetime limit due to the tip damage from electric field with high gradient.
- It can produce high brightness electron beams, but with low average current.

Secondary electron emission sources:

- It provides electron beams with low current densities, high energy spread, poor emittance and very low brightness.

∴ **Thermionic emission** and **photoelectric emission** are currently more preferable emission processes for generation of high brightness electron beams.

Lecture No. 1

- Introduction to electron sources
  - Electron emission processes
- Types of electron guns
  - Conventional thermionic DC guns
  - Photocathode DC guns
  - Thermionic RF guns
  - Photocathode RF guns
- Benefits of RF electron guns
  (as compared to conventional guns)
- Basic principle of RF structure

Conventional Thermionic DC Guns

➢ Electrons emitted by the heated cathode are accelerated by the DC high voltage.

➢ **It consists of two main parts:**

1. Heating filament consists a resistive material, e.g. tungsten, and heated by an electricity.

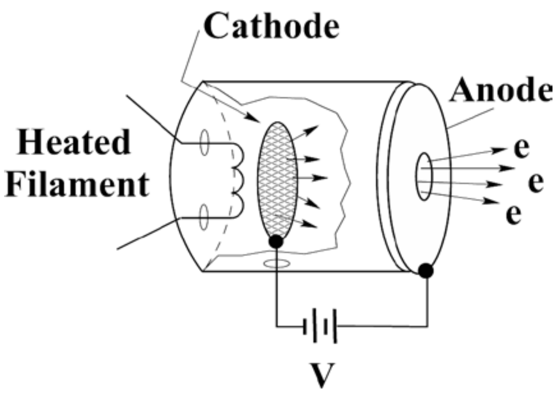

http://lib.convdocs.org/docs/index-269021.html

2. Accelerating region is bounded by two electrodes, known as cathode and anode.

- Electrons leave the cathode surface by thermionic emission with small thermal energy and then emerge into a region of DC electric field and gain the kinetic energy by

$$\Delta E_k = eV$$

- The output electron beam for the gun is a continuous beam, but one can use
  - diode gun: pulse length is controlled by modulating the anode voltage
  - triode gun: pulse length is fast controlled by the grid

- The electron beam pulse length can be reduced by using a buncher system.

Characteristics of Thermionic DC Gun (1)

1. Richardson' s law: current density of the thermionic emission is limited by the heating temperature as

$$j = \frac{4\pi emk^2}{h^3} T^2 e^{-\frac{eW_F}{kT}} = AT^2 e^{-\frac{eW_F}{kT}}$$

$$A = \frac{4\pi emk^2}{h^3}$$

Material	A (A/cm²K²)	W_F (eV)	T (°K)	J (A/cm²)
Tungsten	60	4.54	2500	0.3
Thoriated W	3	2.63	1900	1.16
Mixed oxides	0.01	1	1200	1
Tantalum	60	3.38	2500	2.38
Cs/O/W	0.003	0.72	1000	0.35

Characteristics of Thermionic DC Gun (2)

2. Space charge effect:

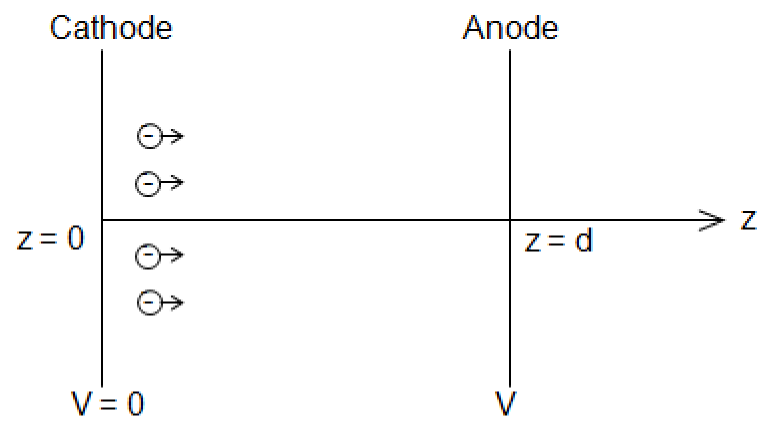

- Electrons emitting from the cathode are accelerated off the cathode surface resulting in the lowering of the potential in the region in front of the cathode that they drift through.

- A stable condition exists when the field is zero or at a constant potential. Any further electric field reduction would repel electrons back to the cathode.

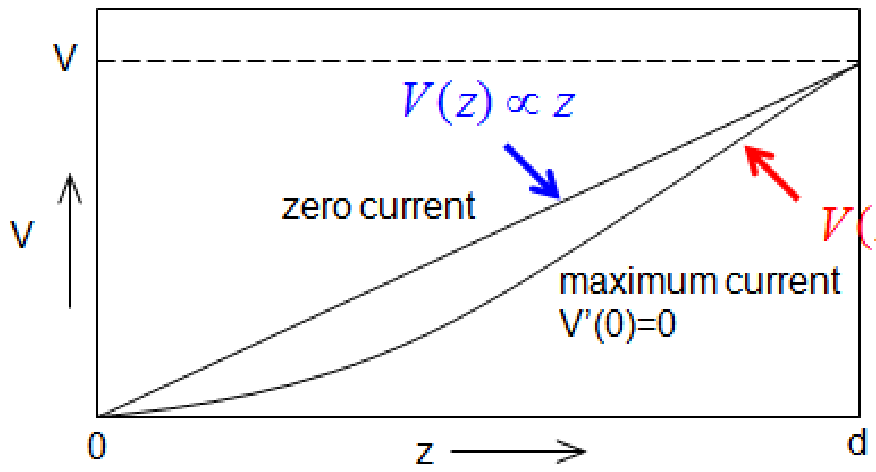

$$V(z) = \left(\frac{3}{2}\right)^{4/3} \left(\frac{J}{\varepsilon_o}\right)^{2/3} \left(\frac{m}{2e}\right)^{2/3} z^{4/3}$$

Characteristics of Thermionic DC Gun (3)

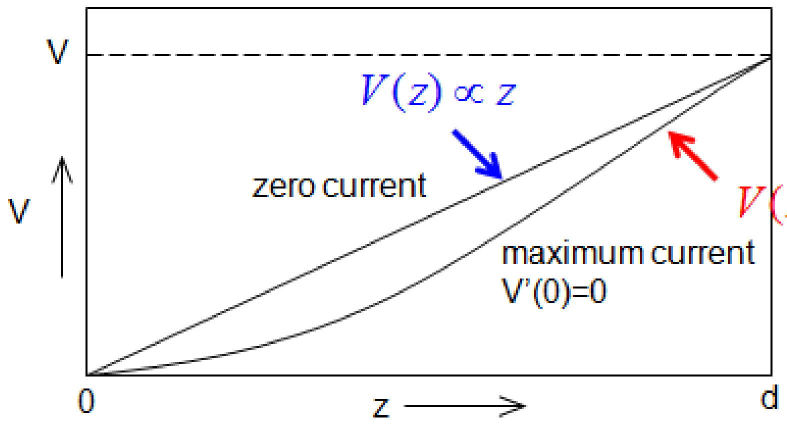

$$V(z) = \left(\frac{3}{2}\right)^{4/3} \left(\frac{J}{\varepsilon_o}\right)^{2/3} \left(\frac{m}{2e}\right)^{2/3} z^{4/3}$$

This stable regime is known as space-charge-limited emission.

→ This effect is governed by the Child-Langmuir's equation, which limits the electron current density that can be extracted from the cathode, as defined by

$$j = \left(\frac{4\varepsilon_o}{9}\right)\left(\frac{2e}{m}\right)^{1/2} \frac{V^{3/2}}{d^2} = \chi \frac{V^{3/2}}{d^2}$$

→ Current density depends mainly on the accelerating voltage (V) and the distance between the cathode and anode (d).

Characteristics of Thermionic DC Gun (4)

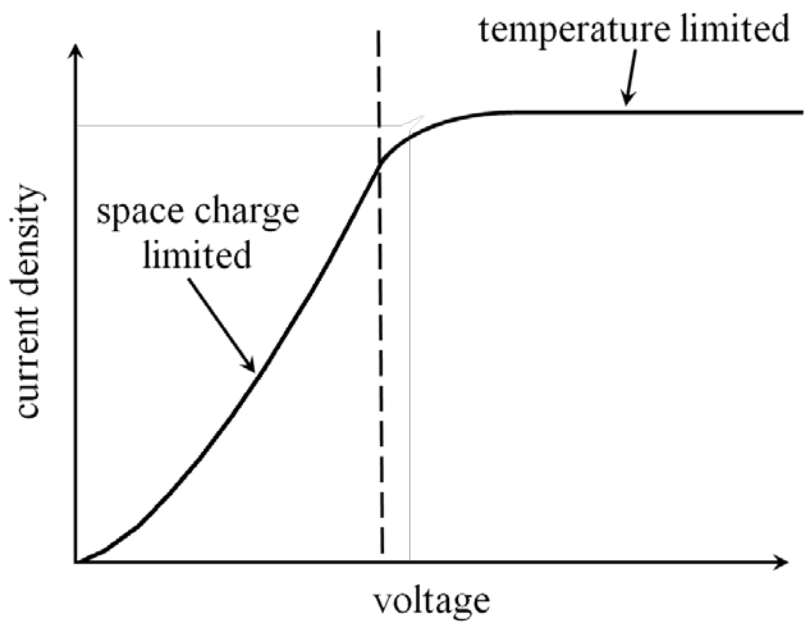

Thermionic emission and space charge limited regimes

- The Child-Langmuir space charge limited current is a maximum current which electrons still can move from cathode to anode while the space charge effect is not high enough to stop the flowing of electrons.
- If the voltage becomes sufficiently high, the Richardson limit for current is reached when the emission becomes temperature limited.

Thermionic DC Gun Injector System

A typical DC injector consists of Electron gun & RF buncher

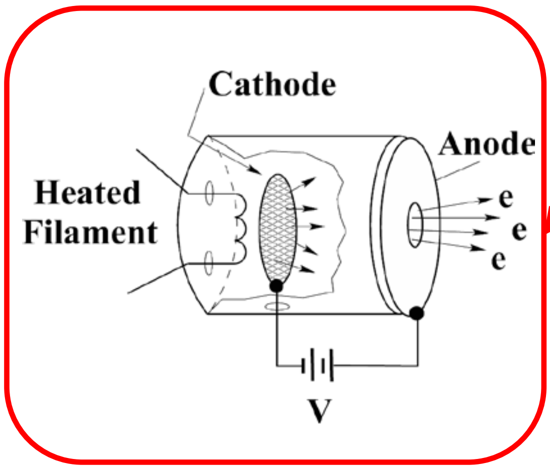

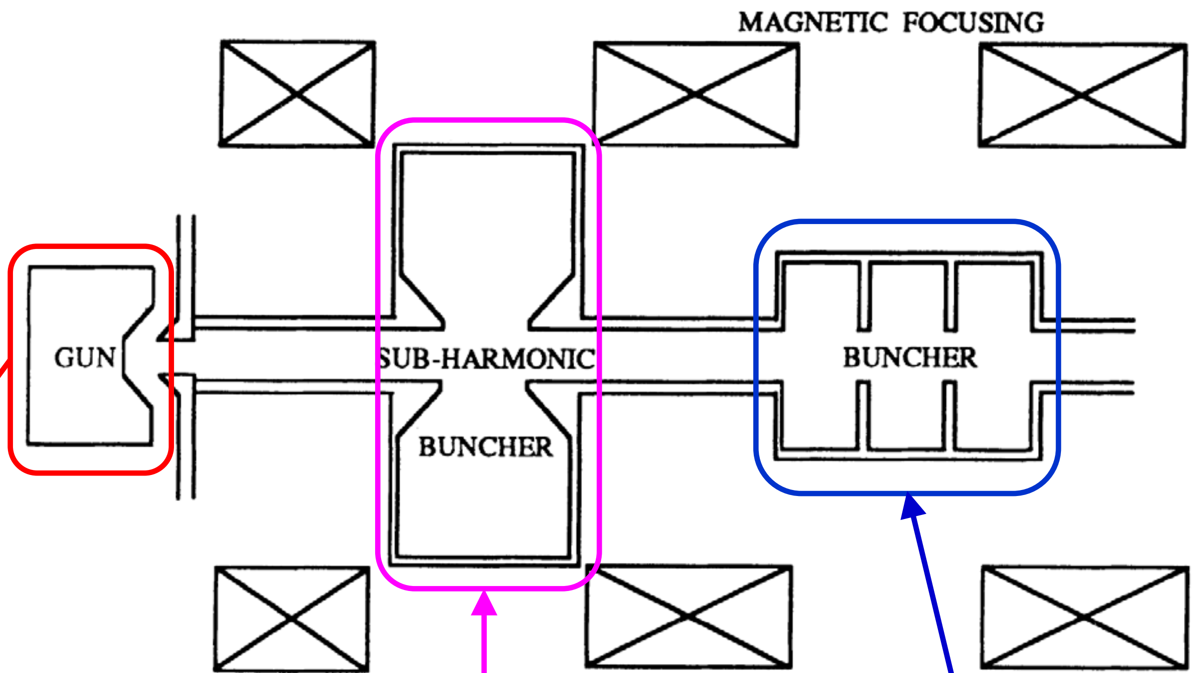

It is used to increase the peak current and to reduce the pulse length.

It is an RF cavity used to reduce the pulse length

C. Travier, Review of Microwave Guns, Particle Accelerators, 1991, Vol. 36, pp.33-74

Buncher & Sub-harmonic Buncher (1)

Electrons enter the **sub-harmonic buncher** and the **buncher** with different RF phases and thus experience different acceleration fields.

→ Velocity modulation is converted into a space modulation after a drift of appropriate length.

→ Electron pulse from the gun is thus transformed into a train of pulses with long tail (one per RF cycle).

Electron beam pulse format

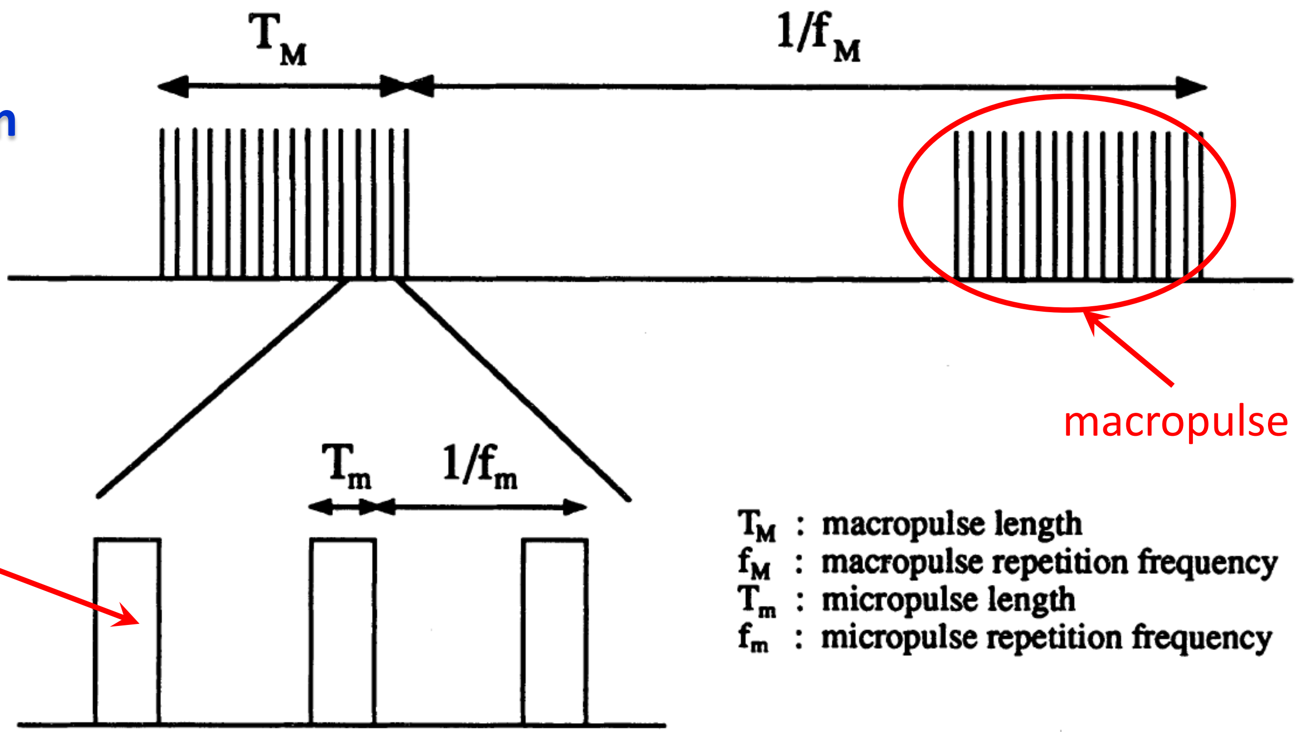

C. Travier, Review of Microwave Guns, Particle Accelerators, 1991, Vol. 36, pp.33-74

Buncher & Sub-harmonic Buncher (2)

The 1 ns gun pulse can be reduced to a few hundred picoseconds in the **sub-harmonic buncher** before entering the buncher where it can be further reduced to a few tens of picoseconds.

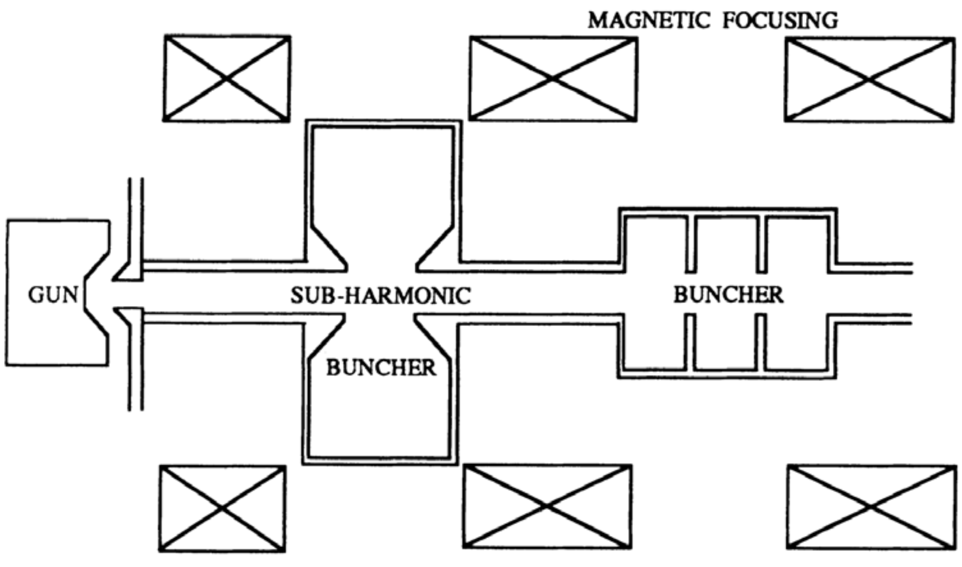

→ This process increases the peak current by an order of magnitude or more, but does not increase the average current.

→ It increases the emittance and energy spread because of the different transverse RF forces experienced by electrons, which leads to reducing of the electron beam brightness.

RF chopper, which is an RF cavity operating with deflecting modes, can be used to cut the long tail of the pulse train and to also select one pulse within the train.

Limitations of Thermionic DC Gun

F. Sannibale, Particle Sources, USPAS, UC Santa Cruz, January 2010

Example of thermionic DC electron gun

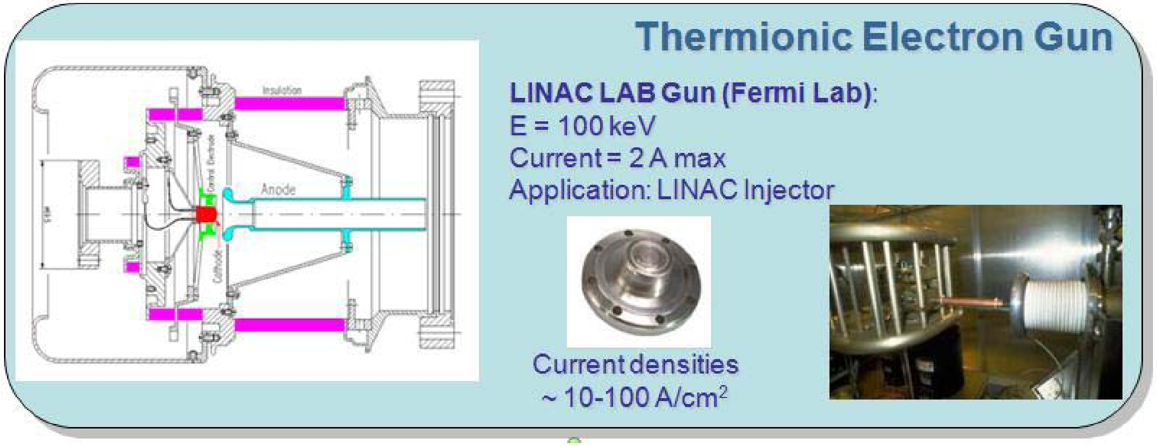

- Current density is limited to few tens of A/cm^2 ($\leq$100 A/cm^2) depending on the cathode material and heating temperature.
- It is difficult to control the bunch distribution since the micropulse length is limited by the cathode grid capacitance (e.g. 1 ns for 1 A electron beam).
- Maximum practical DC voltage is limited to a few hundred kilovolts, therefore the beam energy is limited to a few hundreds keV.

  - The output beam is not yet relativistic, then the space charge effects dominate.
- Emittance growth and bunch length increases due to space charge effects.

  - Normalized emittance in the order of 1 - 10 π mm-mrad.

Photocathode DC Electron Guns

In photocathode DC guns, electrons are emitted from a photocathode by a short laser pulse and then accelerated by the electrostatic field between the cathode and the anode.

→ Electrons move across the accelerating field gap of the gun, which has a large DC potential, and leave the anode hole with the energies depending on the DC potential between the electrodes.

$$\Delta E_k = eV$$

→ The output beam contains of electron pulses with the current and bunch length controlling by the laser pulses.

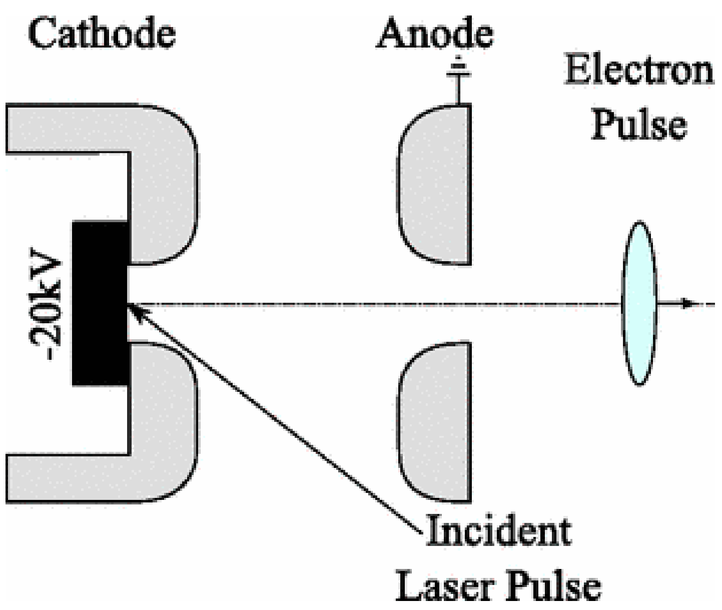

B. L. Rickman et al., Phys. Rev. Lett. 111, (2013) 237401.

Limitations of Photocathode DC Gun

- Current density is limited depending on the cathode material and the laser pulse energy.
- Initial electron bunch length depends on the laser pulse length.
- Maximum practical DC voltage is limited to a few hundred kilovolts, therefore the beam energy is limited to a few hundreds keV.

  - The output beam is not yet relativistic, then the space charge effects dominate.
- Emittance growth and bunch length increases due to space charge effects.

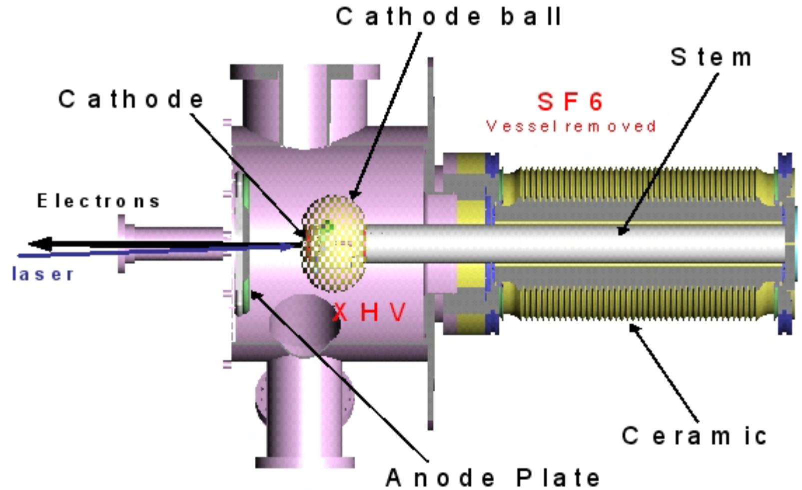

Photocathode DC electron gun at ASTeC, UK http://www.stfc.ac.uk/ASTeC/Alice/accelerator/36004.aspx

Thermionic RF Electron Guns

Thermionic DC guns provide low brightness electron beam due to low accelerating DC field and buncher system.
→ High accelerating radio-frequency (RF) cavity can be utilized to encounter the problem from space charge effects.

Thermionic RF electron gun consists of two main parts.

1. Heating cathode consists of an emissive surface cathode made of a resistive material and heated by an electricity

2. Accelerating region is a RF conducting walled cavity.

→ When the RF-fields in the cavity are in the accelerating phase electrons are accelerated and leave the cathode with velocities depending on the amplitude and phase of the RF-fields.

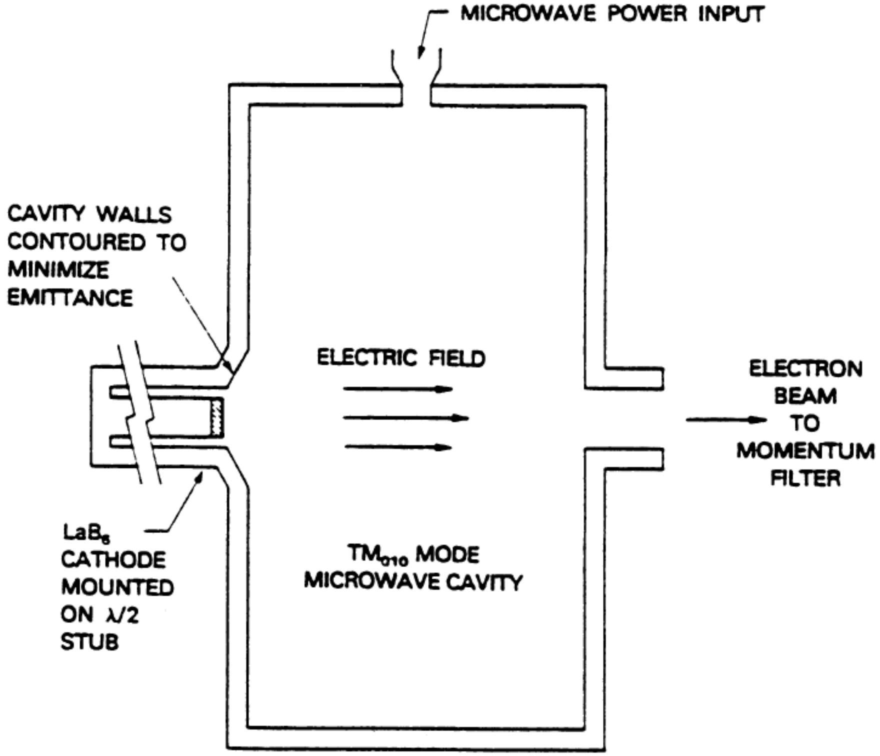

G.A. Westenskow, J.M.J. Madey, Microwave Electron Gun, Laser and Particle Beams Vol. 2, Part 2 (1984) 223.

Acceleration by Time Varying RF Fields

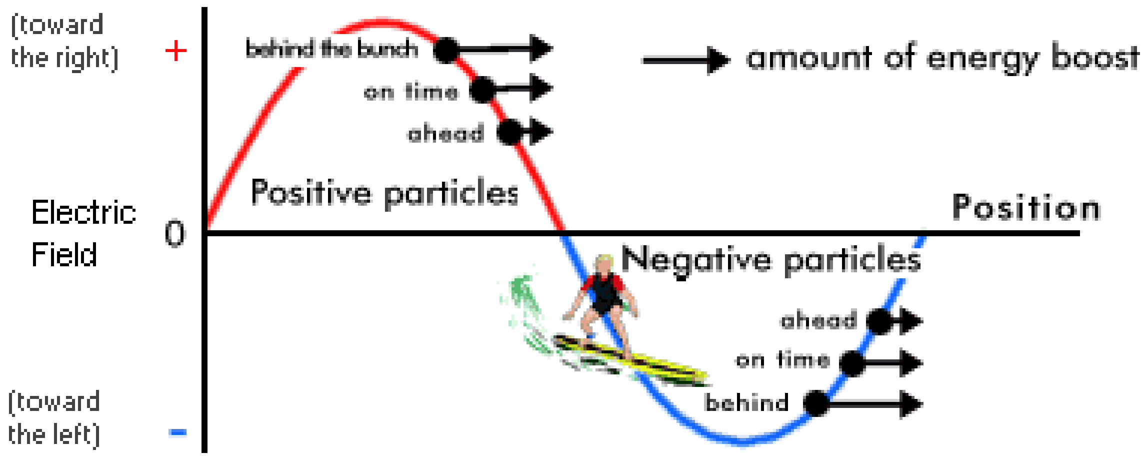

G. Hoffstaetter, USPAS, June 2010

Particles must have the correct phase relative to the accelerating voltage

Accelerating field $E_z = E_{zo}\cos(\omega t)$

Accelerating voltage $V_{rf} = \int E_s(s,t)\,ds$

Energy gain $W = qV = q\int E_o e^{i(\omega t - ks)}\,ds$

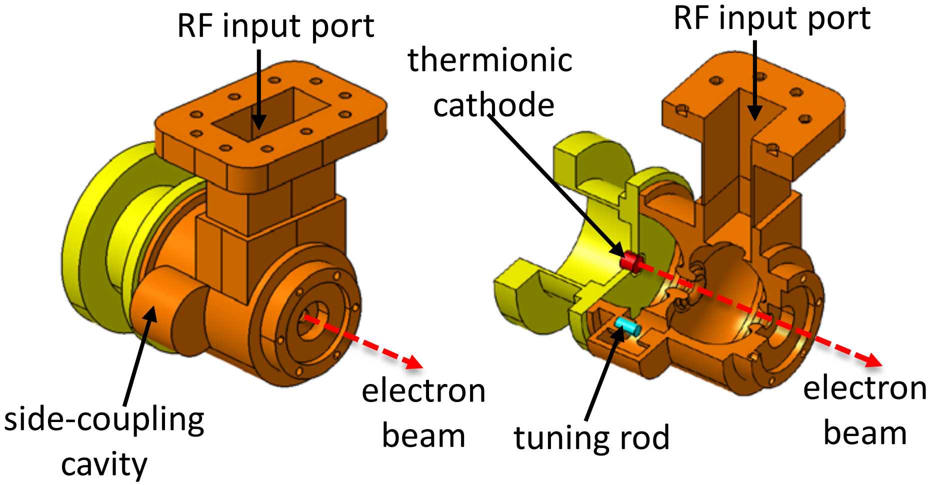

S. Rimjaem et al., Nuc. Instr. and Meth. A 736 (2014) 10-21.

Acceleration by RF Fields

In a **thermionic RF guns**, electrons are continuously emitted by the cathode but can only be extracted and accelerated during half an RF cycle with a too large phase (> 100°)

→ Some electrons do not have enough energy to reach the cavity output and are accelerated backward to hit the cathode (back-bombardment effect).

→ The electron pulse that can exit the cavity is long (~1/4 of RF period) and has a very large energy spread.

→ Magnetic bunching system with energy slits (e.g. α-magnet) can be placed downstream the gun to reduce the pulse length, to increase the peak current and to select a given energy spectrum.

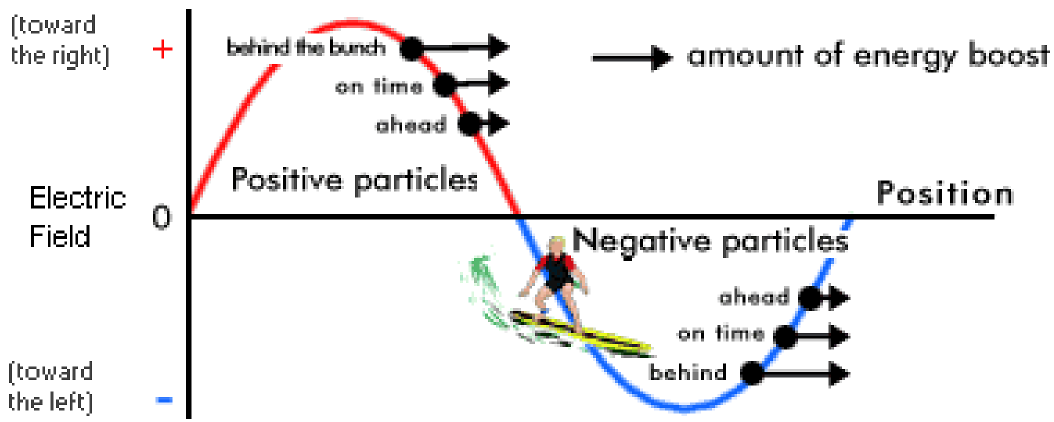

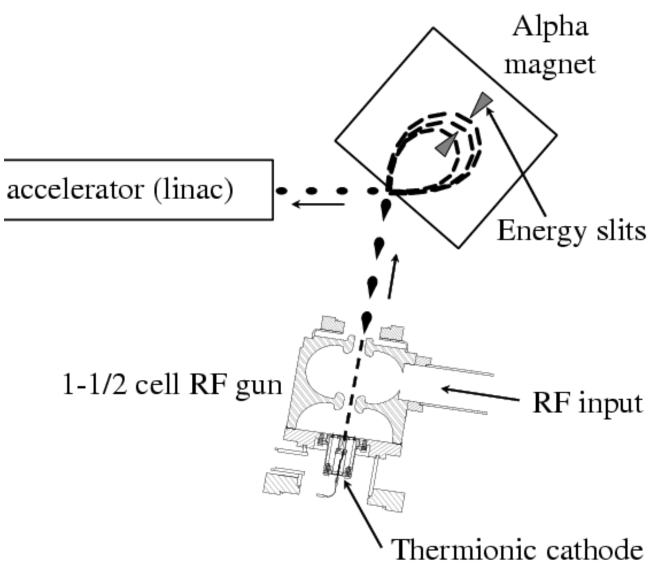

Electron Beam from Thermionic RF Gun

In an RF gun, electron emission occurs continuously giving a train of bunches that varies in energy because of the time-varying RF-field.

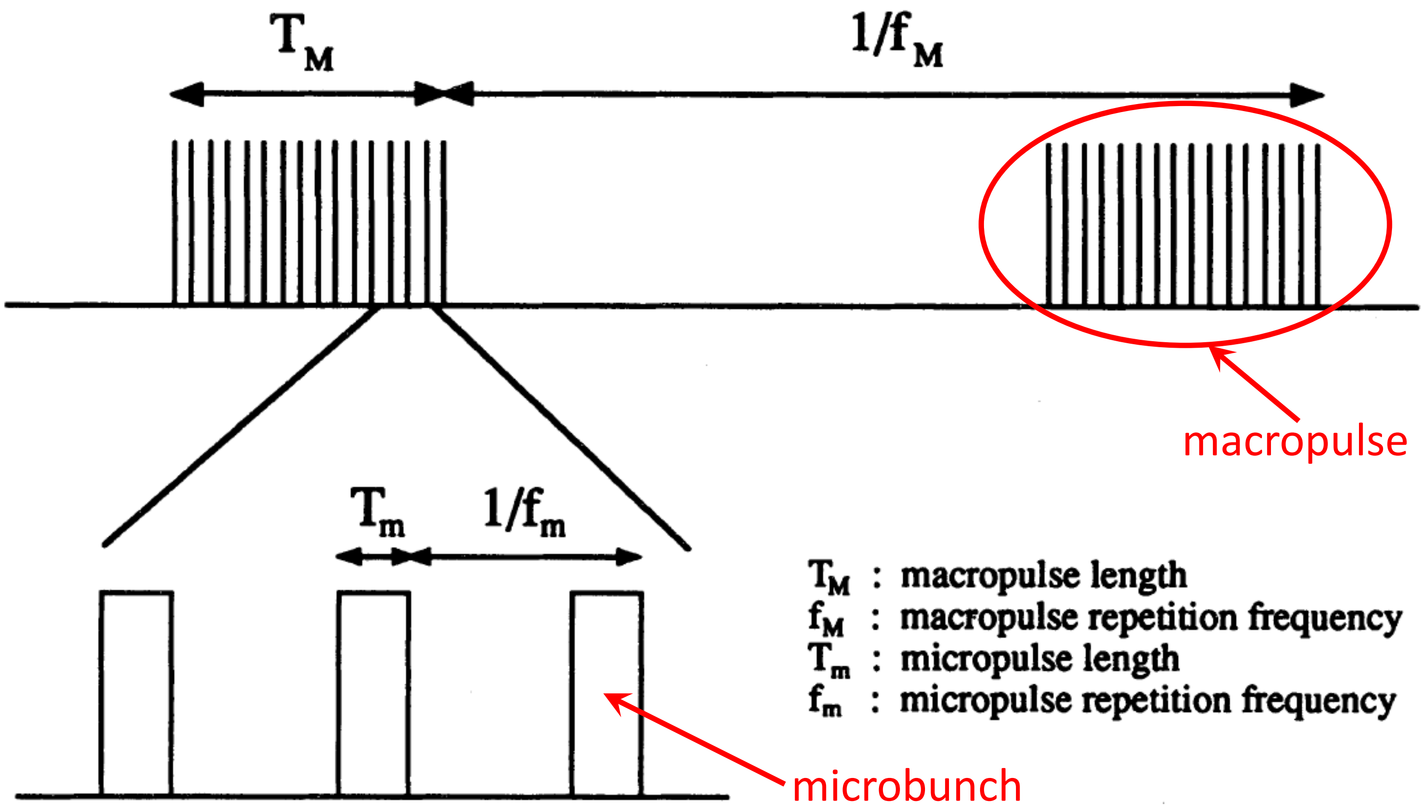

(C. Travier, Review of Microwave Guns, Particle Accelerators, 1991, Vol. 36, pp.33-74)

Electron Beam Pulse Format

Example:
Thermionic RF gun
at Chiang Mai University
(CMU RF-gun)
RF frequency = 2856 MH
Repetition rate = 10 Hz

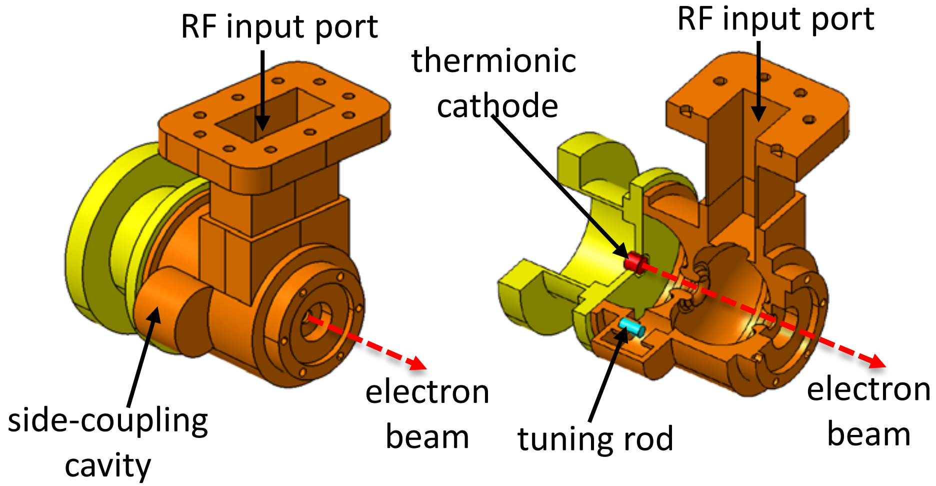

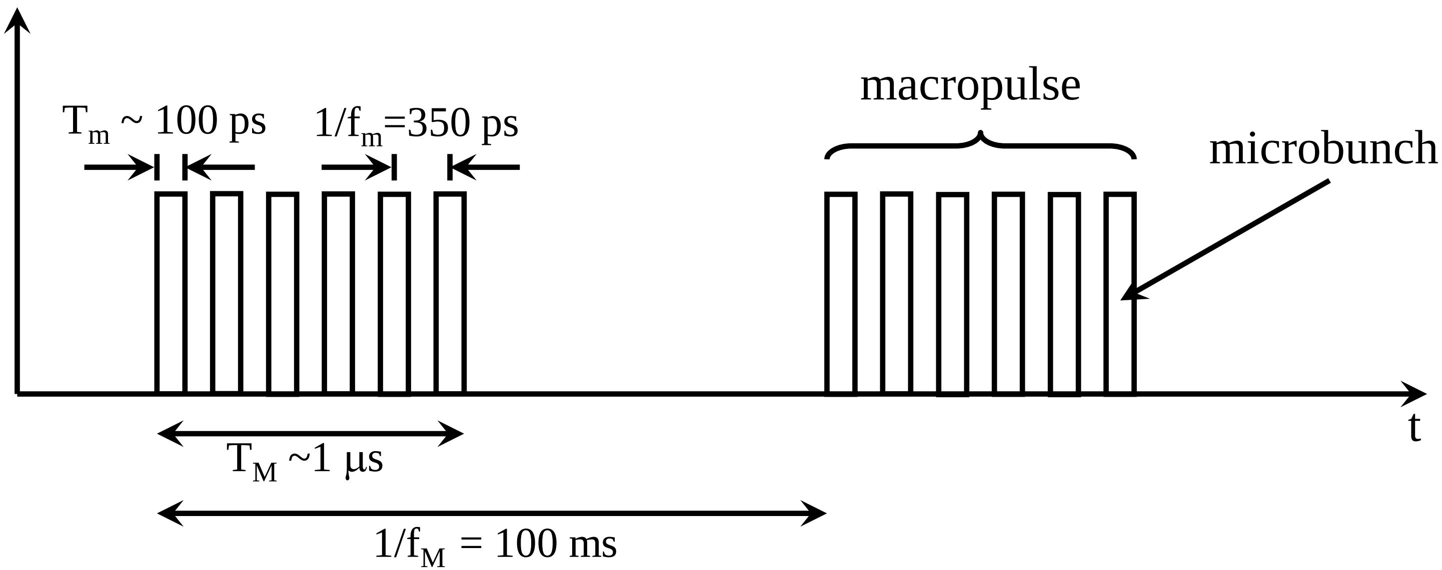

Characteristics of Thermionic RF Gun (1)

1. Richardson' s law: current density of the thermionic emission is limited by the heating temperature as

$$J = \frac{4\pi emk^2}{h^3} T^2 e^{-\frac{eW_F}{kT}} = AT^2 e^{-\frac{eW_F}{kT}}$$

$$A = \frac{4\pi emk^2}{h^3}$$

2. Schottky effect: this effect was discovered by Walter Schottky.

• While an RF field is applied to the RF gun, the work function of the cathode is reduced due to the quantum tunneling through the work function barrier.

→The electric field reduces the potential energy of electrons outside the cathode surface, distorting the potential barrier at the cathode surface.

→The work function of the cathode is reduced by the Schottky correction (W_{qt}),

$$W_F \to W_F - W_{qt}$$

which is related to the RF electric field as $W_{qt}[eV] = 0.012\sqrt{E(kV/cm)}$

Characteristics of Thermionic RF Gun (2)

→ The Richardson' s law becomes $j = AT^2 \exp\left[\frac{-e(W_F - W_{qt})}{kT}\right]$

→ The accelerating electric on the cathode surface expressed by $E = E_0 \sin \omega t$

where E_o is the maximum electric field and $\omega = 2\pi f$ where f is the resonant frequency, then the Richardson's law with Schottky's correction becomes

$$\frac{j}{AT^2} = \exp\left[\frac{-e(W_F - 0.012\sqrt{E_0(kV/cm)\sin(2\pi f)t})}{kT}\right]$$

Conclusion:

- In thermionic RF gun, higher heating temperature provides higher current density of electron beam.
- Applying of electric field in the RF gun reduces the work function barrier of the cathode and results in increasing of the electron beam current density.

Limitations of Thermionic RF Gun

- Beam energy is in the order of a few MeV to a few tens MeV.
- The back-bombardment electrons heat the cathode and thus results in current increase during the macropulse.

  - This leads to unstable beam operation and cathode degradation.
- Peak current is limited by the thermionic cathode current density.
- The output beam has a long bunch and large energy spread.

  - This requires a magnetic bunch compressor, which induces emittance growth and particle losses.

Thermionic RF guns can produce high brightness beams, but they cannot produce very high peak current.

Photocathode RF Electron Guns

- A photocathode placed in RF cavity is illuminated by laser pulses.

$\rightarrow$ Short electron bunches are produced via photoelectric process with the bunch length depending on the laser pulse length.

$\rightarrow$ Electron bunches are accelerated inside the RF cavity of high accelerating gradient and gain energy to reach the relativistic velocity in a very short distance.

- The RF cavity is optimized and the laser phase with respect to RF phase is adjusted to minimize the emittance.

$\rightarrow$ Low emittance electron beam.

- Solenoid magnets are used to focus the beam for counteracting the space charge effects (Coulomb force).

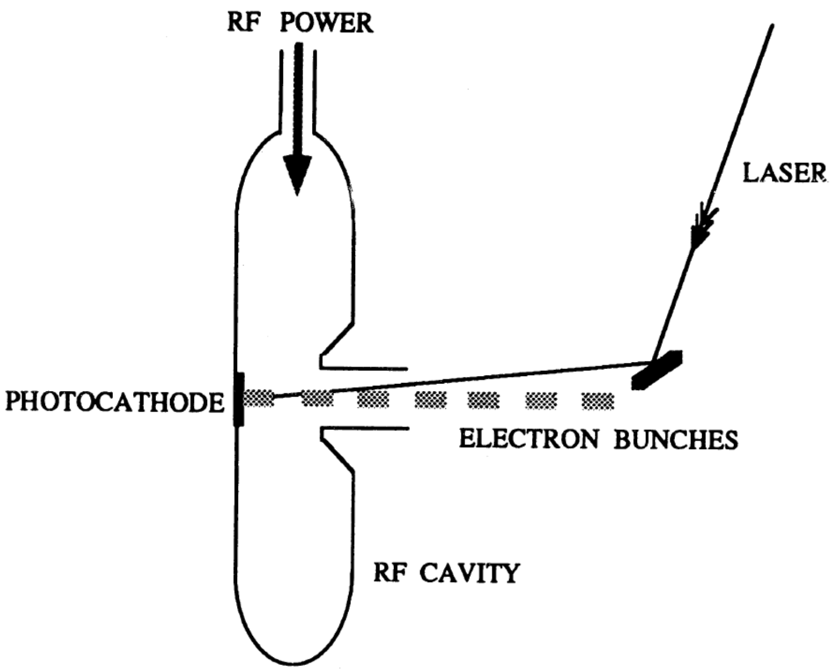

C. Travier, Review of Microwave Guns, Particle Accelerators, 1991, Vol. 36, pp. 33-74.

Example: Photocathode RF Gun @ PITZ, DESY

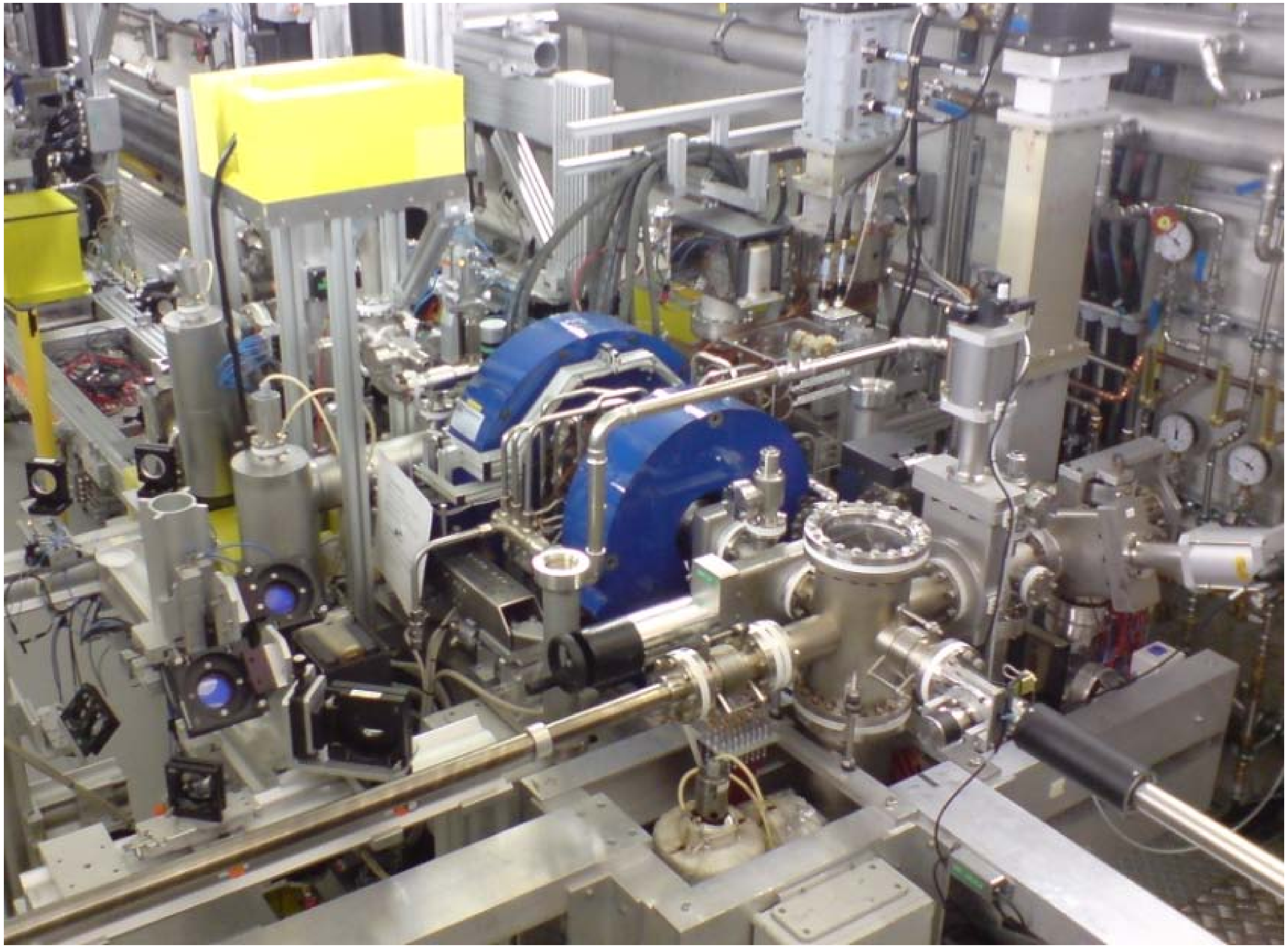

http://pitz.desy.de/

Example: Photocathode RF Gun @ PITZ, DESY

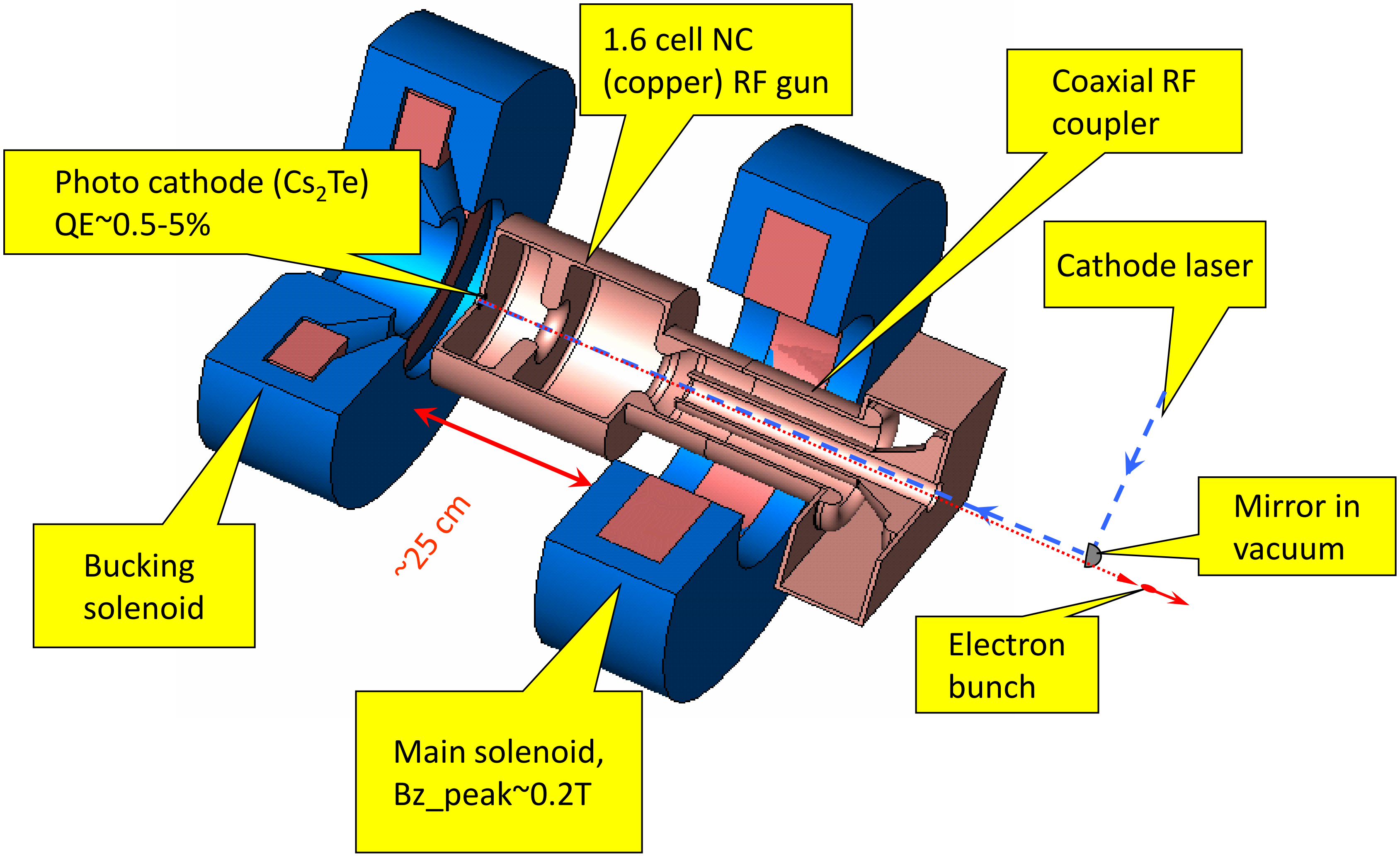

http://pitz.desy.de/

Example: Photocathode Laser @ PITZ

- Ytterbium-doped YAG laser (Yb:YAG)
  - IR input pulses
- UV output pulses
  - λ = 257 nm
  - pulse repetition rate = 1 MHz
  - up to 800 micro bunches/train
  - micro bunch energy: up to 10 μJ
  - bunch spacing: 0.2 – 1 μs
- can generate a broad variety of longitudinal pulse shapes of flat-top and Gaussian

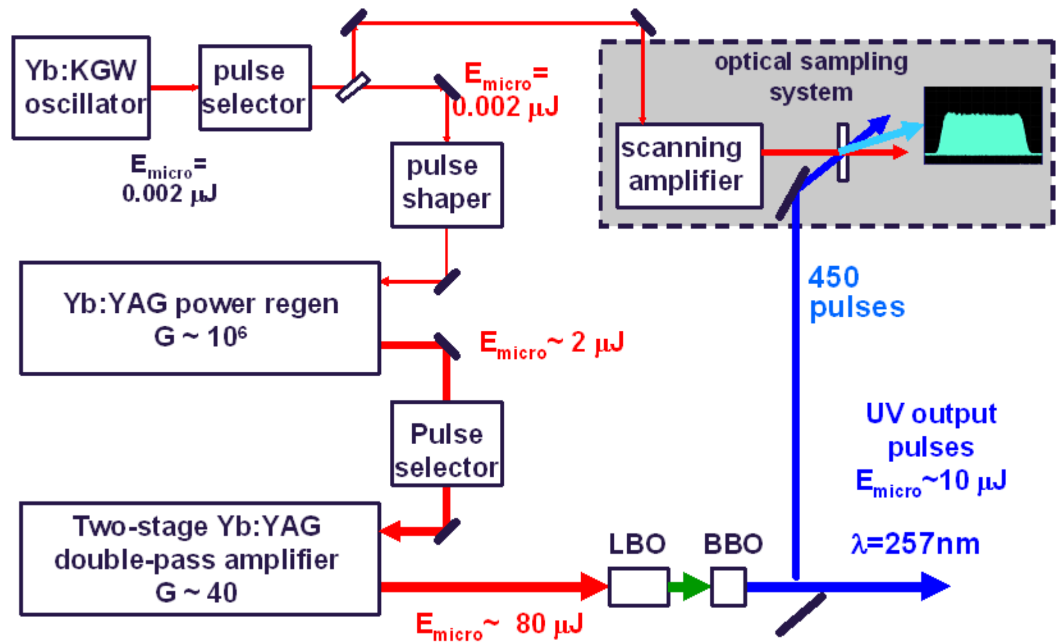

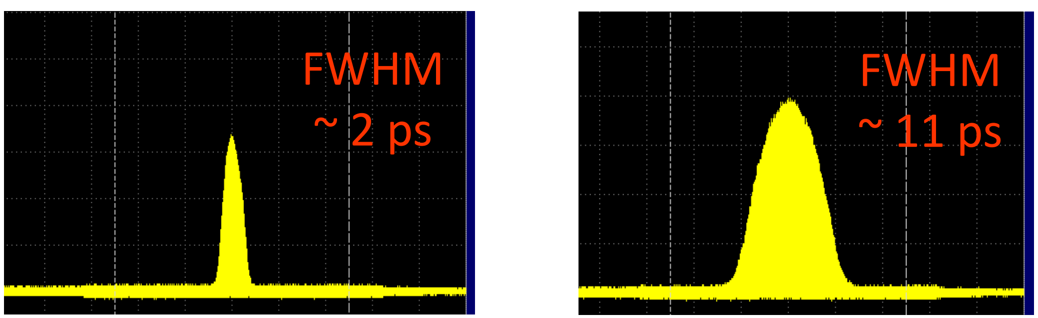

Gaussian pulses of different durations (FWHM = 2 -14 ps)

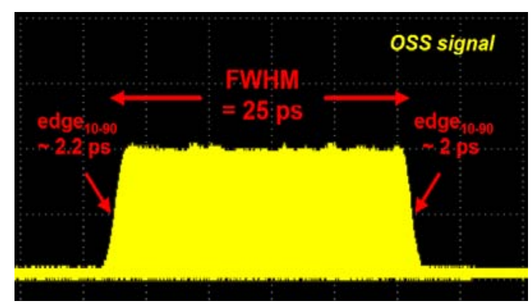

Flat-top pulses of different durations and rise/fall time (max. flat-top ~25 ps FWHM)

Advantages of Photocathode RF Guns

- Electron bunches have relativistic kinetic energy (MeV scale).
- Photo-cathodes can deliver much higher current densities than thermionic cathodes.
- The output beams have lower emittance value than the thermionic guns.
- The pulse format of electron bunches from photocathode RF gun is more flexible than that of conversional DC-gun and that of thermionic RF-gun
  → The laser can generate a broad variety of longitudinal pulse shapes of Gaussian , flat-top or ellipsoid.

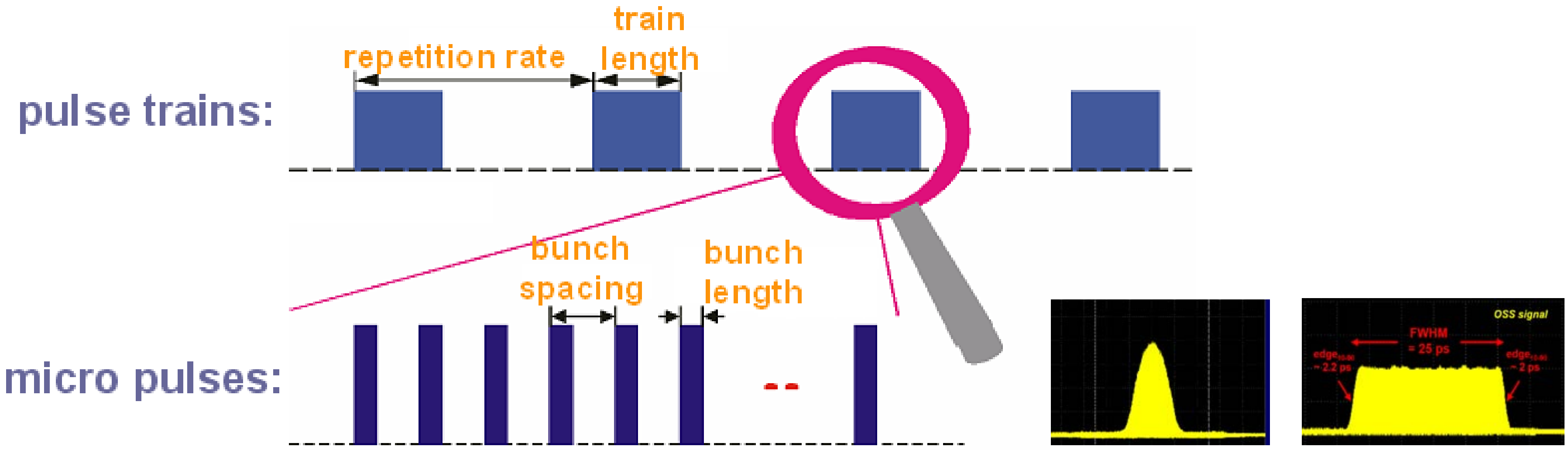

Lecture No. 1

- Introduction to electron sources
  - Electron emission processes
- Types of electron guns
  - Conventional thermionic DC guns
  - Photocathode DC guns
  - Thermionic RF guns
  - Photocathode RF guns
- **Benefits of RF electron guns**
  (as compared to conventional guns)
- Basic principle of RF structure

Benefits of RF Electrons Guns

- RF guns accelerate electrons with high accelerating field in the order of MV/m.

→ Rapid acceleration of electrons in the RF cavity results in the reduction of emittance growth from the space charge forces.

- The RF-guns can produce relativistic electron bunches of higher current with no additional extensive buncher system.

→ This leads to a compact and economical structure to produce high- brightness electron beams with MeV kinetic energies.

- Thermionic RF guns are simple, compact, and economical compared to a photo-cathode guns.

→ The thermionic RF-gun is normally used as an electron injector for IR FELs, coherent THz sources and Synchrotron radiation facilities.

Lecture No. 1

- **Introduction to electron sources**
  - Electron emission processes
- **Types of electron guns**
  - Conventional thermionic DC guns
  - Photocathode DC guns
  - Thermionic RF guns
  - Photocathode RF guns
- **Benefits of RF electron guns**
  (as compared to conventional guns)
- **Basic principle of RF structure**

Standing Wave RF Structure

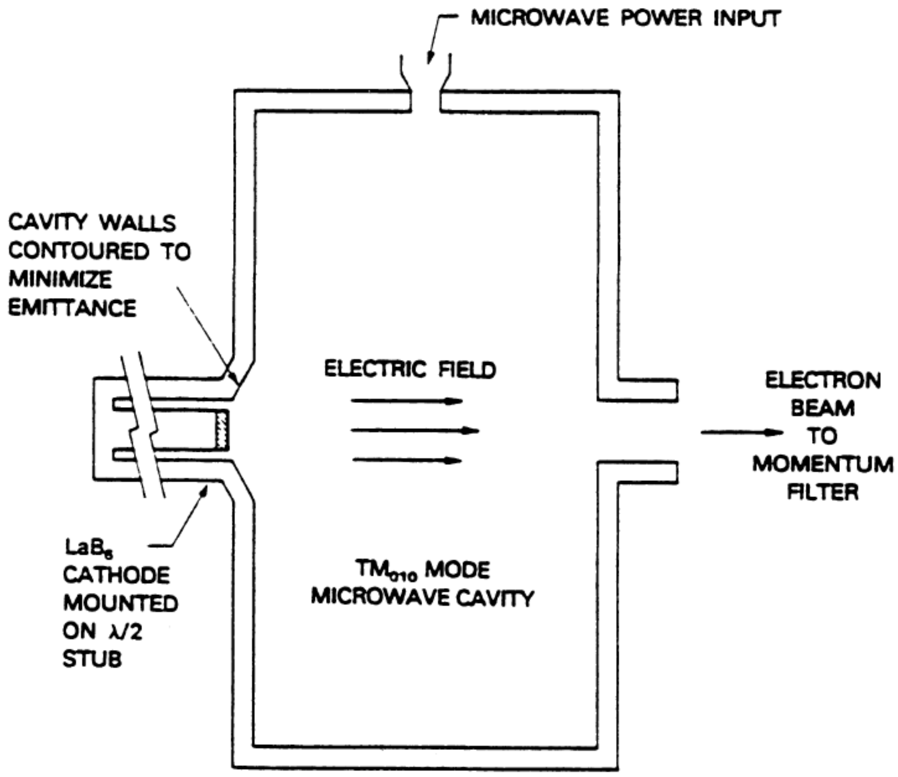

G.A. Westenskow, J.M.J. Madey, Microwave Electron Gun, Laser and Particle Beams Vol. 2, Part 2 (1984) 223.

Infinite circular conducting waveguide

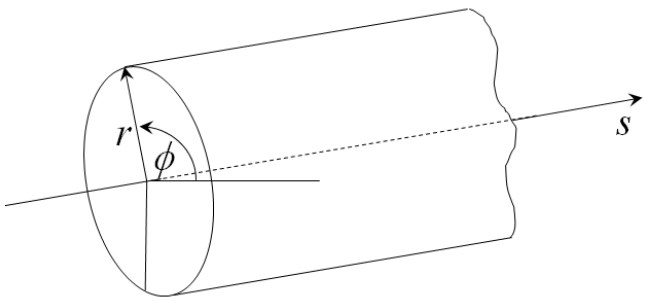

pillbox RF cavity (simplest RF structure)

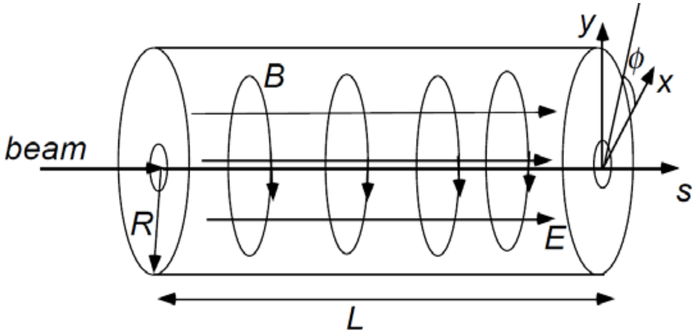

The cavity is operated in the TM_{010} mode:

$\rightarrow$ longitudinal E field

$\rightarrow$ transverse B field.

Pill-box Cavity (1)

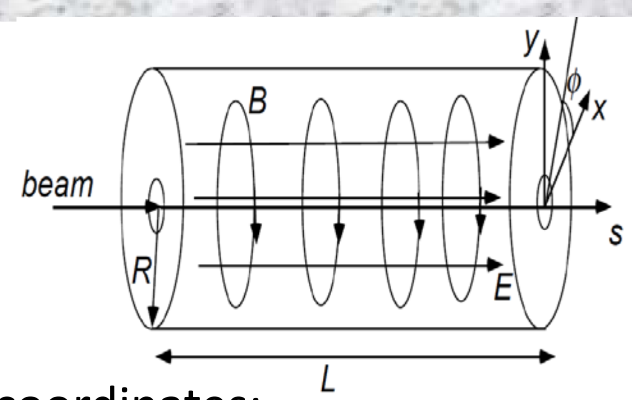

wave equations in cylindrical coordinates:

$$\nabla^2 \vec{E} + k^2 \vec{E} = 0 \quad \Rightarrow \quad E_r, E_\phi, E_s \qquad (1)$$

$$\nabla^2 \vec{B} + k^2 \vec{B} = 0 \quad \Rightarrow \quad B_r, B_\phi, B_s \qquad (2)$$

Wave equation of electromagnetic fields in cylindrical coordinates:

$$\frac{\partial^2 E_s}{\partial r^2} + \frac{1}{r}\frac{\partial E_s}{\partial r} + \frac{1}{r^2}\frac{\partial^2 E_s}{\partial \varphi^2} + \frac{\partial^2 E_s}{\partial z^2} + k^2 E_s = 0,$$

$$\frac{\partial^2 H_s}{\partial r^2} + \frac{1}{r}\frac{\partial H_s}{\partial r} + \frac{1}{r^2}\frac{\partial^2 H_s}{\partial \varphi^2} + \frac{\partial^2 H_s}{\partial z^2} + k^2 H_s = 0$$

Solution in a form of Bessel functions is

$$E_s(r, \varphi, s, t) = E_0 J_n(k_c r) e^{i(\omega t - n\varphi - ks)} \qquad (3)$$

Boundary conditions of the lowest mode (TM_{010}) at the cavity wall is

$$E_{\parallel} = B_{\perp} = 0$$

Electric & Magnetic Fields in TM_{010} Pill-box Cavity

Electric and magnetic field components inside the TM_{010} cavity are

$$E_s(r,t) = E_o J_o(k_c r)\cos\omega t \qquad (4)$$

$$B_\phi(r,t) = -\frac{E_o}{c} J_1(k_c r)\sin\omega t \qquad (5)$$

where $k_c = \frac{2\pi}{\lambda}$ and $c = \frac{\omega}{k_c}$ when $J_o(k_c r)$ and $J_1(k_c r)$ are Bessel functions.

- Electric field E_s is maximum at r =0 and it reduces when the radius increases.
- Electric field is constant along longitudinal direction.
- Magnetic field is zero at all locations along the cavity axis or at r =0.

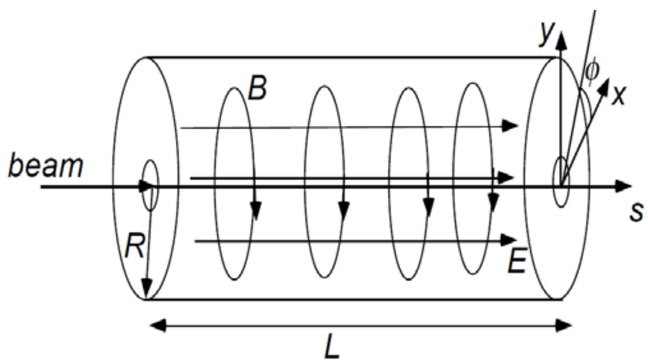

Longitudinal electric field and Transverse magnetic field in TM_{010} pill-box cavity.

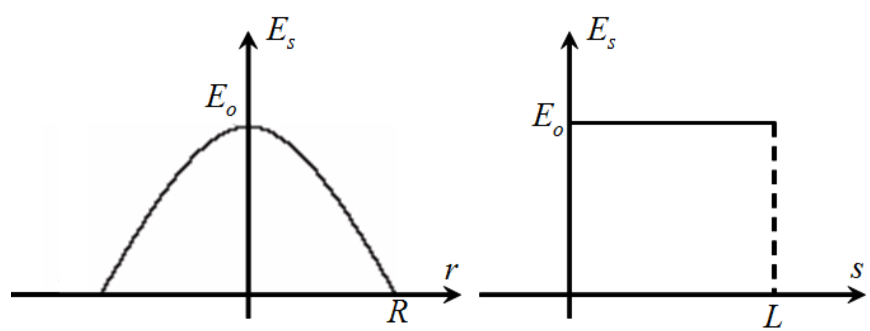

Maximum energy gain in pillbox cavity with length L.

Electric field versus radial and longitudinal distance of TM_{010} pill-box cavity.

Resonant Frequency & RF Wavelength

- Parameters of the TM_{010} mode of the pill-box RF cavity can be defined when inside the cavity is free space $\mu = \varepsilon = 1$ and consider the boundary condition at $J_0(2.405) = 0$ and $k_c R = 2.405$.

- Resonant frequency is

$$f_{rf} = \frac{\omega}{2\pi} = \frac{k_c c}{2\pi\sqrt{\mu\varepsilon}R} = \frac{2.405c}{2\pi R}$$

$$f_{rf} = \frac{\omega}{2\pi} = \frac{2.405c}{2\pi R} \qquad (6)$$

Bessel functions $J_o(x) = J_o(k_c r)$

$J_1(x) = J_1(k_c r)$

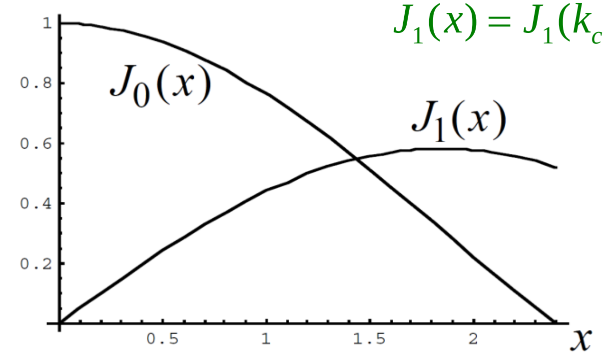

- RF wavelength is

$$\lambda_{rf} = \frac{c}{f_{rf}} = \frac{2\pi}{2.405}R \qquad (7)$$

Cavity Length & Radius

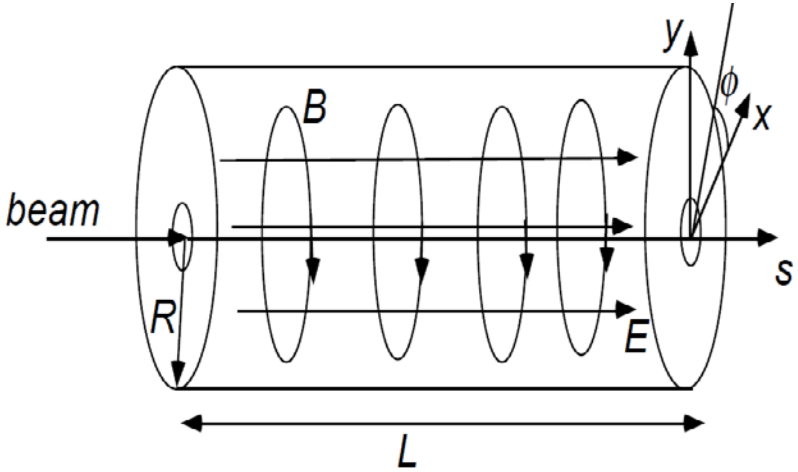

Synchronicity condition of π-mode leads to the length of the cavity as

$$L = \frac{vT_{rf}}{2} = \beta \frac{\lambda_{rf}}{2} \qquad (8)$$

From equation (6) and (7) we can define the cavity radius as

$$R = 2.405 \frac{c}{2\pi f} \qquad (9)$$

Energy Gain & Accelerating Voltage

- Energy gain of charge "e" can be calculated from

$$W = eV_{acc} = e\int_{-L/2}^{L/2} (E_o \cos \omega t)ds \qquad (10)$$

- Accelerating voltage is

$$V_{acc} = \int_{-L/2}^{L/2} (E_o \cos \omega \frac{s}{v})ds = E_o \frac{2v}{\omega} \sin \frac{\omega L}{2v} \qquad (11)$$

- Transit time factor is

$$T = \frac{V_{acc}}{E_o L} = \frac{\sin(\omega L / 2v)}{\omega L / 2v} \qquad (12)$$

This is the parameter which is used to consider the length of the RF cavity.

Figure of Merit of RF Cavity (1)

Acceleration in the RF cavity can be explained by considering the relation between stored energy (W_s) and cavity wall loss in one RF cycle $(2\pi/\omega)$ through a parameter called Quality factor (Q-factor), which is defined as

$$Q = 2\pi \frac{Stored\ energy}{energy\ loss\ in\ 1\ cycle} = \frac{\omega W_s}{P_l}$$

Higher Quality factor $\rightarrow$ higher stored energy $\rightarrow$ higher acceleration

- Stored energy can be found from

$$W_s = \frac{1}{2\mu_o} \int_{cavity\ volume} B^2 dV$$

- Cavity wall losses is

$$P_i = \frac{R_w}{2\mu_o^2} \int_{cavity\ surface} B^2 ds \qquad (13)$$

where $R_w = \rho_c / \delta$ is surface resistivity, ρ_c is resistivity and δ is skin depth.

Figure of Merit of RF Cavity (2)

- Skin depth is a intrinsic property of materials, which can be calculated from

$$\delta = \sqrt{\frac{2\rho_c}{\mu_o \omega}} = \sqrt{\frac{2}{\mu_o \omega \sigma_c}} \qquad (14)$$

where $\sigma_c = \frac{1}{\rho_c}$ is the conductivity of the RF cavity.

- The cavity wall losses becomes

$$P_i = \frac{\delta \omega}{4\mu_o} \int_{cavity\ surface} B^2 ds \qquad (15)$$

- The quality factor is

$$Q_i = \frac{\omega W_s}{P_i} = \frac{2\int B^2 dV}{\delta \int B^2 dS} \qquad (16)$$

The quality factor strongly depends on the size and the surface resistivity of the RF cavity.

Figure of Merit of RF Cavity (3)

- The cavity wall losses is expressed in terms of the accelerating voltage and the shunt impedance as

$$P_i = \frac{V_{acc}^2}{R_S} \qquad (17)$$

where R_s is the shunt impedance and V_{acc} is the accelerating voltage.

- Shunt impedance per unit length of the RF cavity with the length "L" is

$$r_s = \frac{V_{acc}^2}{P_i L} = \frac{E_o^2 L}{P_i} T^2 \qquad (18)$$

- Considering the quality factor, we get the R-over-Q ratio , which depends only on size and shape of the RF cavity as

$$\frac{r_s}{Q} = \frac{V_{acc}^2}{\omega W_s L} \qquad (19)$$

Figure of Merit of RF Cavity (4)

- The cavity wall loss is proportionally to the stored energy as

$$Q_i = \frac{dW_s}{dt} = \frac{\omega W_s}{P_i} \qquad (20)$$

- Since, the stored energy is exponential decay as

$$W_s = W_{so} e^{-\omega t/Q} \qquad (21)$$

Thus, the filling time becomes

$$t_f = \frac{2Q}{\omega} \qquad (22)$$

End of Lecture No. 1

Questions
&
Discussion

Lecture Outline

Lecture No. 1

- Electron accelerators and sources
- Types of electron guns
- Benefits of RF electron guns

Lecture No. 2

- Design and construction of RF gun
- Low power tests and tuning of RF gun
- RF power source and high power tests

Lecture No. 3

- Operation of RF electron gun
- Generation and applications of ultra short electron bunches produced by RF gun

Lecture No. 2

- **Design and Construction of RF Gun**
  - Principle, design and simulation of RF gun
  - Fabrication of RF gun
- **Low Power Tests and Tuning of RF Gun**
  - Low power tests and RF measurements
  - Tuning of RF gun
- **RF Power Source and High Power Tests**
  - Introduction to RF source, transmission and coupling system required for RF gun
  - High power tests and conditioning of RF gun
- **High Power Tests and Commissioning of RF Gun**
  - Conditioning of RF gun
  - Cathode preparation

Maximum Acceleration

Synchronicity condition of π-mode leads to the length of the cavity as

$$L = \frac{vT_{rf}}{2} = \beta\frac{\lambda_{rf}}{2} \qquad (11)$$

Transit time factor for maximum acceleration $\sin(\omega L/2v) = \sin 90^o$ and $\beta = \frac{v}{c}$ is

$$T = \frac{\sin(\omega L/2v)}{\omega L/2v} = \frac{\sin 90^o}{\omega L/2v} = \frac{2v}{\omega L} = \frac{2(\lambda_{rf} f_{rf})}{(2\pi f_{rf})(\beta\lambda_{rf}/2)}$$

$$T = \frac{\sin 90^o}{\omega L/2v} = \frac{2}{\pi}; \quad \beta \approx 1 \qquad (11)$$

Maximum voltage:

$$V_{acc} = E_o LT = \frac{2E_o L}{\pi} \qquad (12)$$

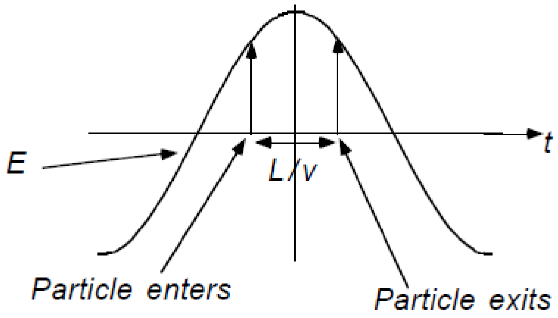

Maximum energy gain in pillbox cavity with length L.

Shape Optimization

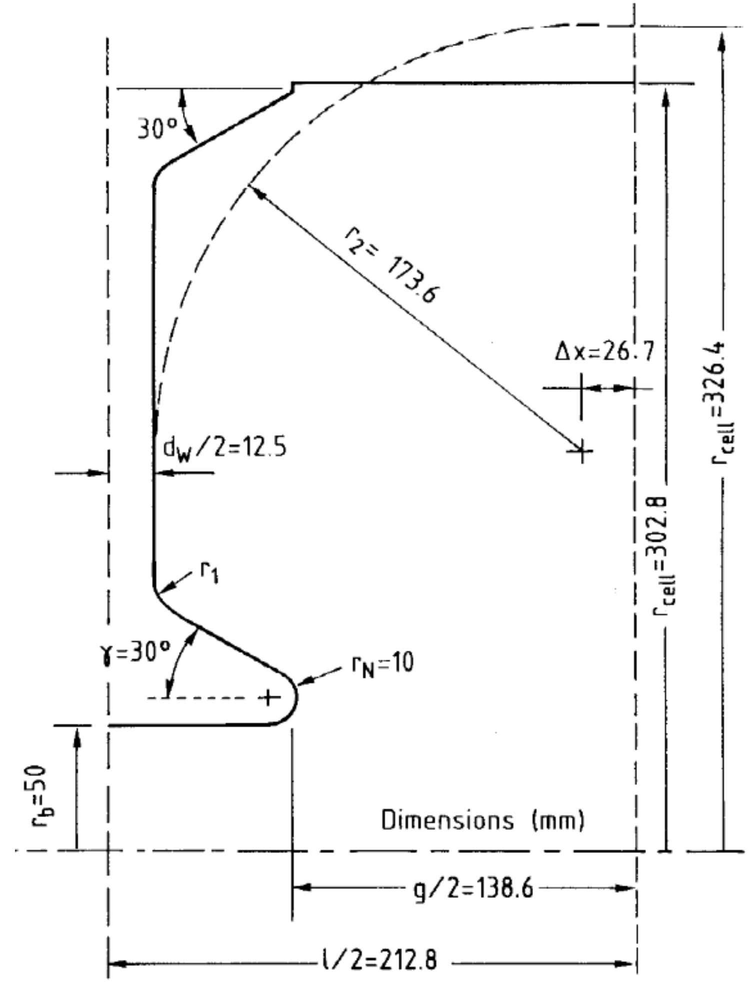

One quadrant of an optimized cell for the LEP copper RF system.

H. Henke, RF Structures (Design), Physics and Technology of Linear Accelerator Systems, Proceedings of JAS 2002.

Thermionic RF Gun @ CMU

- Half-cell and full-cell are π excitation mode
- Side-coupling cavity leads the whole RF-gun to $\pi/2$ excitation mode

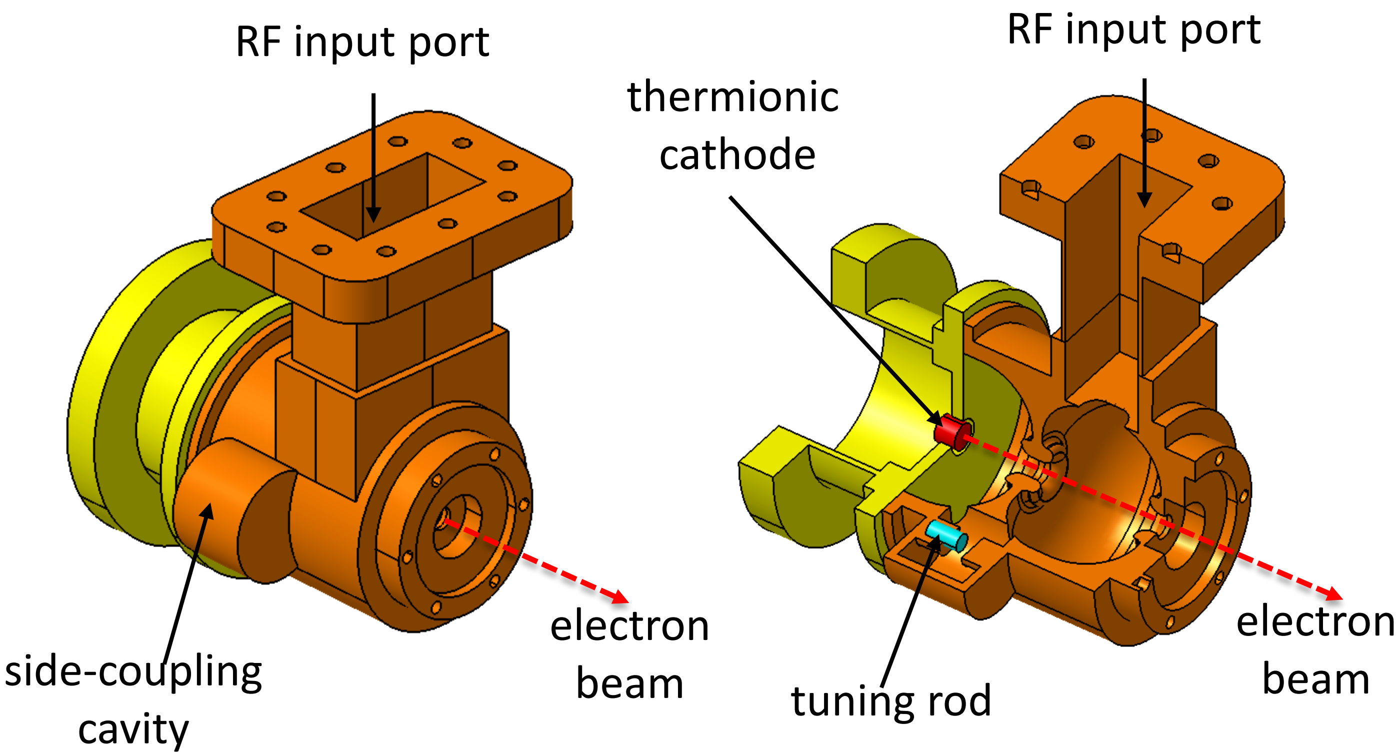

S. Rimjaem et al., Nuc. Instr. and Meth. A 736 (2014) 10-21.

Design and Simulations of RF-gun

Available online at www.sciencedirect.com
SCIENCE DIRECT®
ELSEVIER
Nuclear Instruments and Methods in Physics Research A 533 (2004) 258–269
NUCLEAR INSTRUMENTS & METHODS IN PHYSICS RESEARCH Section A
www.elsevier.com/locate/nima

Femtosecond electron bunches from an RF-gun

Sakhorn Rimjaem[a,*], Ruy Farias[b], Chitrlada Thongbai[a], Thiraphat Vilaithong[a], Helmut Wiedemann[c]

[a] *Fast Neutron Research Facility, Physics Department, Chiang Mai University, P.O. Box 217, Chiang Mai 50202, Thailand*
[b] *Laboratorio National de Luz Sincrotron, LNLS, Campinas, Brazil*
[c] *Applied Physics and SSRL,/SLAC Stanford University, Stanford, CA, USA*

Received 8 December 2003; received in revised form 3 May 2004; accepted 27 May 2004
Available online 29 July 2004

2D RF Simulations for 2 Cavities Together

SUPERFISH (LANL) was used to study

- Shape optimization
- RF-parameters
- Accelerating field distribution

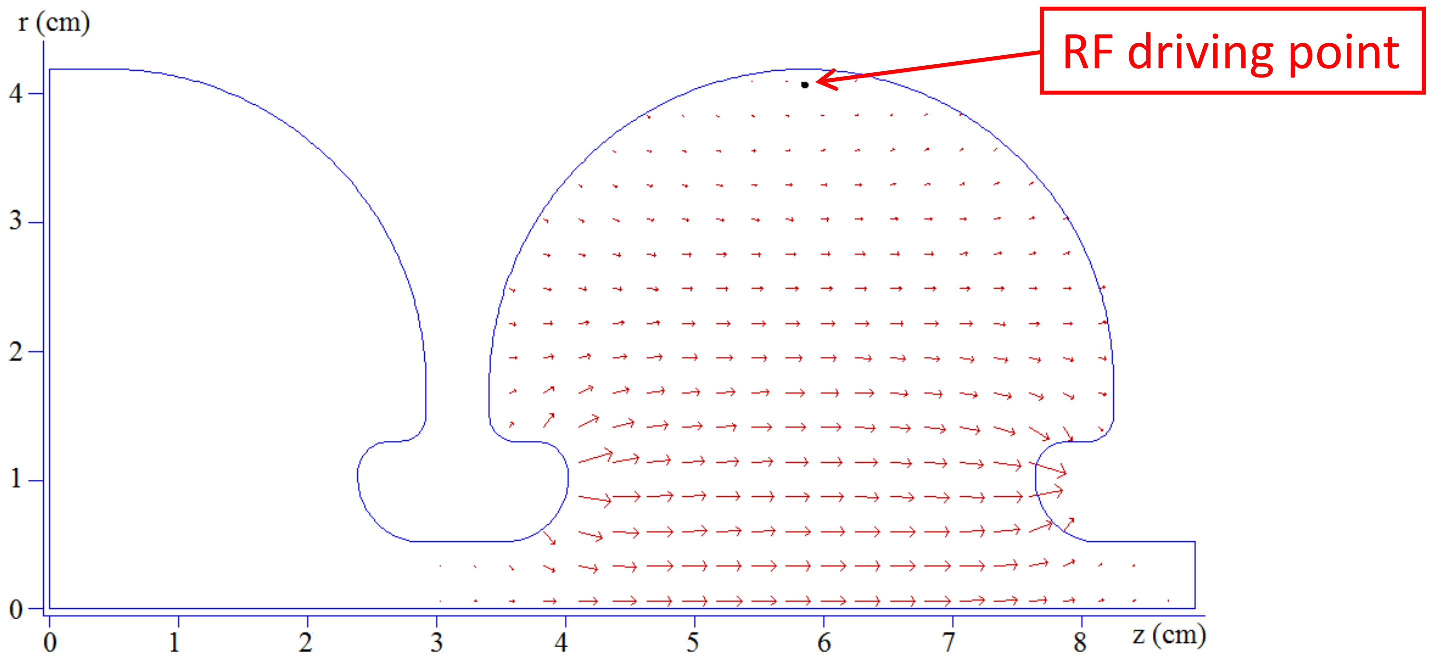

2D internal geometry and SUPERFISH computed electric field vectors of the one and half cells RF-gun (only half of the RF-gun cross-section is shown).

2D RF Simulations for 2 Cavities Separately

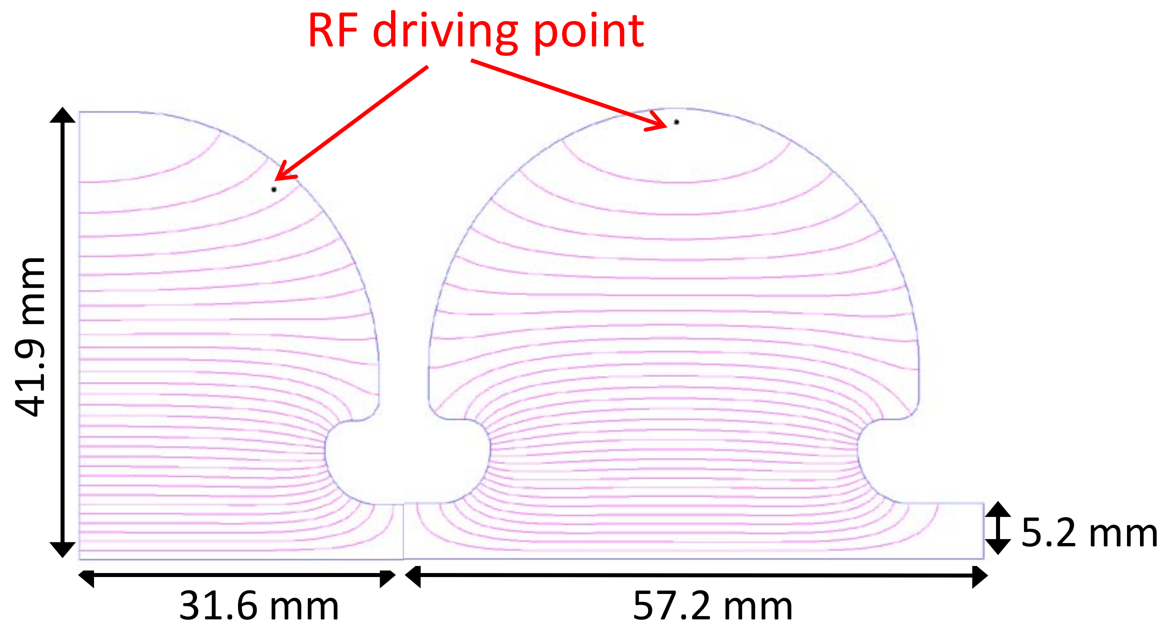

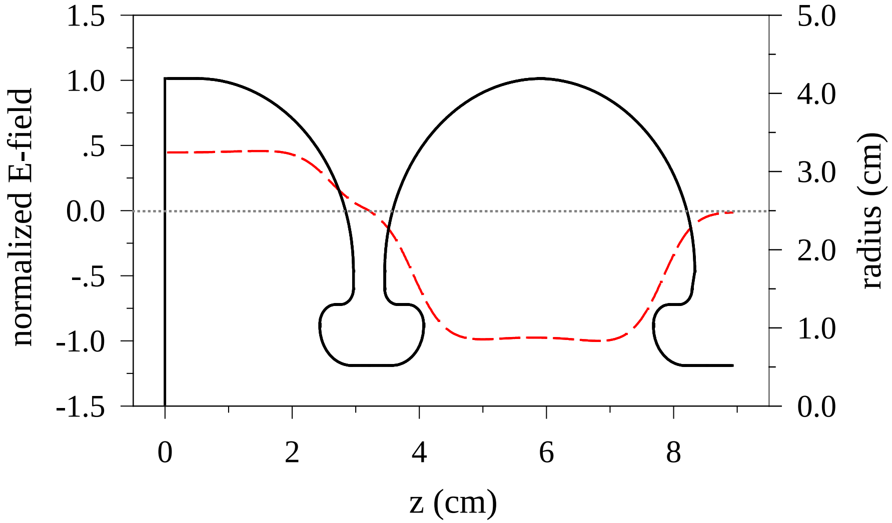

Parameters for the design RF-gun

Parameter	HC	FC
Cavity length (mm)	32.1	58.1
Effective length (mm)	25.1	38.7
Radius (mm)	24.64	24.64

Beam Dynamic Study

PARMELA (LANL)

- Track particles through RF-fields obtained from SUPERFISH
- Solve Maxwell's equations for EM field including space charge effect
- Results show both longitudinal and transverse distributions

Beam Optics (H. Wiedemann)

- Simulate beam optics in the alpha magnet, linac and other components
- Used to optimize the electron beam size through the beam line

BCompress (H. Wiedemann)

- Study beam dynamics from gun exit to experimental stations
- Determine locations of experimental stations, electron bunch length, bunch charge, peak current

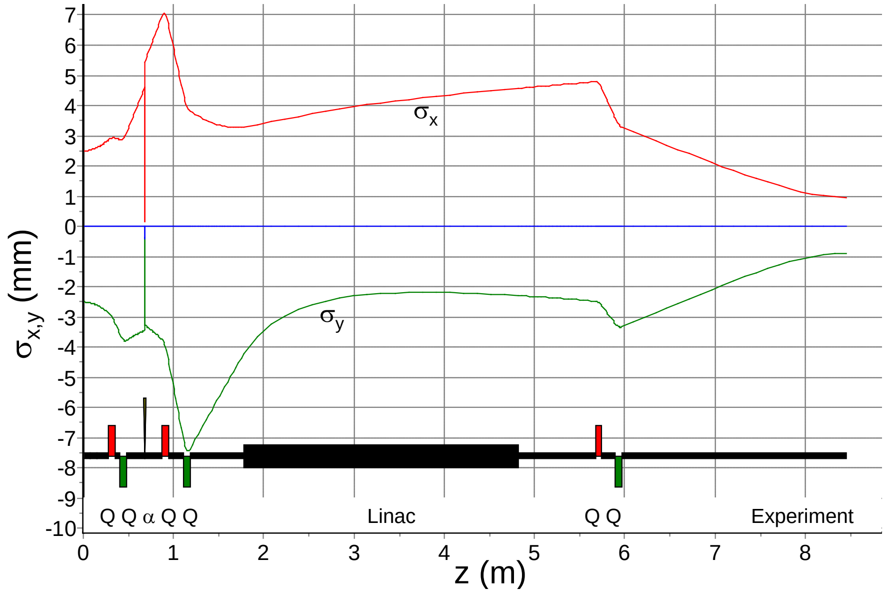

S. Rimjaem et al., Nucl. Inst. And Meth. A 533, 2004

Longitudinal Beam Dynamics

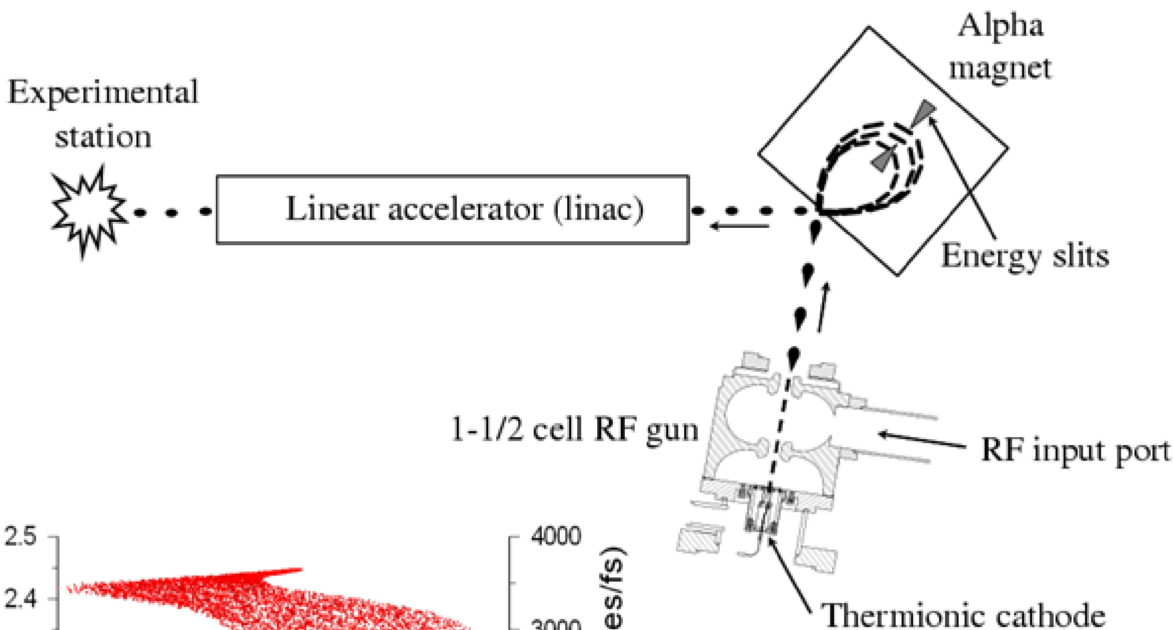

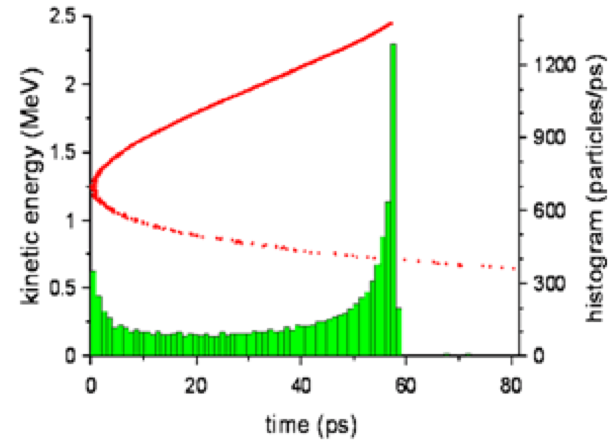

at α-magnet exit

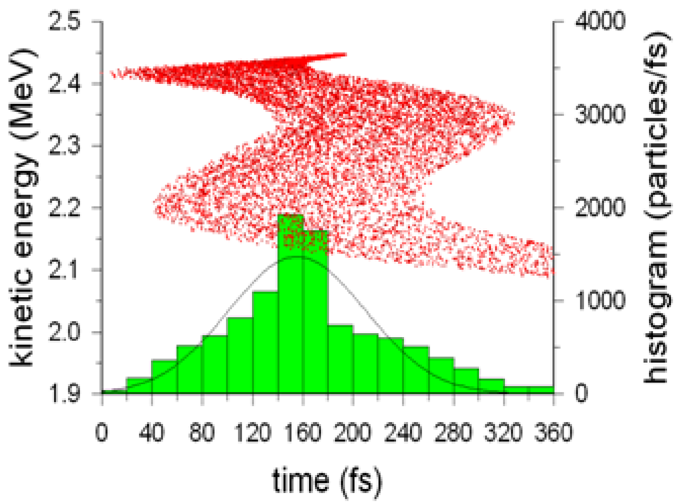

at experimental station (l_b~53 fs)

100,000 simulated macroparticles per bunch with cathode current of 2.9 A and each macroparticle represents a charge of 10.15 fCb or 6.34×10^4 electrons

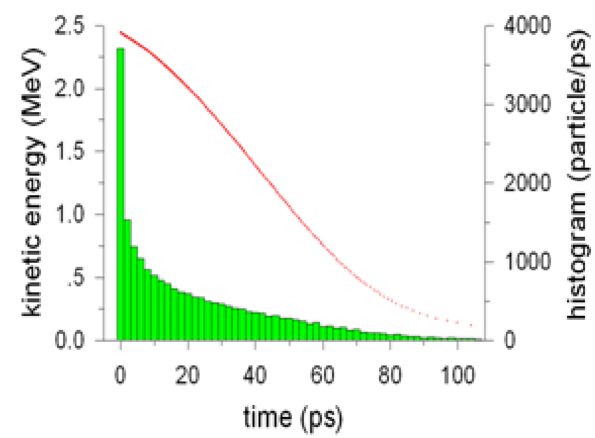

at RF-gun exit (l_b~10 ps)

Transverse Beam Dynamics

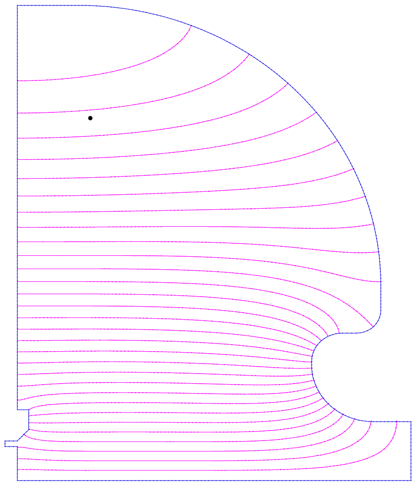

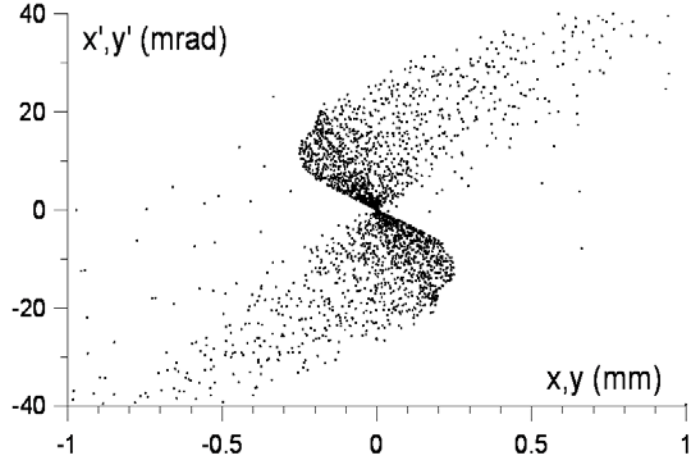

Nose-cone @ cathode

- divergence ~10 mrad
- limit bunch length ~120 fs

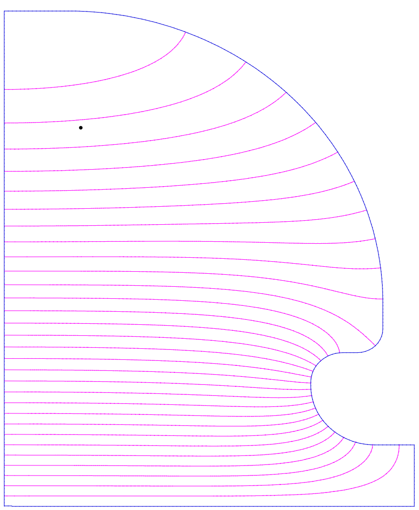

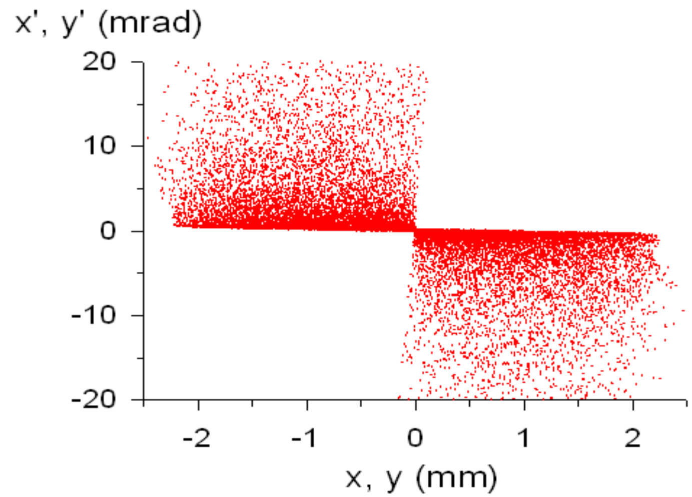

CMU RF-gun

- flat cathode
- bigger iris radius
- divergence ~1 mrad
- $\varepsilon_{n,rms}$~3.8 mm-mrad
- bunch length ~53 fs

S. Rimjaem et al., Nucl. Inst. And Meth. A 533, 2004

RF Gun & Beam Parameters

Parameter	Design RF-gun	Actual RF-gun
Cavity length of HC/FC (mm)	32.1 / 58.1	31.6 / 57.2
Effective length of HC/FC (mm)	25.1 / 38.7	24.9 / 39.2
f_{rf} of HC/FC (MHz)	2863.6 / 2825.0	2880.6 / 2868.8
Q_0 of HC/FC	15263 / 13022	15692/ 13343
β= v/c at gun exit	0.9851	0.9849
Max. kinetic energy (MeV)	2.45	2.44
Ave./max. field in HC (MV/m)	23.9 / 29.9	22.7 / 28.7
Ave./max. field in FC (MV/m)	45.0 / 67.6	46.9 / 68.5
Ave. field ratio	1.88	2.07
Max. field ratio	2.26	2.39
Cathode radius (mm)	3	3
Cathode emission current (A)	2.9	2.9
Cathode current density (A/cm^2)	10	10
Charge per bunch @ experiment (pCb)	94	94
Peak current @ experiment (A)	707	682
Bunch length, rms @ experiment (fs)	53	55

3D Cylindrical Symmetric Model

SUPERFISH 7.19: 2D simulations

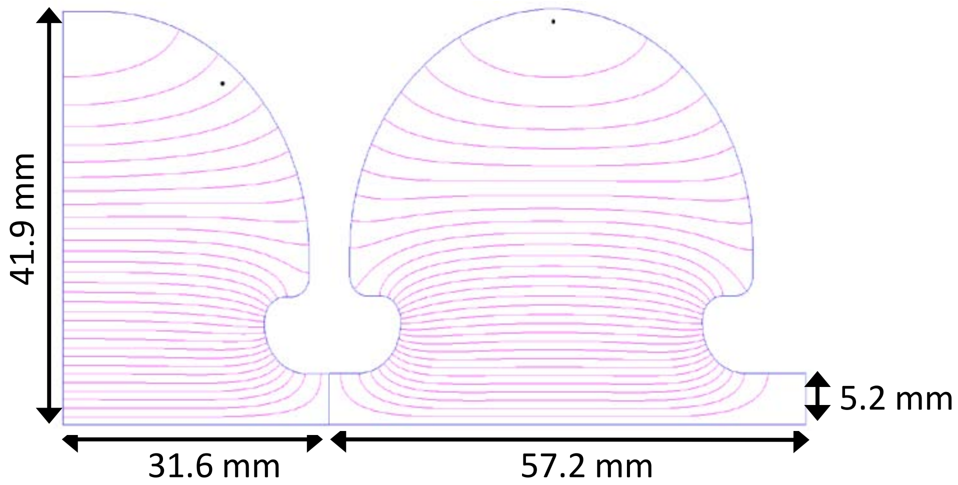

CST Microwave Studio 2012@: 3D simulations

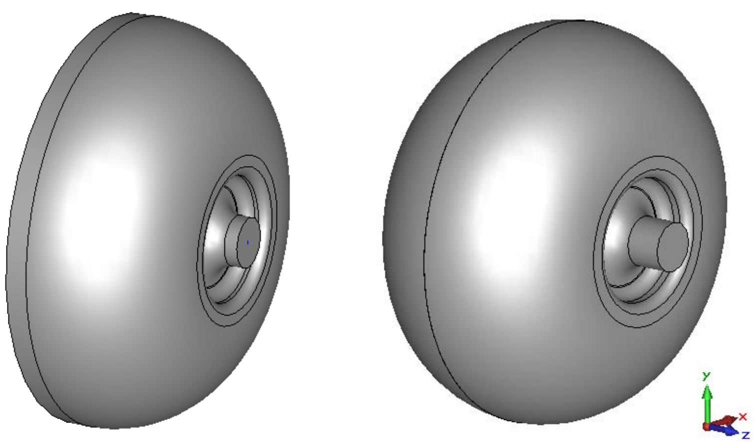

PARMELA distribution @ gun exit

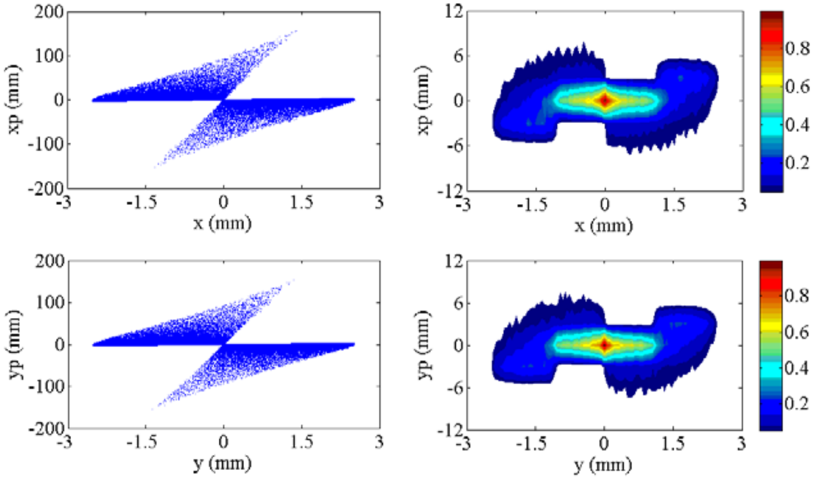

5 cm after gun exit

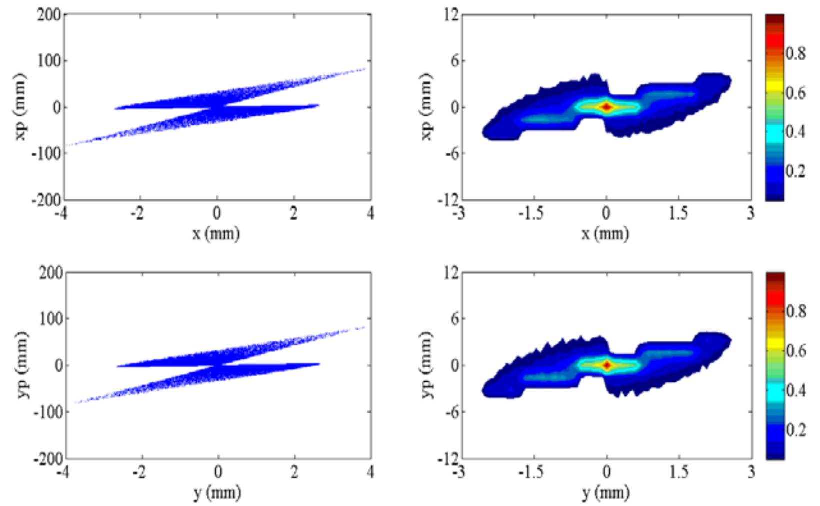

Study of Asymmetric Side-coupling RF-gun

Nuclear Instruments and Methods in Physics Research A 736 (2014) 10–21

ELSEVIER

Contents lists available at ScienceDirect

Nuclear Instruments and Methods in Physics Research A

journal homepage: www.elsevier.com/locate/nima

NUCLEAR INSTRUMENTS & METHODS IN PHYSICS RESEARCH

RF study and 3-D simulations of a side-coupling thermionic RF-gun

CrossMark

S. Rimjaem [a,b,*], K. Kusoljariyakul [a,b], C. Thongbai [a,b]

[a] *Department of Physics and Materials Science, Faculty of Science, Chiang Mai University, Chiang Mai 50200, Thailand*
[b] *Thailand Center of Excellence in Physics (ThEP), Commission on Higher Education, Bangkok 10400, Thailand*

3D CST MWS RF-gun Model (1)

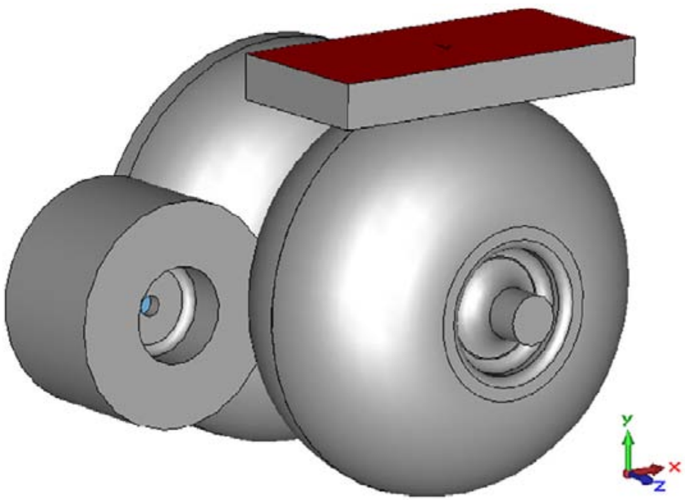

Parameter	3-D model	Measurement
$f_{\pi/2}$	2856.4 MHz	2856 MHz @ 27.5°C
Q_o	15272	12979
Q_l	2074	1586
Q_{ext}	2400	1741
β_{rf}	6.36	7.3
E_{p2}/E_{p1}	1.98	2.00
$\langle E_2 \rangle / \langle E_1 \rangle$	1.69	1.73

Electric field distributions

yz-plane

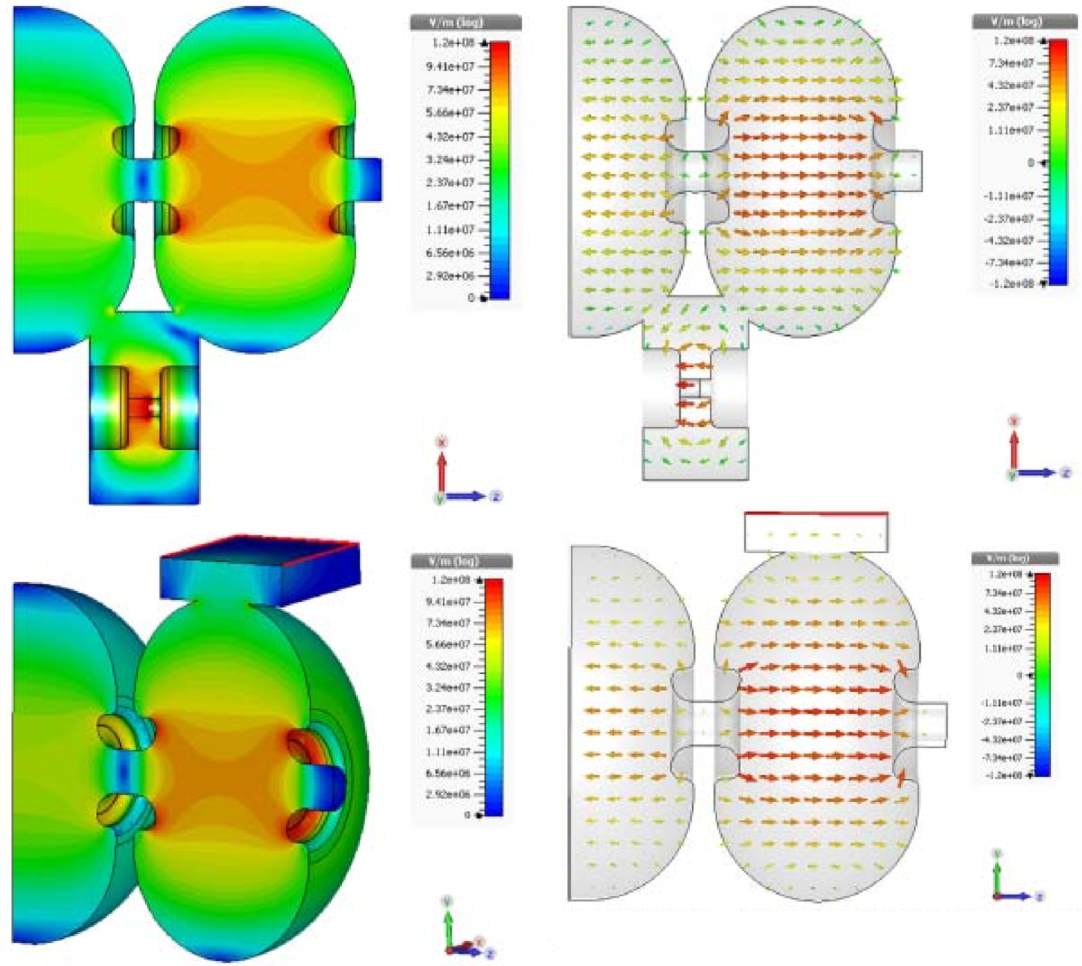

3D CST MWS RF-gun Model (2)

Magnetic field distributions in xy-plane @ z = 0, 20, 41, 58 mm

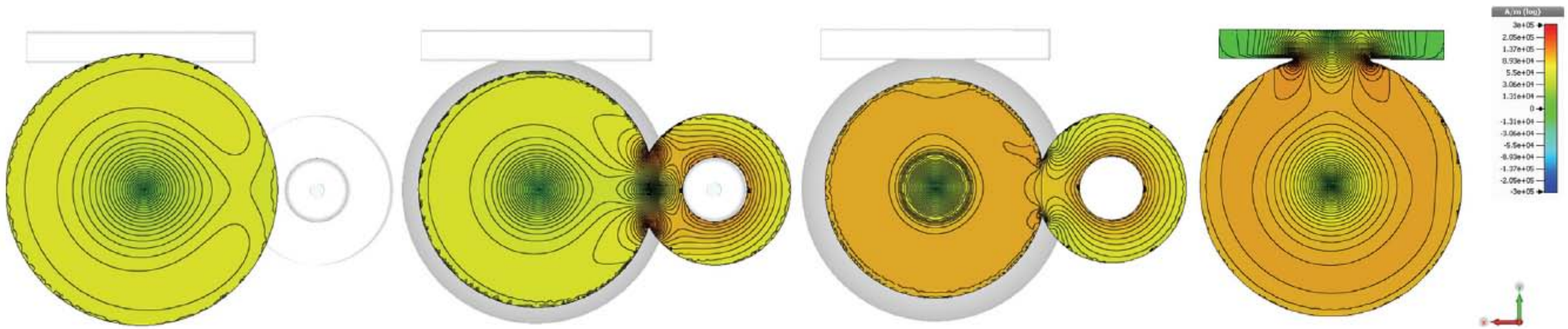

@ gun exit (emit. Increases 10.8%)

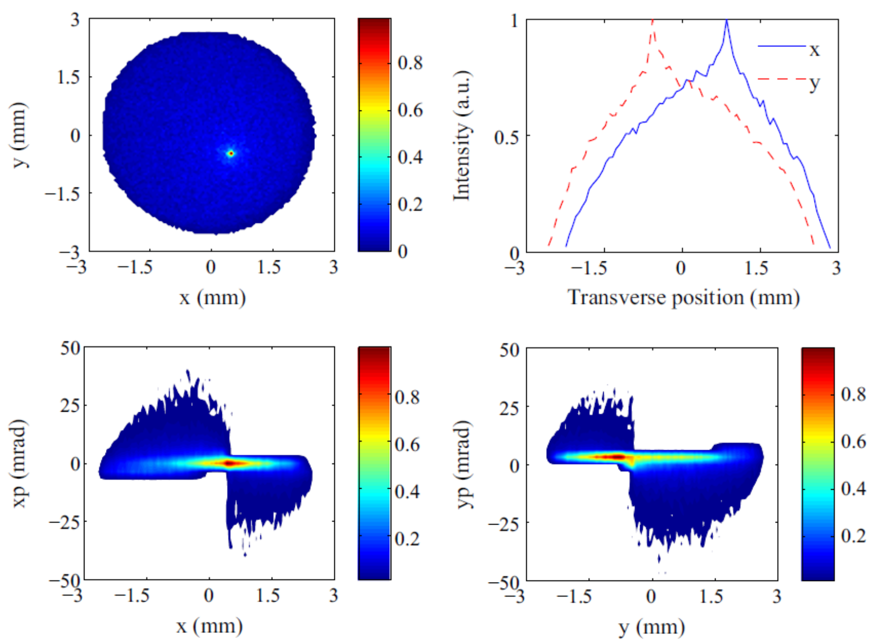

@ 5 cm after gun exit (emit. Increases 17.2%)

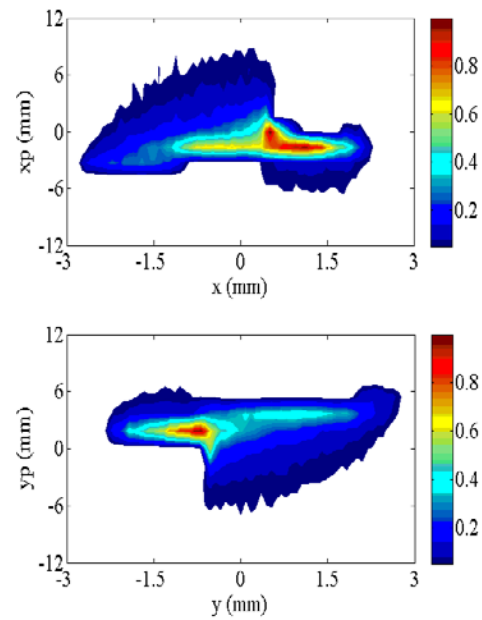

Compared Results of SUPERFISH & CST MWS

Parameter	SUPERFISH field	MWS field	Unit
Ave. field in half cell (E_1)	25.91	25.91	MV/m
Max. field in half cell (E_{p1})	31.91	31.80	MV/m
Ave. field in full cell	44.82	43.78	MV/m
Max. field in full cell	64.29	62.86	MV/m
Ave. field ratio (E_2/E_1)	1.73	1.69	
Max. field ratio (E_{p2}/E_{p1})	2.00	1.98	
Ave. beam kinetic energy	1.96	1.94	MeV
Max. beam kinetic energy	2.53	2.49	MeV
Bunch charge	0.21	0.21	nC
Horizontal centroid position	0.028	0.846	mm
Vertical centroid position	−0.032	−0.575	mm
Horizontal rms beam size	1.145	1.154	mm
Vertical rms beam size	1.146	1.183	mm
Horizontal rms emittance	16.25	17.79	mm · mrad
Vertical rms emittance	16.25	18.21	mm · mrad

On-axis Electric Field and Longitudinal Distribution

On-axis electric field distributions

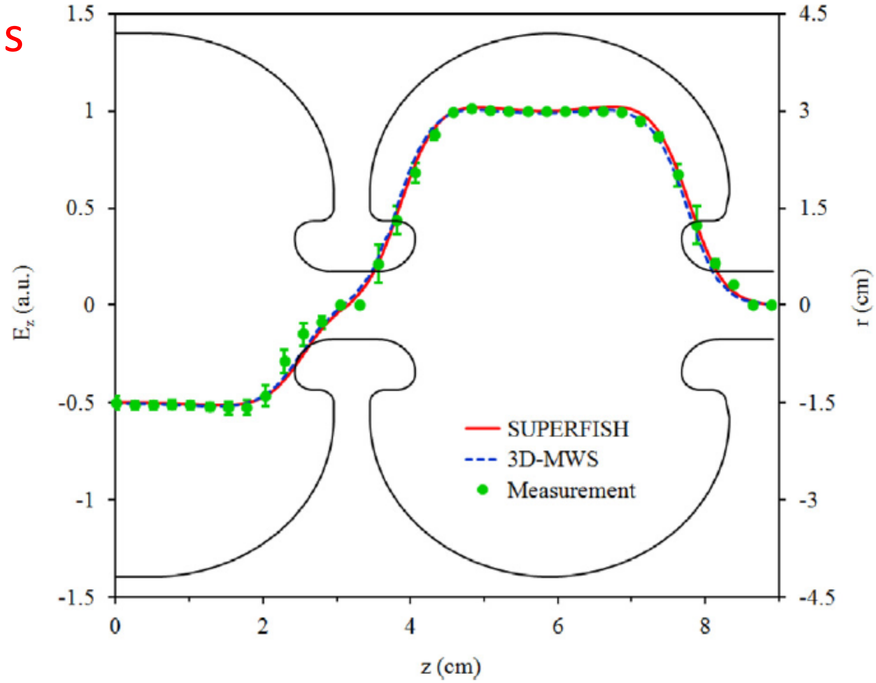

Longitudinal particle distributions

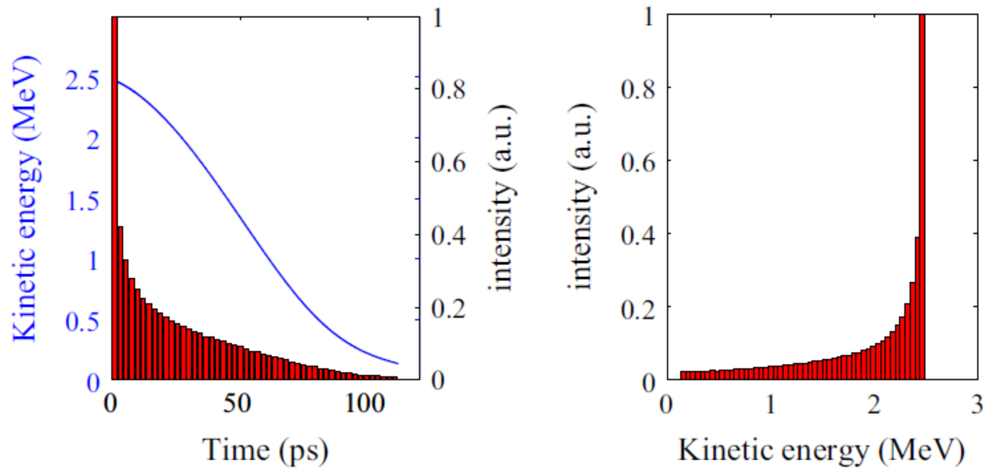

Rotation of Side-coupling Cavity Plane

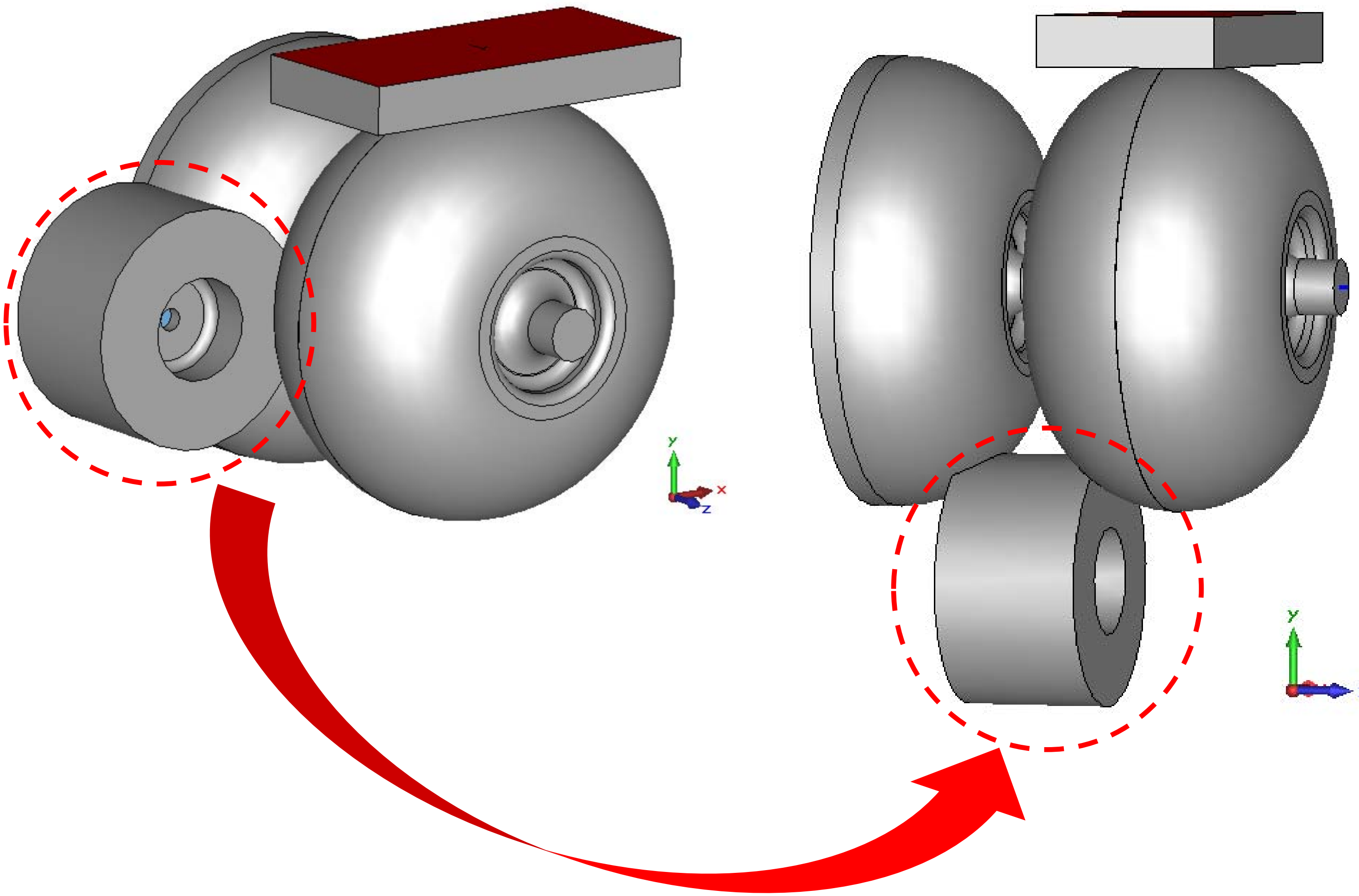

Rotate side-coupling cavity from
horizontal coupling to be vertical coupling

Vertical On-axis Side-coupling Cavity RF-gun (1)

yz-plane

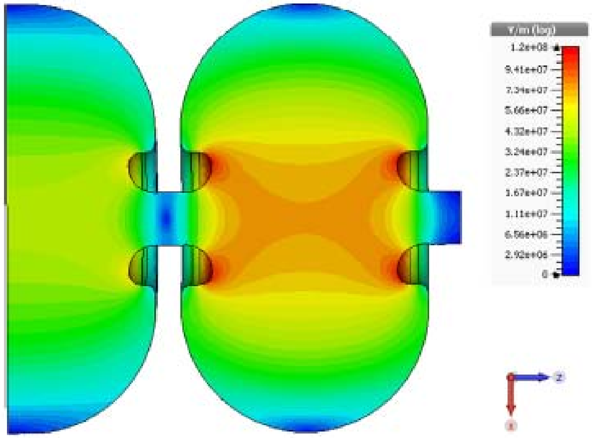

Parameter	Value
Resonant frequency in π/2-mode ($f_{\pi/2}$)	2855.8 MHz
Unloaded quality factor (Q_o)	15,271
Loaded quality factor (Q_l)	2053
External quality factor (Q_{ext})	2372
RF-coupling coefficient (β_{rf})	6.44
Peak electric field ratio (E_{p2}/E_{p1})	2.00
Average electric field ration (E_2/E_1)	1.72

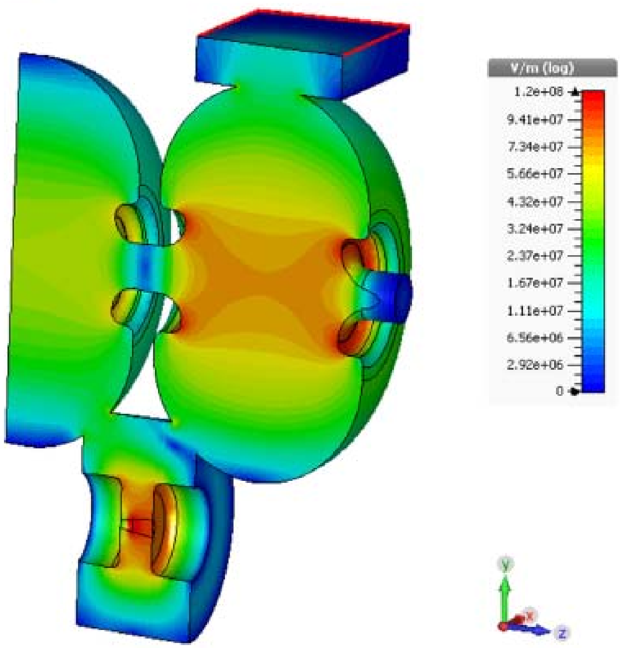

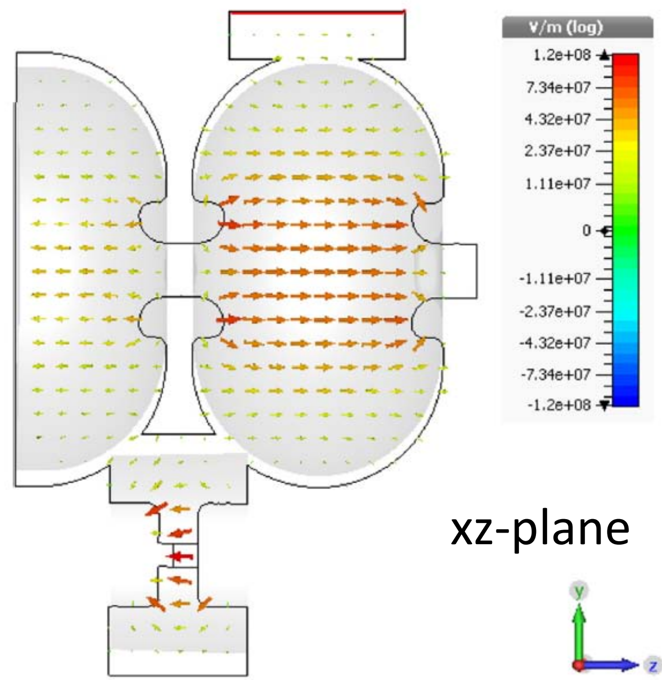

xz-plane

Vertical On-axis Side-coupling Cavity RF-gun (2)

Magnetic field distributions in xy-plane @ z = 0, 20, 41, 58 mm

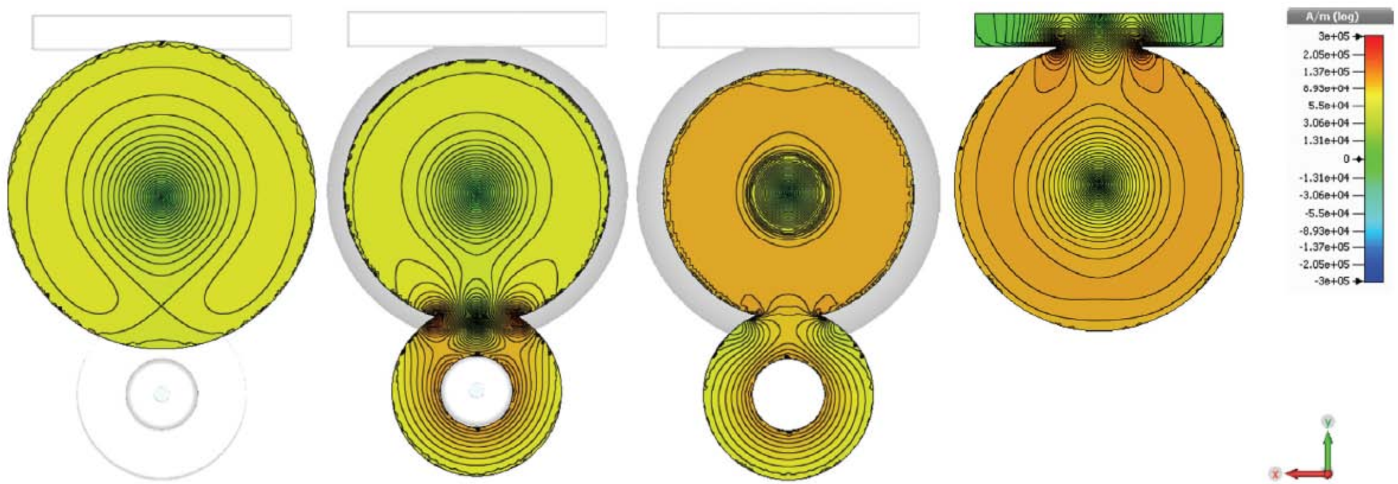

gun exit (emit. Increases 0.9%)

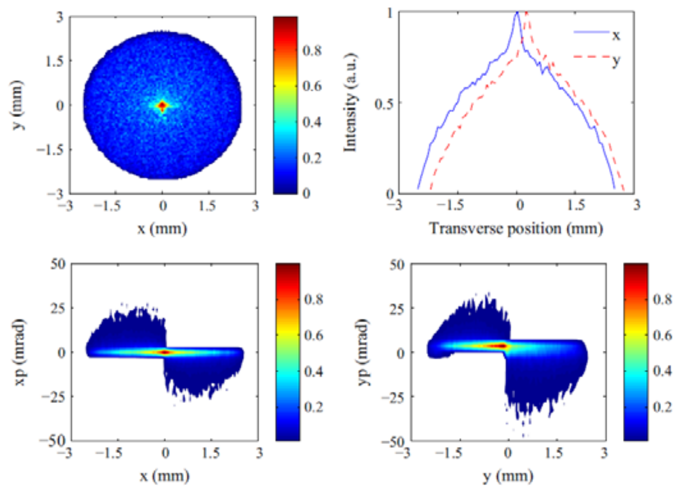

5 cm after gun exit (emit. Increases 0.7%)

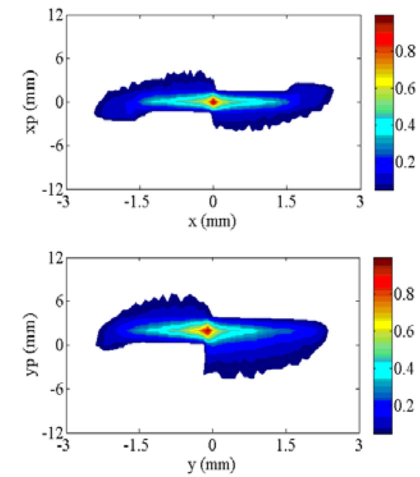

Improvement of Transverse Phase Space Distribution

Parameter	SUPERFISH	H-coupling	V-coupling	Unit
E_{p2}/E_{p1}	2.00	1.98	2.01	
$\langle E_2 \rangle / \langle E_1 \rangle$	1.73	1.69	1.72	
$\langle E_1 \rangle$	25.91	25.91	25.91	MV/m
$\langle E_2 \rangle$	44.82	43.78	44.56	MV/m
E @ cathode	31.91	31.80	31.41	MV/m
Max. kinetic energy	2.53	2.49	2.51	MeV
Mean kinetic energy	1.96	0.94	1.96	MeV
X-centroid position	0.028	0.846	0.027	mm
Y-centroid position	-0.032	-0.575	0.250	mm
Xrms beam size	1.145	1.154	1.163	mm
Yrms beam size	1.146	1.183	1.118	mm
X-emittance @ gun exit	16.25	17.79	15.80	mm-mrad
Y-emittance @ gun exit	16.25	18.21	17.22	mm-mrad
X-emittance @ 5 cm	10.89	12.07	10.25	mm-mrad
Y-emittance @ 5 cm	10.82	12.68	11.33	mm-mrad

Lecture No. 2

- **Design and Construction of RF Gun**
  - Principle, design and simulation of RF gun
  - **Fabrication of RF gun**
- **Low Power Tests and Tuning of RF Gun**
  - Low power RF measurements
  - Tuning of RF gun
- **RF Power Source and High Power Tests**
  - Introduction to RF source, transmission and coupling system required for RF gun
  - High power tests and conditioning of RF gun
- **High Power Tests and Commissioning of RF Gun**
  - Conditioning of RF gun
  - Cathode preparation

Materials

- Normal conducting RF cavities are typically made of Oxygen Free High Conductivity copper (OFHC copper) due to its strength, hardness, high conductivity.
- **Connections, flanges and vacuum components**
  - Stainless steel
  - Copper plating of stainless steel (for area where contact to the RF field)
- Superconducting RF cavities are made of Niobium

Table 1: Some characteristics of metals

	el. cond.	density	yield strength (R_p 0.2 %)	tensile strength	Brinell hardness	melting temperature
	MS m^{-1}	g/cm^3	MPa	MPa		°C
Ag	62.6	10.5	30	130…160	15…36	960.5
Cu soft	59	8.94	100…150	200 … 250	40 … 50	1083
Cu hard	55		300…450	400 … 490	80 … 120	
Cu-OFS	58	8.92	70…360	220…450	50…100	1083
CuZr	53.8	8.89	42…500	200…530		980
Cu-Al_2O_3	49.3	8.8	410…560	480…580		1080
Au	45.4	19.29		100…300	13…75	1063
Al	38	2.7	25…200	70…250	15 … 70	658
Mo	20.8	10.2	400	700…1200	150	2630
W	18.2	19.3	1500	400…4000	250	3380
Pd	9.8	11.97		200…400	40…100	1552
Nb	6.6	8.57		500	120	2477
SS 316LN	1.1	7.9	300	600	180	1350

E. Jensen, Fabrication and Testing of RF Structures, Physics and Technology of Linear Accelerator Systems, Proceedings of JAS 2002.

Machining

There are several techniques for machining the RF gun and its components.

→ To choose the technique, one should consider required surface properties, e.g. tolerance, surface finish, contamination from other materials.

Table 3: Surface roughness obtained with different machining operations.

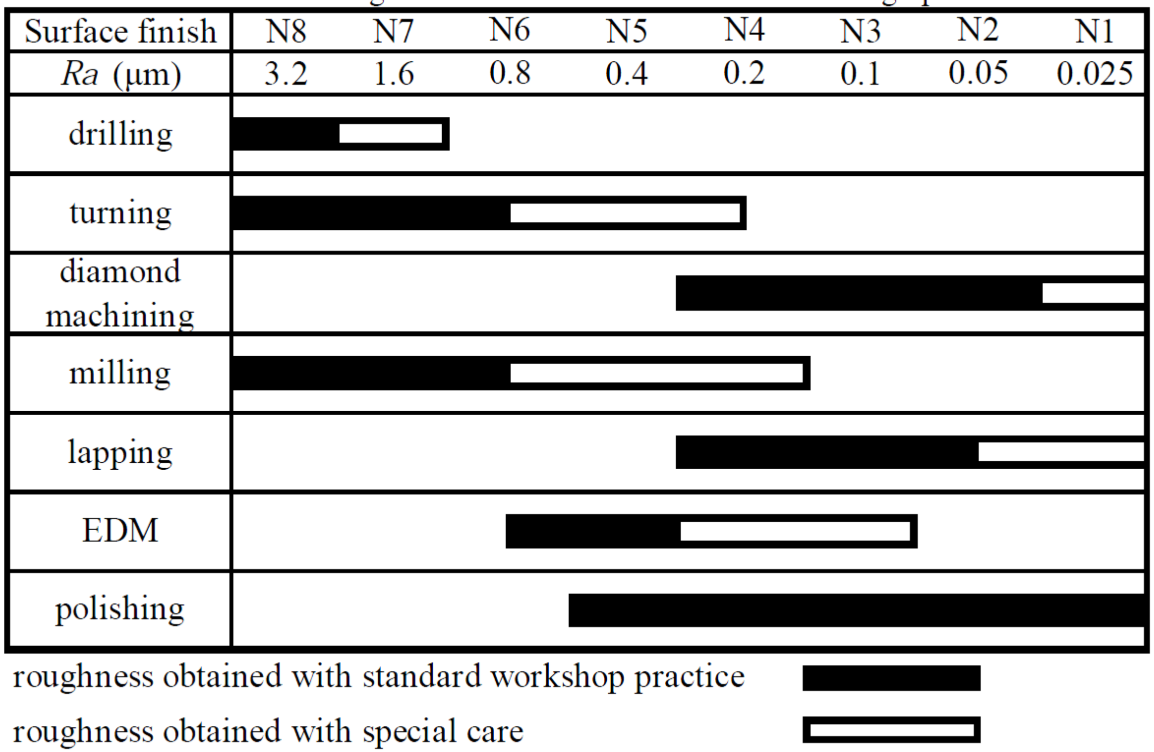

EDM (electric discharge machining)

Rule of thumb:
Ra should not exceed a quarter of the skin-depth.

E. Jensen, Fabrication and Testing of RF Structures, Physics and Technology of Linear Accelerator Systems, Proceedings of JAS 2002.

Joining Techniques

- TIG (tungsten inert gas) welding is characterized by the use of an inert gas (Ar) flow to shield the heated area around the joint from the oxidizing atmosphere.
- EBW (electron-beam welding) uses a finely (sub mm) focused electron beam to vaporize the work-piece near the joint to be.
- Diffusion bond is created between smooth surfaces .
- Vacuum brazing is the preferred brazing technique.
  - Different brazing alloys behave differently when becoming liquid.

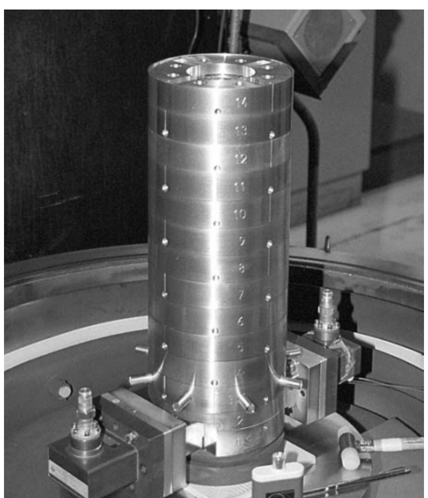

Cells of an S-band structure being stacked inside a vacuum brazing furnace.

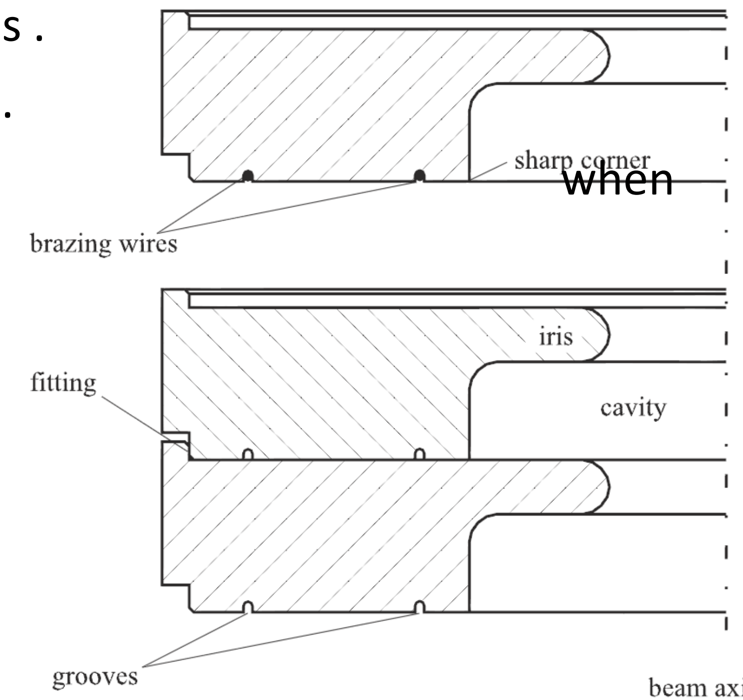

E. Jensen, Fabrication and Testing of RF Structures, Physics and Technology of Linear Accelerator Systems, Proceedings of JAS 2002.

Example: Fabrication of CMU RF-gun

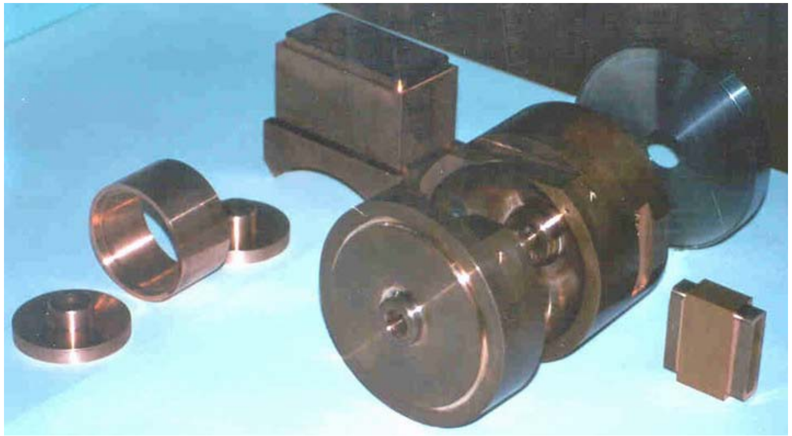

Cavities and related components fabrication

- Oxygen Free High Conductivity copper (OFHC copper)
- CNC machining

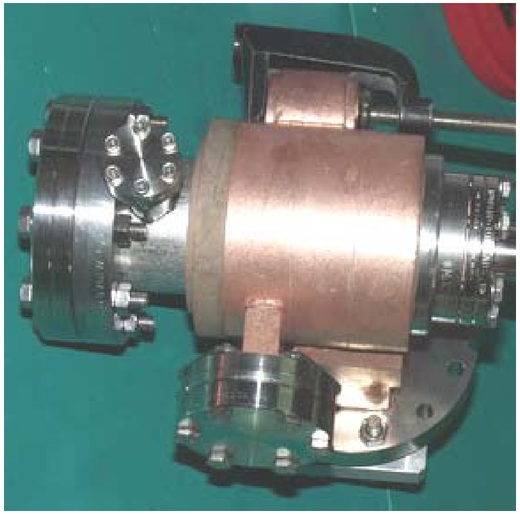

RF-gun forming

- Welding (SST components)
- High temperature brazing in free-O_2 environments

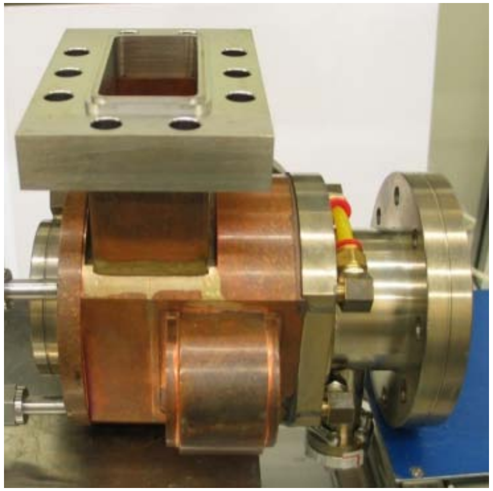

completed RF gun

Lecture No. 2

- **Design and Construction of RF Gun**
  - Principle, design and simulation of RF gun
  - Fabrication of RF gun
- **Low Power Tests and Tuning of RF Gun**
  - Low power RF measurements
  - Tuning of RF gun
- **RF Power Source and High Power Tests**
  - Introduction to RF source, transmission and coupling system required for RF gun
  - High power tests and conditioning of RF gun
- **High Power Tests and Commissioning of RF Gun**
  - Conditioning of RF gun
  - Cathode preparation

RF Frequency Measurements

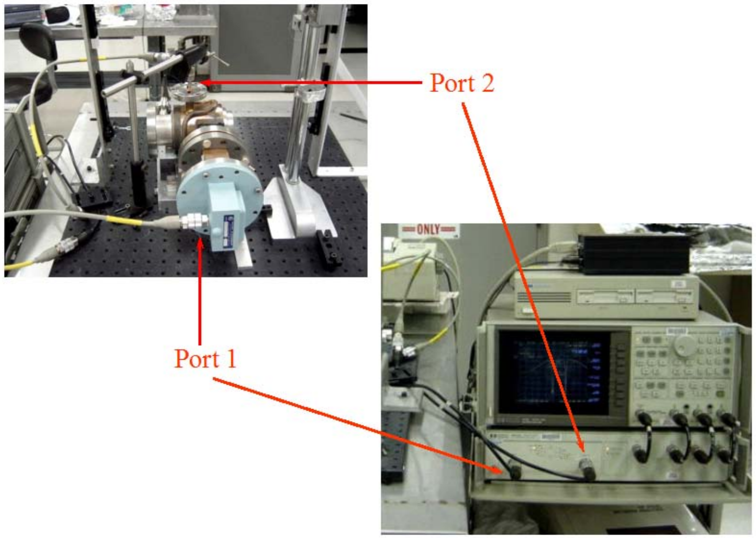

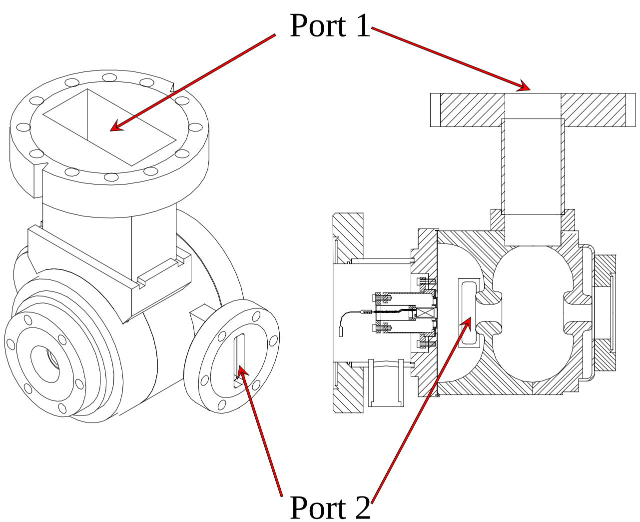

RF-measurements

- Before and after the RF-gun brazing process
- Using network analyzer
- Input RF-power level = 1 dB (10 mW)
- RF-power input port → waveguide at FC
- Output pick up port → vacuum port at HC

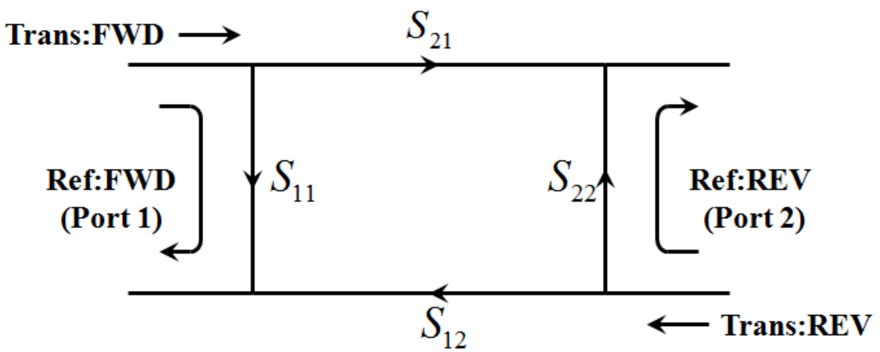

Parameter	Value
f_{rf} of HC/FC (MHz)	2854.6 / 2858.3
f_{rf} of whole gun (MHz)	2855.3

RF Measurements Using Smith Chart

Identification of the half-power points from the Smith Chart representation showing seven frequencies (f_0; f_1; f_2; f_3; f_4; f_5 and f_6). Q_0 locus is given by $x = r$, Q_L by $x = r \pm 1$ and Q_{ext} by $x = \pm 1$

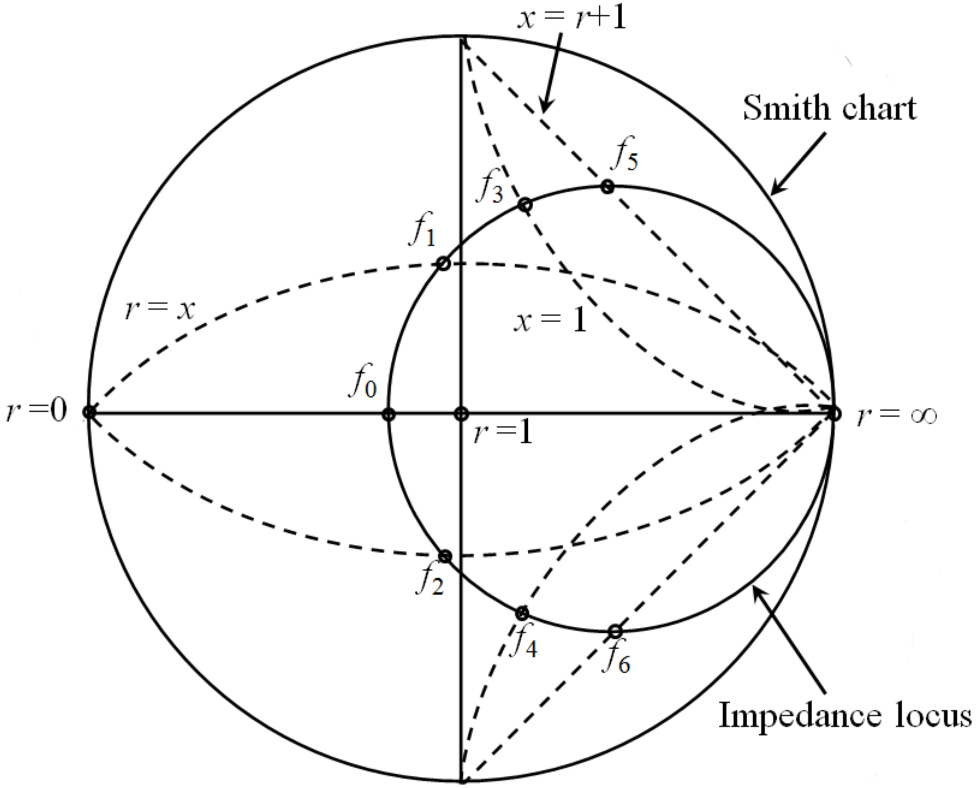

The quality factors are

$$Q_0 = \frac{f_0}{f_1 - f_2}, \quad Q_{ext} = \frac{f_0}{f_3 - f_4}, \quad Q_L = \frac{f_0}{f_5 - f_6}$$

The RF coupling coefficient can be calculated from

$$\beta_{rf} = \frac{Q_0}{Q_{ext}}$$

Results of RF Measurements Using Smith Chart

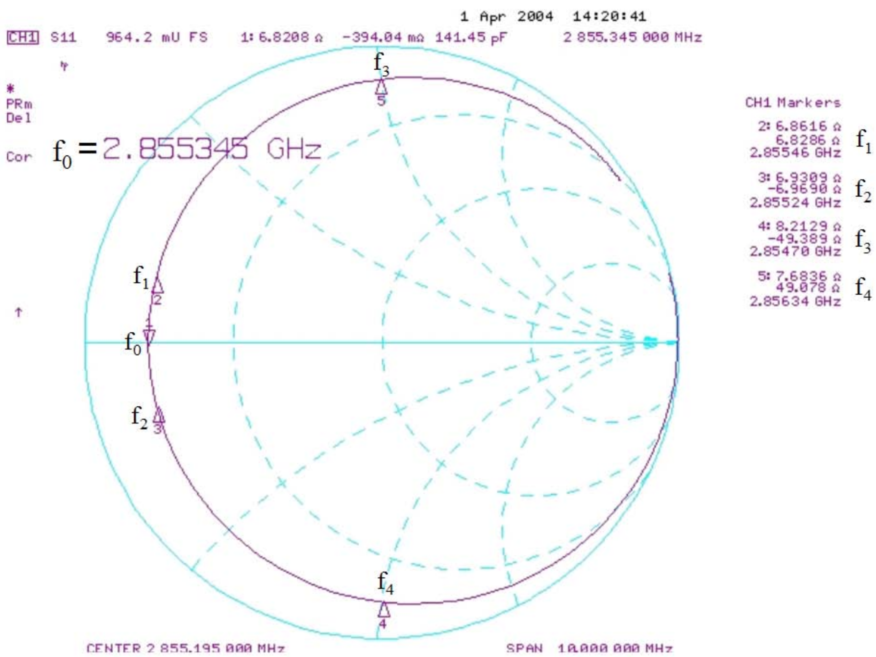

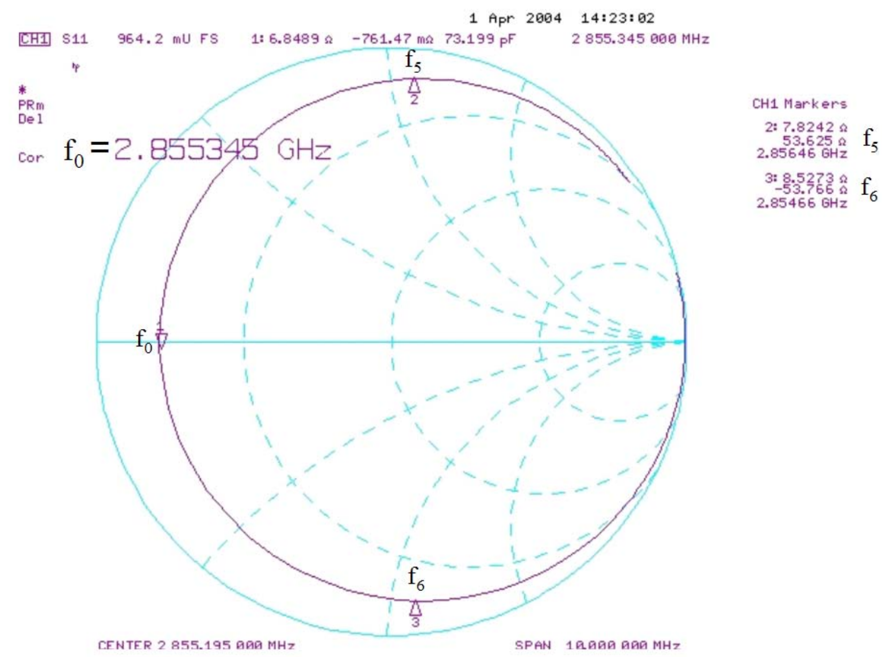

$$Q_0 = \frac{f_0}{f_1 - f_2}, \quad Q_{ext} = \frac{f_0}{f_3 - f_4}, \quad Q_L = \frac{f_0}{f_5 - f_6}$$

$$\beta_{rf} = \frac{Q_0}{Q_{ext}}$$

Unloaded quality factor (Q_o)	12,979
Loaded quality factor (Q_l)	1586
External quality factor (Q_{ext})	1741
RF-coupling coefficient (β_{rf})	7.3

On-axis Field Profile Measurements

Schematic diagram of the bead-pull set-up.

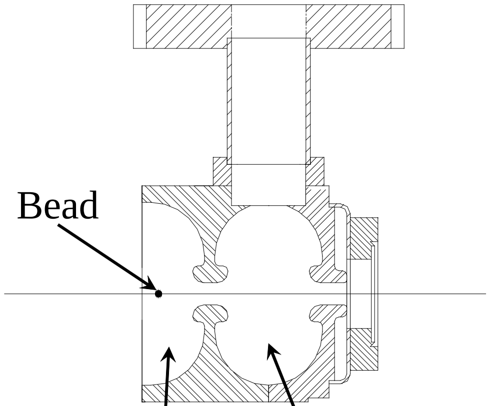

Slater's Perturbation $\frac{\Delta\omega}{\omega} = \frac{\Delta U_M - \Delta U_E}{U} = \frac{\int_{\Delta V} (\mu H^2 - \varepsilon E^2) dV}{\int_V (\mu H^2 + \varepsilon E^2) dV}$

Bead-pull measurement

- 2.36 mm diameter dielectric bead
- Resonant frequency shift $E_z \; \alpha \; \sqrt{\Delta\omega} = \sqrt{f - f_0}$

On-axis Field Profile Measurements

Measured on-axis electric field distribution inside the RF-gun.

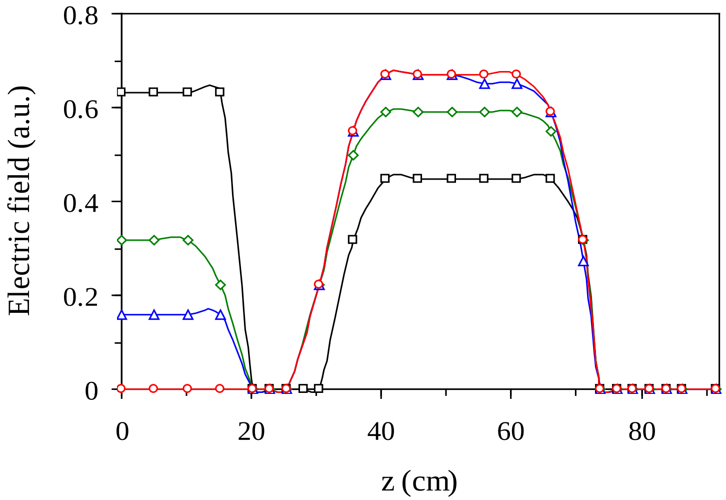

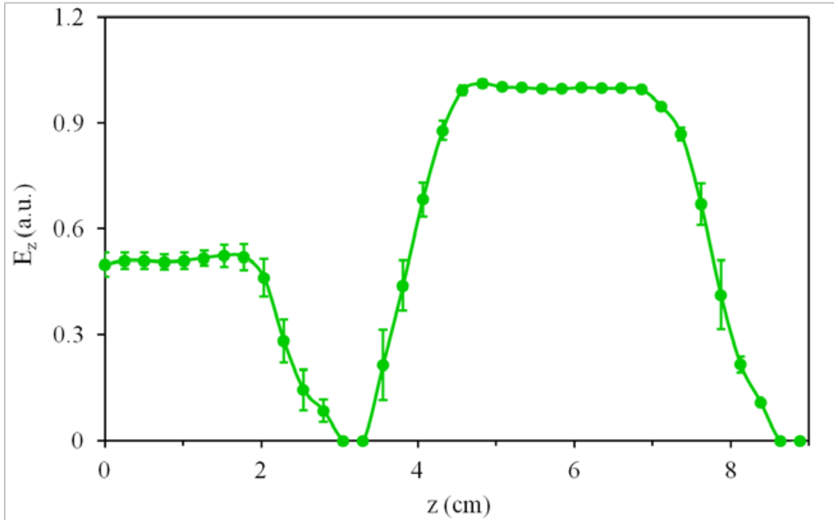

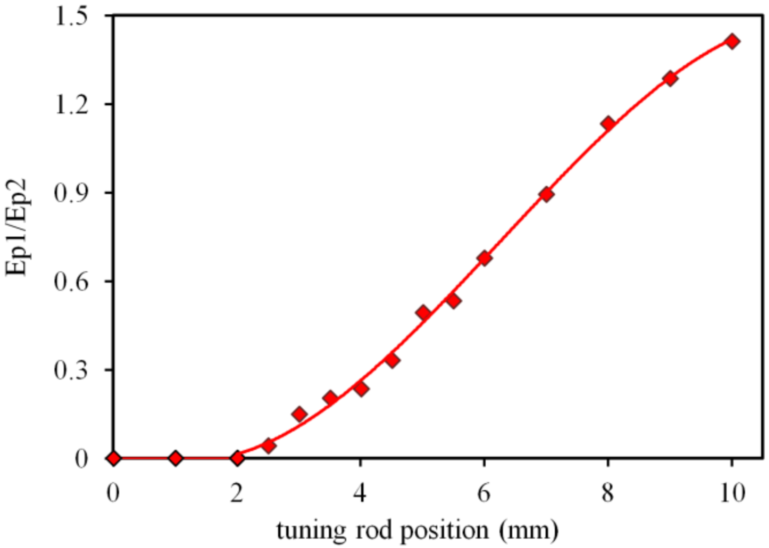

$$\frac{E_{p2}}{E_{p1}} = 2.00 \qquad \frac{E_{ave,2}}{E_{ave,1}} = 1.73$$

Measured field ratio vs. the tuning rod position.

Summary of RF Parameters of RF Gun

Measured RF-parameters of the RF-gun in π/2 operation mode obtained from the low-power RF-measurements. The measurements were performed at the room temperature of 25 °C and in ambient air.

Parameter	Value
Resonant frequency in π/2- mode ($f_{\pi/2}$)	2855.3 MHz
Frequency separation between π/2 and π modes	7.9 MHz
Unloaded quality factor (Q_o)	12,979
Loaded quality factor (Q_l)	1586
External quality factor (Q_{ext})	1741
RF-coupling coefficient (β_{rf})	7.3
Peak field ratio (E_{p2}/E_{p1})	2.00
Average field ratio (E_2/E_1)	1.73

S. Rimjaem et al., Nuc. Instr. and Meth. A 736 (2014) 10-21.

Lecture No. 2

- **Design and Construction of RF Gun**
  - Principle, design and simulation of RF gun
  - Fabrication of RF gun
- **Low Power Tests and Tuning of RF Gun**
  - Low power RF measurements
  - Tuning of RF gun
- **RF Power Source and High Power Tests**
  - Introduction to RF source, transmission and coupling system required for RF gun
  - High power tests and conditioning of RF gun
- **Commissioning of RF Gun**
  - Conditioning of RF gun
  - Cathode preparation

RF System for CMU RF Gun

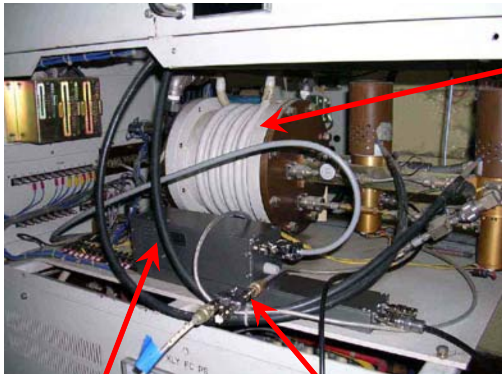

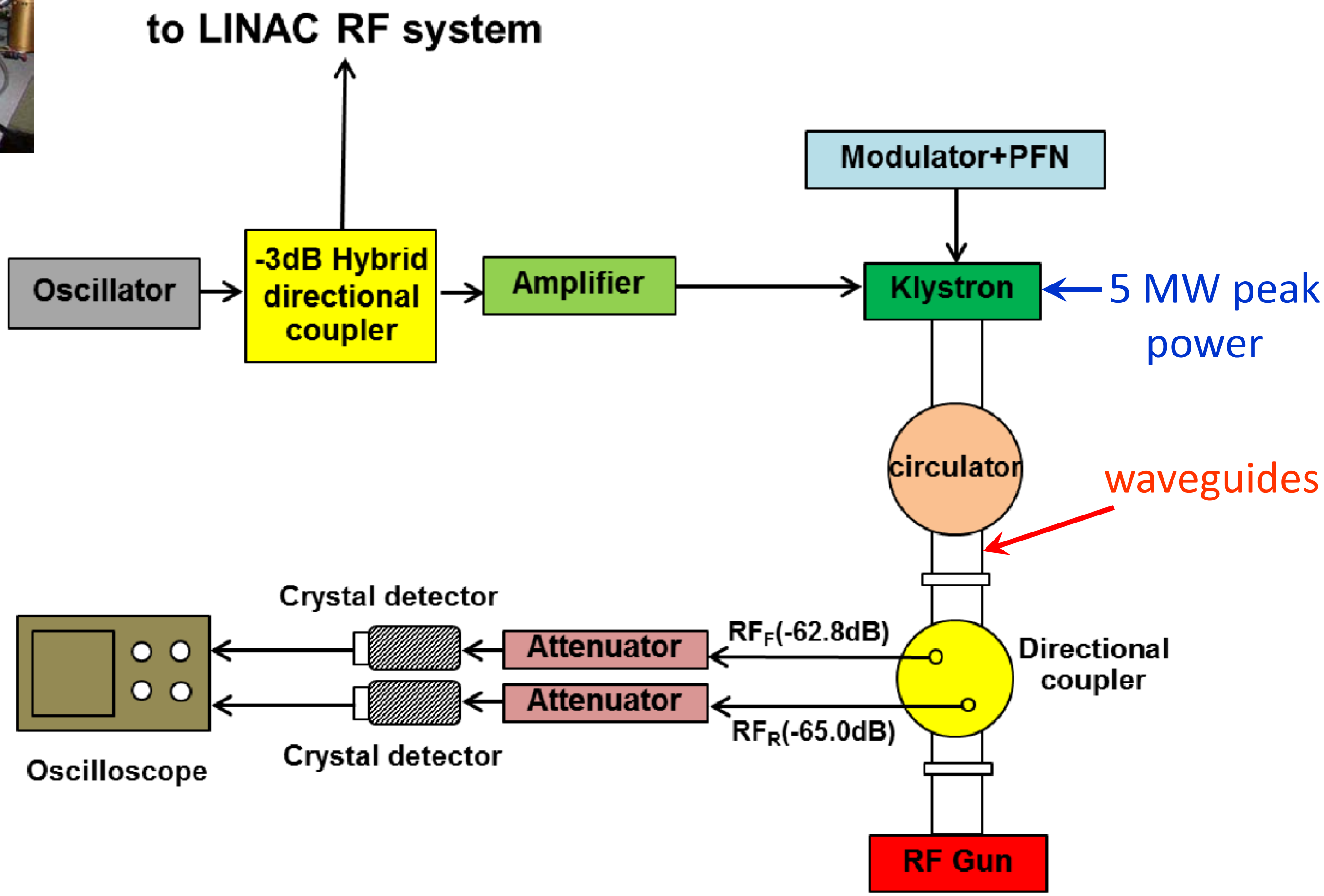

High Power RF Source

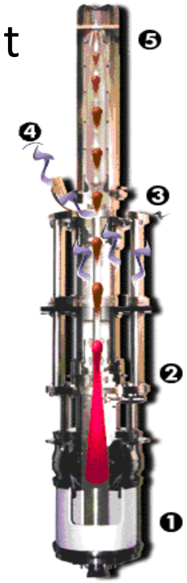

www2.slac.stanford.edu/vvc/accelerators/klystron.html

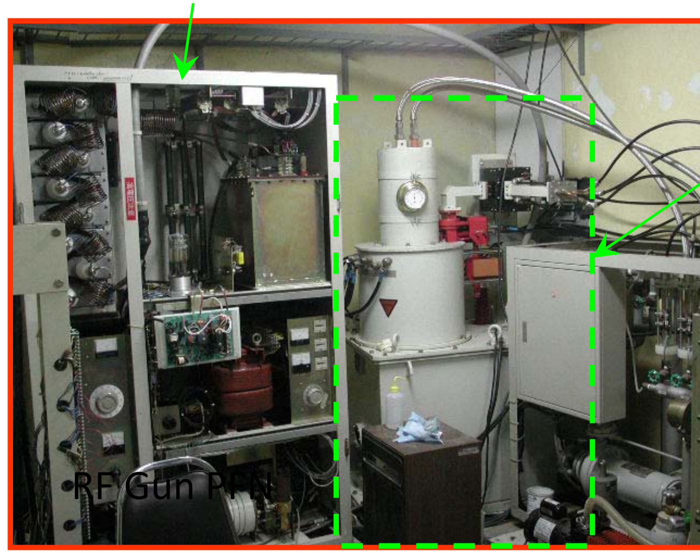

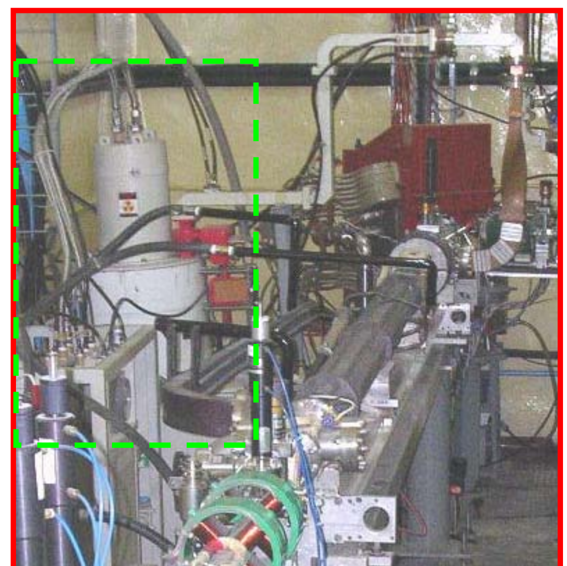

High Power RF Tests

RF-gun Temperature and Thermal expansion

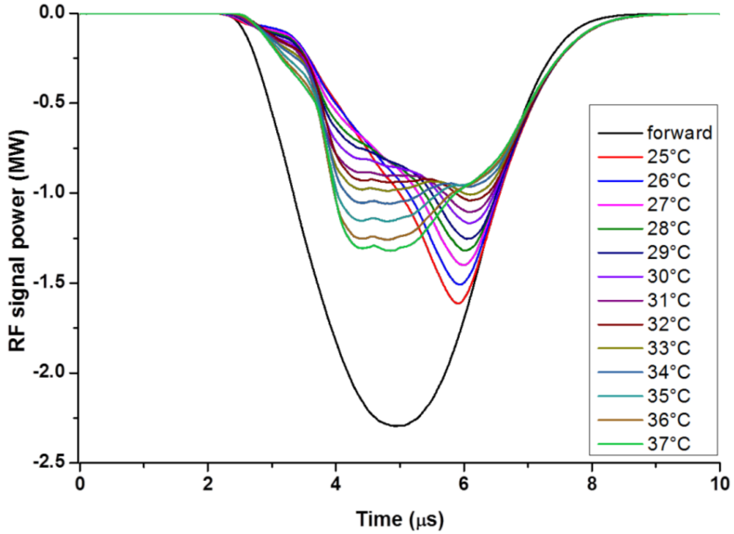

RF power signal vs. time at different gun temperatures.

Directional coupler
Crystal Detector

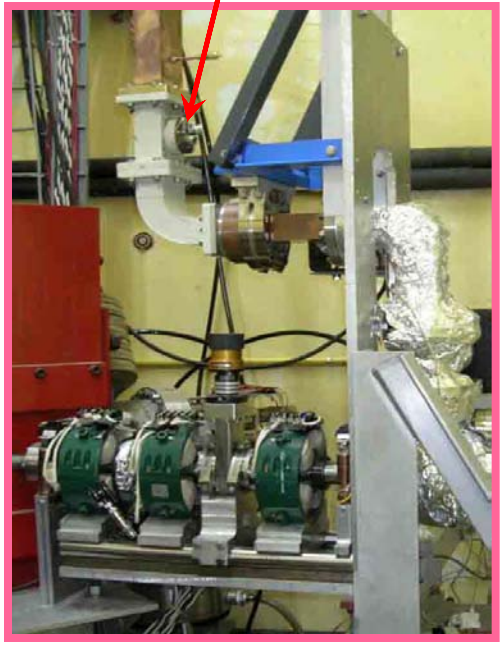

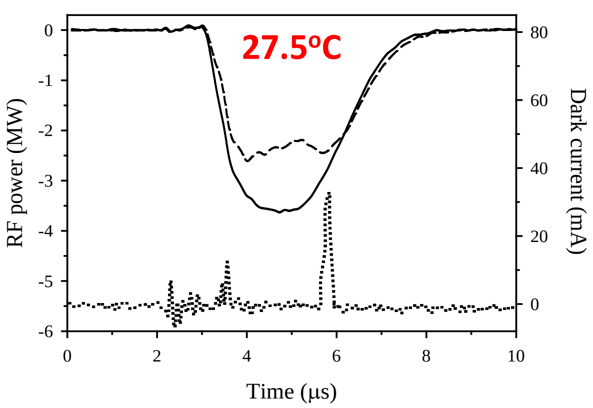

Cavity absorption power ~ 1.46 MW

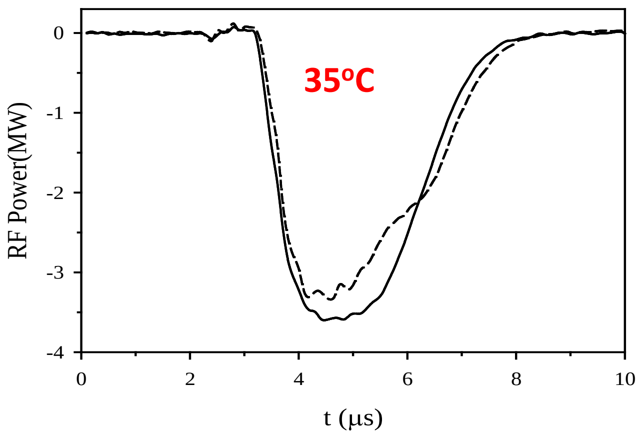

Frequency de-tuned of 362 kHz (small cavity absorption)

$$\frac{\Delta f}{\Delta T} \approx -\frac{2.405c}{2\pi a}\alpha$$

$$\approx -48.3\ kHz/^{o}C$$

RF Parameters of the CMU RF Gun

The RF-coupling coefficient (βrf) can be determined from the input (Pi) and reflected (Pr) power measurements in the steady state as

$$\beta_{rf} = \frac{1 \pm \sqrt{P_r/P_i}}{1 \mp \sqrt{P_r/P_i}}$$

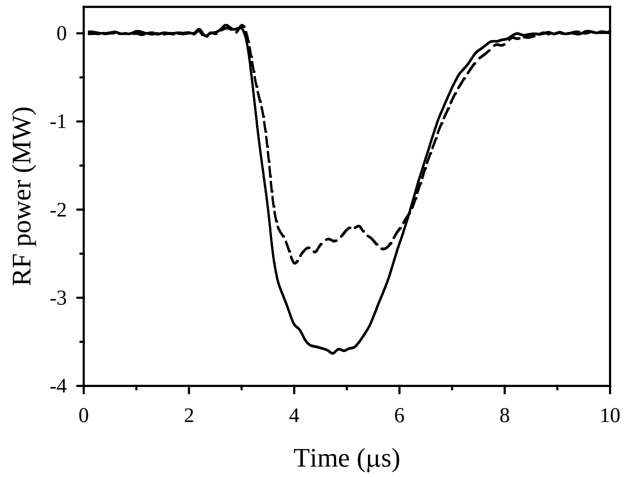

High-power RF parameters, typical operating condition and electron beam-loading parameters of the PBP-CMU RF-gun.

Parameter	Value	Unit
Resonant frequency in π/2-mode	2856	MHz
Operating temperature	27.5	°C
Input RF peak power	3.55	MW
Dissipation RF power	1.36	MW
External RF-coupling coefficient	8.3	

S. Rimjaem et al., Nuc. Instr. and Meth. A 736 (2014) 10-21.

End of Lecture No. 2

Questions
&
Discussion

Lecture Outline

Lecture No. 1

- Electron accelerators and sources
- Types of electron guns
- Benefits of RF electron guns

Lecture No. 2

- Design and construction of RF gun
- Low power tests and tuning of RF gun
- RF power source and high power tests

Lecture No. 3

- Operation of RF electron gun
- RF gun applications
- Generation and applications of ultra short electron bunches produced by RF gun

Lecture No. 3

- **Operation of RF Electron Gun**
  - Cathode preparation
  - Operation conditions
  - Measurements of electron beam properties
- **RF Gun Applications**
  - Electron sources for high energy physics accelerator
  - Electron sources for direct applications
  - Electron sources for light sources
- **Generation and Applications of Ultra Short Electron Bunches Produced by RF Gun**
  - Generation and applications of ultra short electron bunches at Chiang Mai University

Thermionic Cathode Preparation

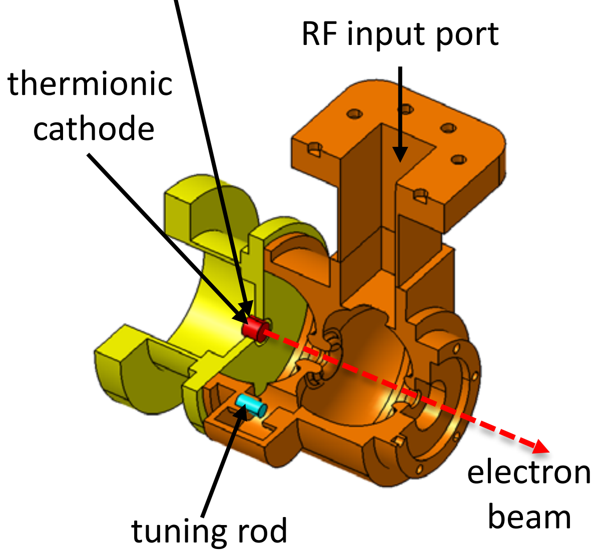

Thermionic cathode

- Dispenser tungsten cathode coated with barium oxide
- Flat circular emitting surface of 3 mm radius

Cathode Tests

Cathode tests (Pyrometric measurements)

- To activate the cathode to temperature > 1050 °C
- Measure the cathode temperature by using an optical Pyrometer
- Required for new cathode or when cathode experiences poor vacuum or chemical contamination.

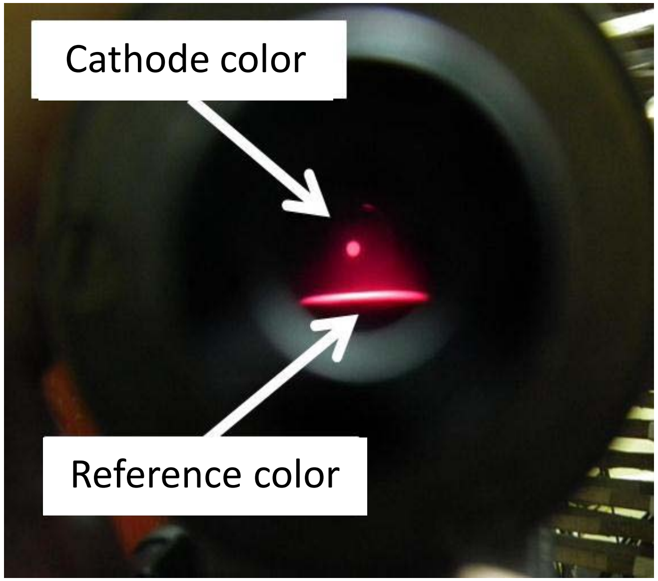

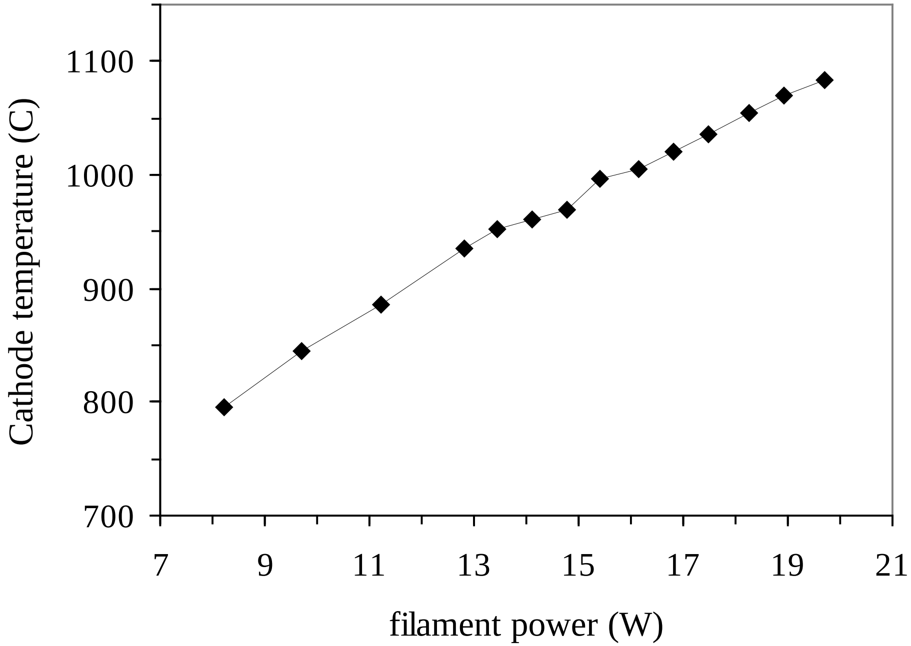

Operating temperature ~900-1000°C
(cathode heating power ~ 13-17 W)

Lecture No. 3

- **Operation of RF Electron Gun**
  - Cathode preparation
  - Operation conditions
  - Measurements of electron beam properties
- **RF Gun Applications**
  - Electron sources for high energy physics accelerator
  - Electron sources for direct applications
  - Electron sources for light sources
- **Generation and Applications of Ultra Short Electron Bunches Produced by RF Gun**
  - Generation and applications of ultra short electron bunches at Chiang Mai University

Beam Energy Measurements (RF Gun)

Using energy slit inside alpha magnet vacuum chamber: E_{max}=2-2.4 MeV

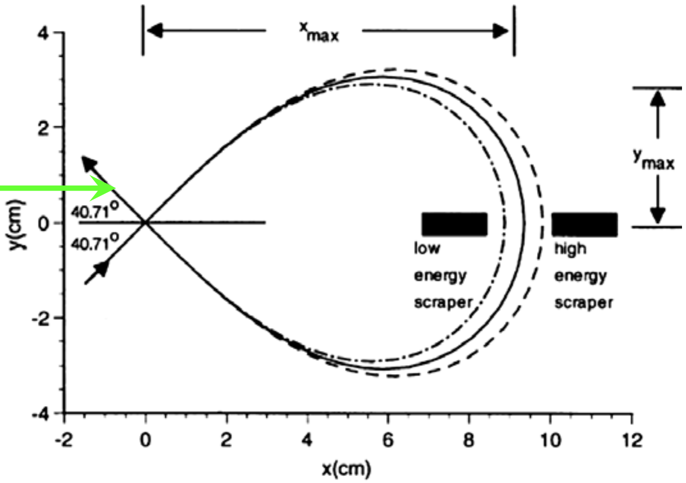

$$x_{max} = 75.05\sqrt{\frac{cp}{mc^2 g}}$$

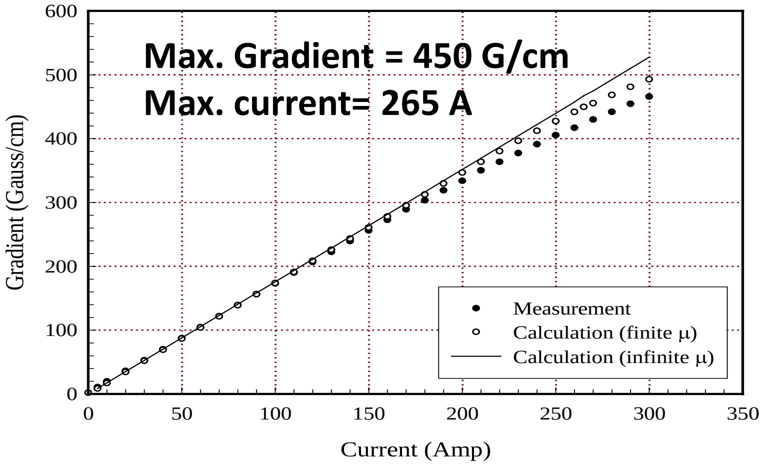

Energy Measurements (Linac)

Dipole magnet is used as electron beam dump + energy spectrometer.

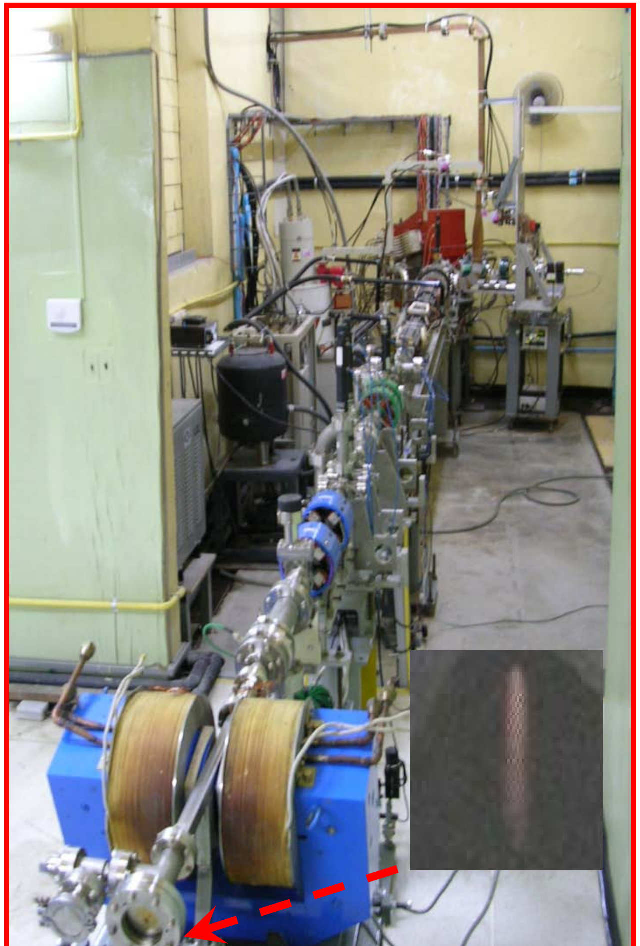

10-15 MeV electron beam

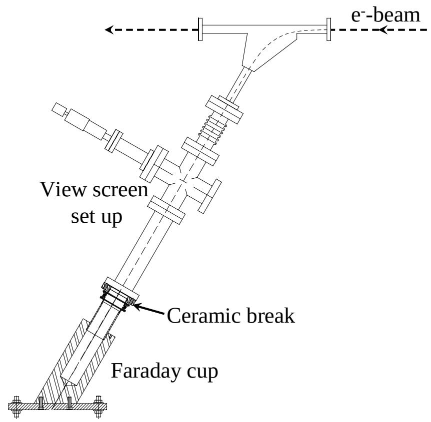

Deflect electron beam 60° respect to beam axis

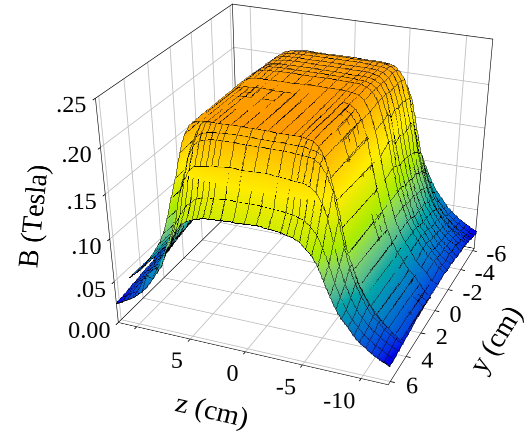

Actual 3D-field distribution of dipole magnet

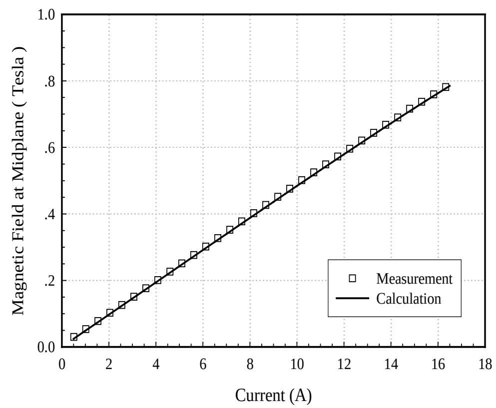

B~0.8 Tesla at current of 16 A

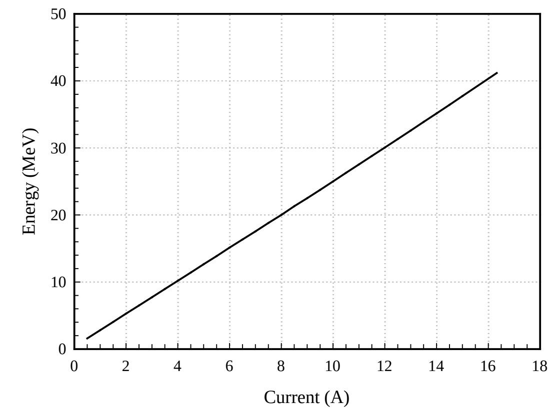

$$E(GeV) = \frac{0.2998 \int B_y dz}{\beta \alpha}$$

Beam Current and Beam Power

Current Monitor

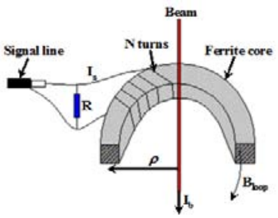

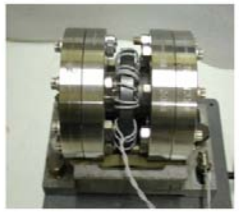

Schematic model of current transformer

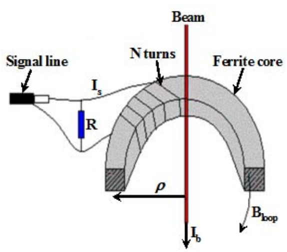

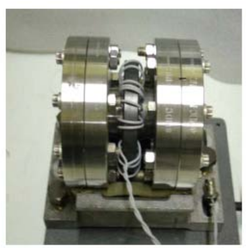

Actual current transformer

$$I_b = N_s I_s = \frac{N_s}{R} V_s = \frac{8}{50} V_s = 0.16\, V_s$$

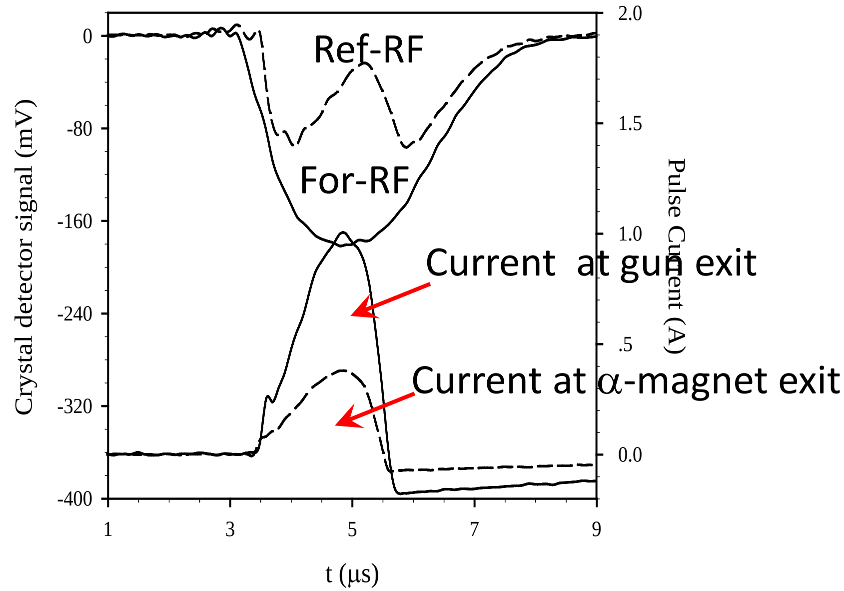

Peak current of ~ 1 A at ~2 MeV from RF-gun

- Beam power P_b~I_b×E_{kin} = 2 MW
- Cavity wall losses P_{cy} ~ 1.46 MW
- P_{cy}+P_b = 3.46 MW

Peak current of 0.4-0.5 A at α- magnet exit (50-60% is filtered out by the energy slits).

Beam Profile Measurements

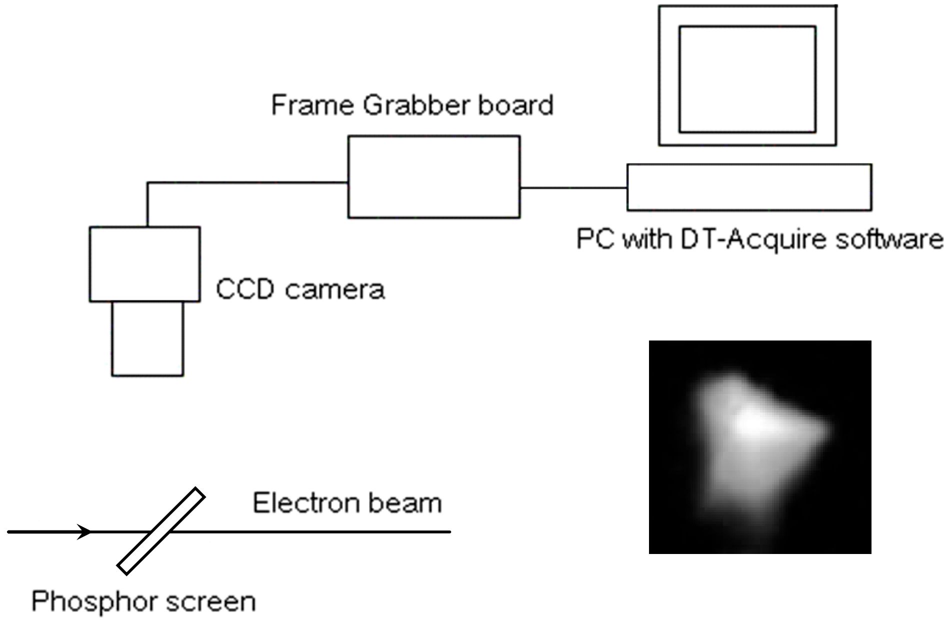

Schematic layout of beam profile measurement setup and a 2.4 MeV electron beam image (SC2)

- -Phosphor screen (Gd_2O_2:Tb deposited on Al-plate)
- -CCD camera
- -Frame grabber broad (DT3315 Data-Translation)
- -PC with DT-Acquire software

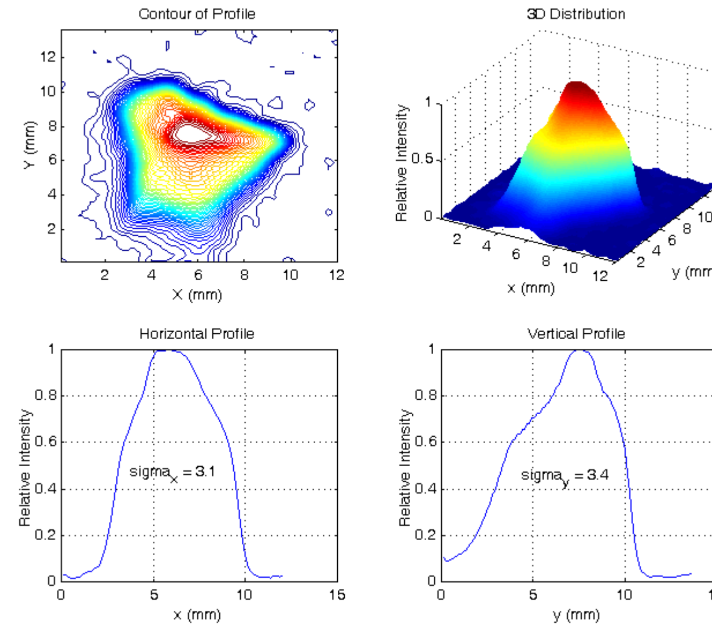

Relative intensity distribution of electron beam in 2D and 3D and the horizontal and vertical beam profiles

(MATLAB code BAP, S. Chumphongphan)

Operation Conditions & Beam Measurements

High-power RF parameters, typical operating condition and electron beam-loading parameters of the PBP-CMU RF-gun.

Parameter	Value	Unit
Resonant frequency in $\pi/2$-mode	2856	MHz
Operating temperature	27.5	°C
Input RF peak power	3.55	MW
Dissipation RF power	1.36	MW
External RF-coupling coefficient	8.3	
Maximum kinetic energy	~2.5	MeV
Beam current	0.7–1	A
RF-pulse length (FWHM)	~2.8	μs
RF repetition rate	10	Hz
Beam-pulse length (FWHM)	1–2	μs
Charge per micro-bunch	~0.2-0.25	nC

Lecture No. 3

- **Operation of RF Electron Gun**
  - Cathode preparation
  - Operation conditions
  - Measurements of electron beam properties
- **RF Gun Applications**
  - Electron sources for high energy physics accelerator
  - Electron sources for direct applications
  - Electron sources for light sources
- **Generation and Applications of Ultra Short Electron Bunches Produced by RF Gun**
  - Generation and applications of ultra short electron bunches at Chiang Mai University

Electron Source for High Energy Physics Accelerator

Example: the International e^- - e^+ Linear Collider (ILC)

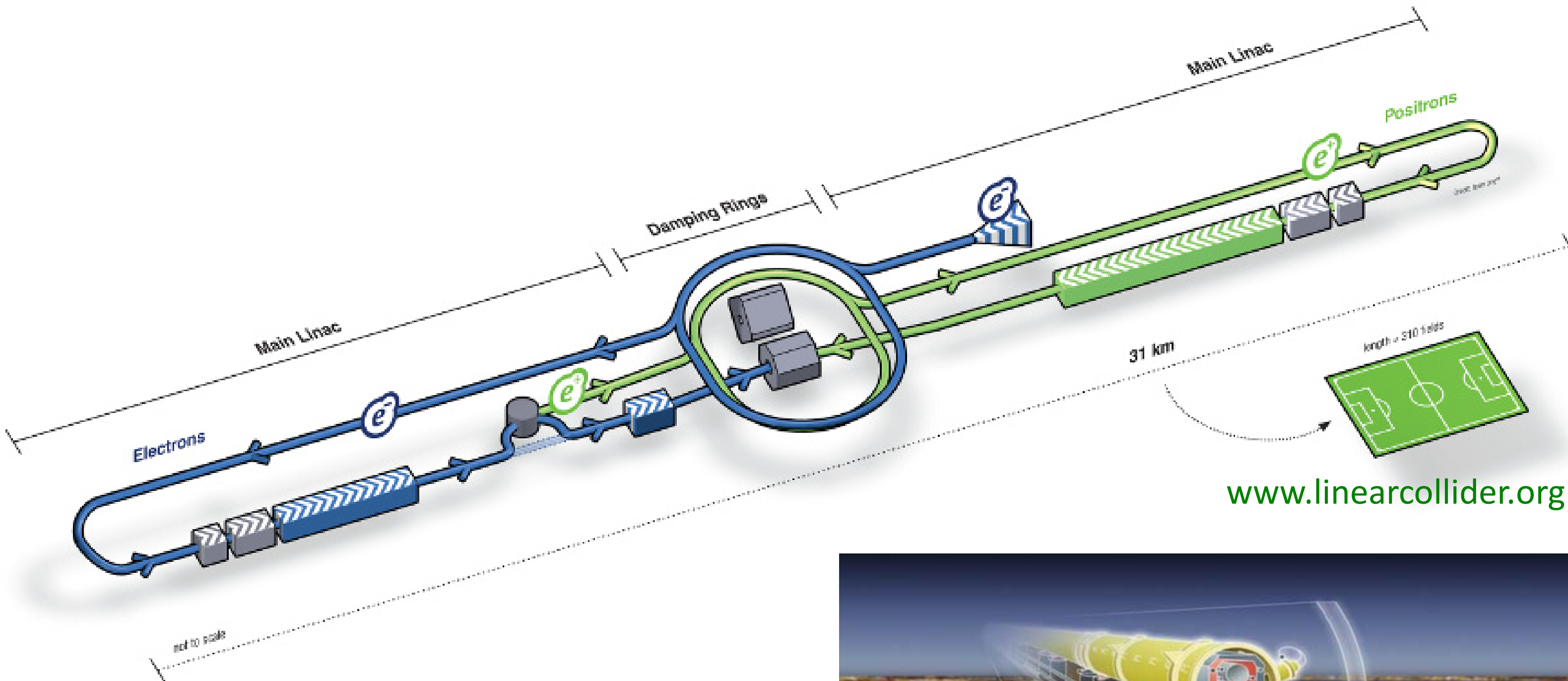

www.linearcollider.org

It is initially planned to have a collision energy of 500 GeV, with the possibility for a later upgrade to 1000 GeV (1 TeV).

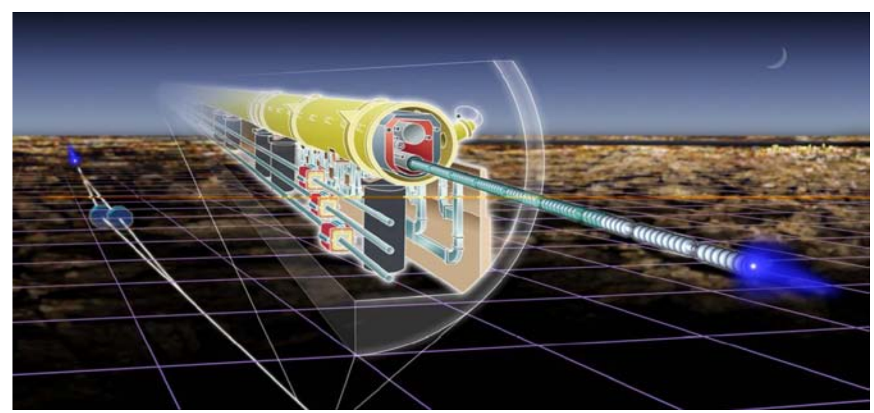

(A. Sessler and E. Wilson, Engines of Discovery: A Century of Particle Accelerators)

Electron sources for direct applications

Examples:

- Ultrafast time-resolved electron diffraction for studying dynamic of chemical reaction

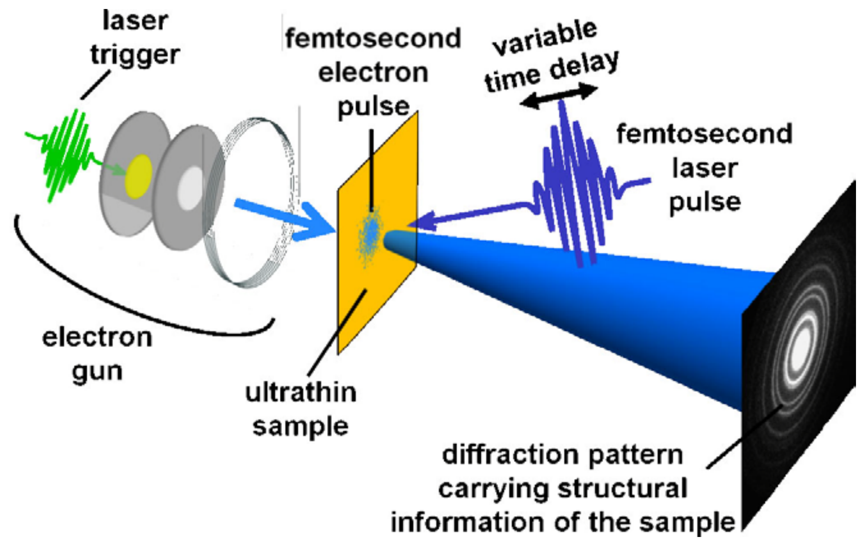

http://www.fhi-berlin.mpg.de/pc/PCres_methods.html

- Ultrafast electron pulse radiolysis

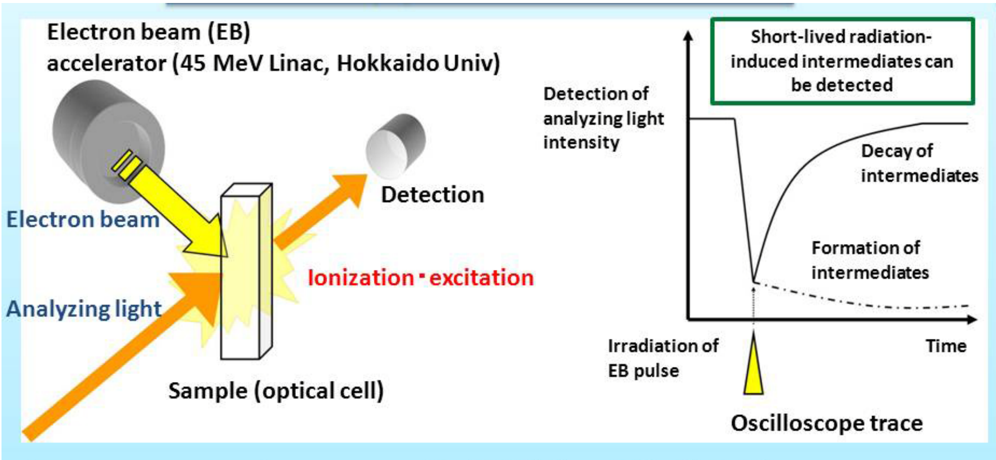

http://labs.eng.hokudai.ac.jp/labo/qsre/field/summary/semiconductor/

Electron source for light sources

Accelerating charges emit electromagnetic radiation

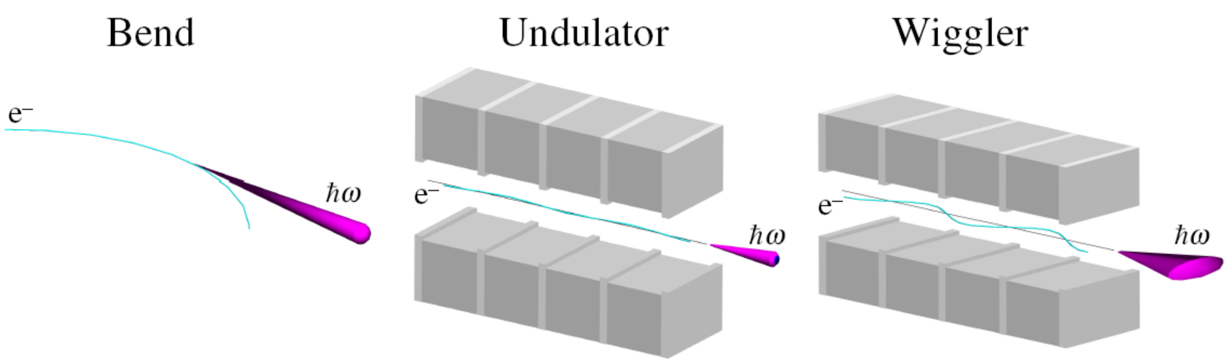

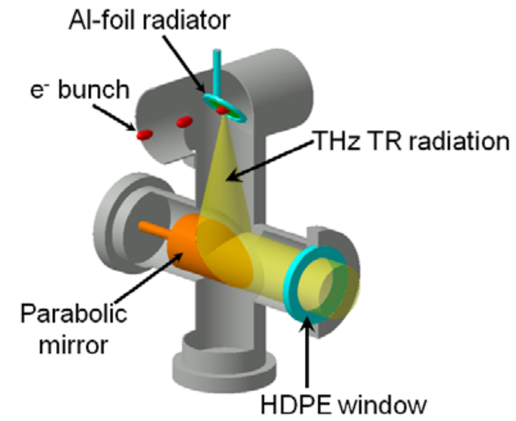

Radiation brightness

- In geometric optics, spectral brightness is defined as photon flux density in phase space about a certain frequency (number of photons per unit time per unit area per unit solid angle):

$$B = \frac{d^2 I}{dA d\Omega} = \frac{d^2 I}{dx dx' dy dy'} \propto \frac{2 I_p}{\varepsilon_x \varepsilon_y}$$

I - *electron beam current*
A - *transverse area*
Ω - *the divergence*
x, y – *transverse* coordinates
x', y' - indicate derivatives with respect to *z*

∴We need electron beams with small emittance and high peak current.

Synchrotron Light Sources

Thermionic DC guns
Thermionic RF guns

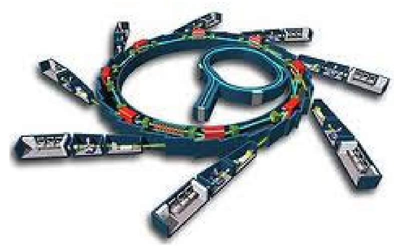

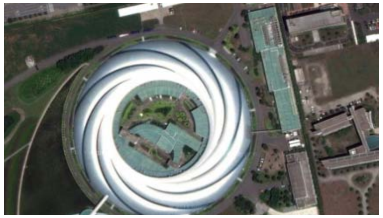

Shanghai light source (China)

Spring 8 (Japan)

Siam Photon (Thailand)

PETRAIII @ DESY (Germany)

Diamond (UK)

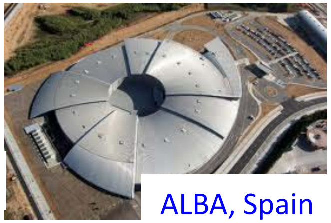

ALBA, Spain

ESRF, France

NSLS (USA)

APS (USA)

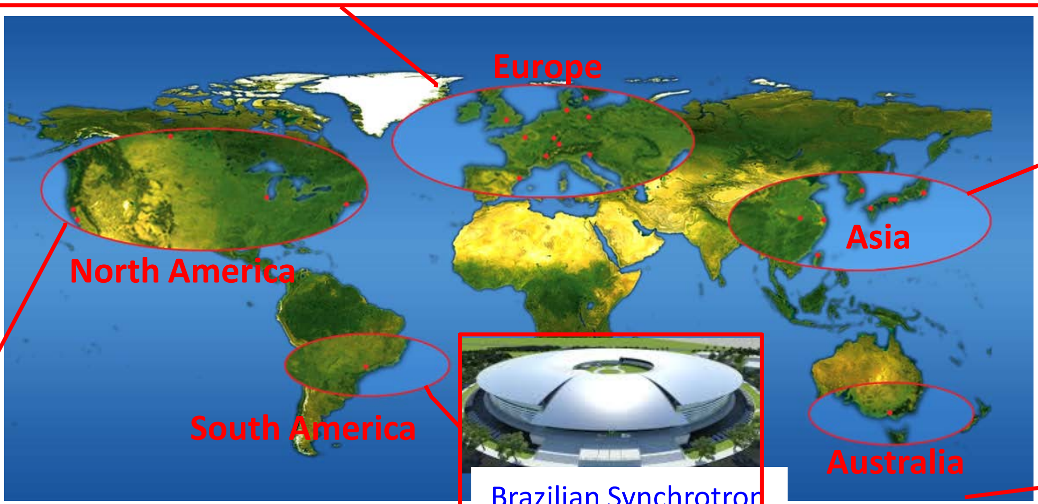

Brazilian Synchrotron

Australia light source (Australia)

Evaluation of Light Sources

- 1st Generation (1970s): Many HEP rings are parasitically used for X-ray production
- 2nd Generation (1980s): Many dedicated X-ray sources (light sources)
- 3rd Generation (1990s): Several rings with dedicated radiation devices (wigglers and undulators)
- 4th Generation (Present): Free Electron Lasers (FELs) driven by linear accelerators

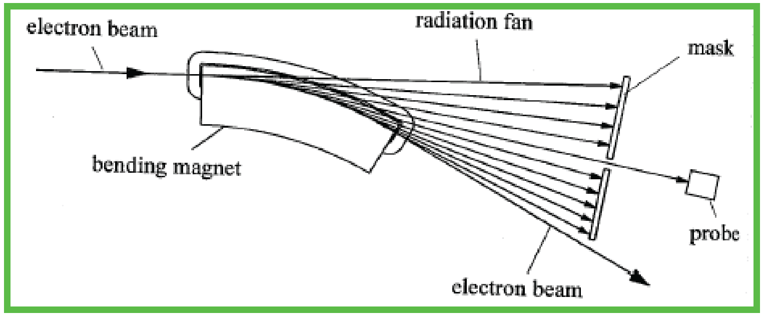

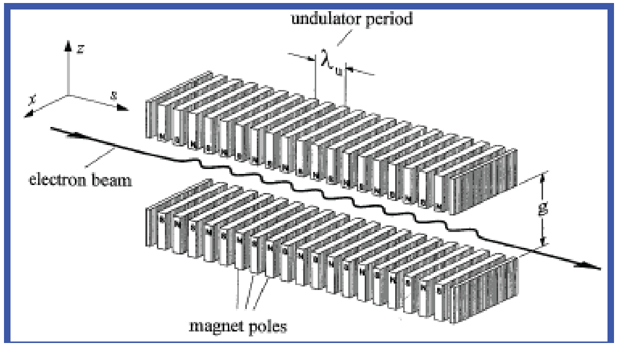

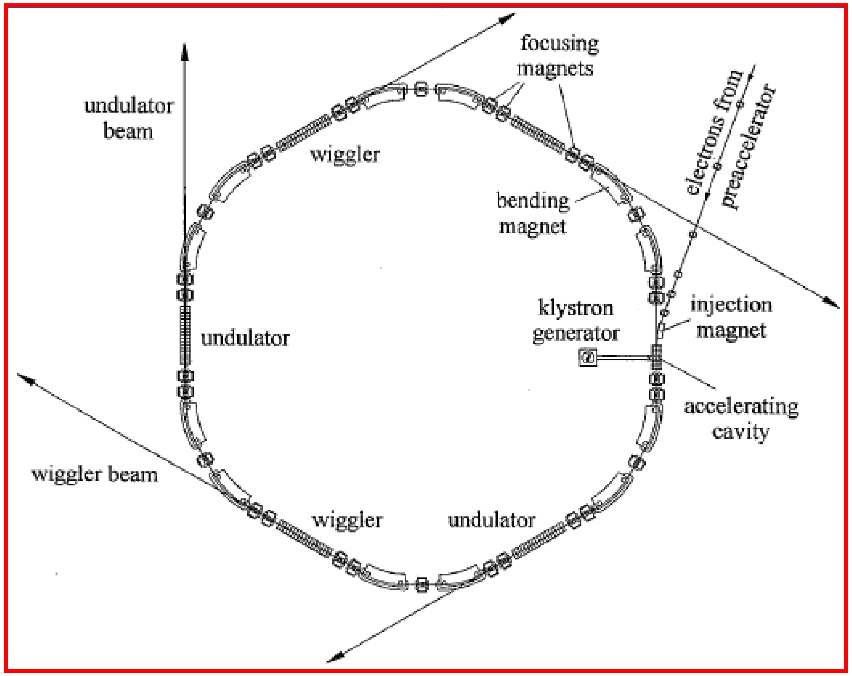

K. Wille, *The Physics of Particle Accelerators: An Introduction*, Oxford University Press, 2000.

4^{th} Generation Light Sources (XFELs)

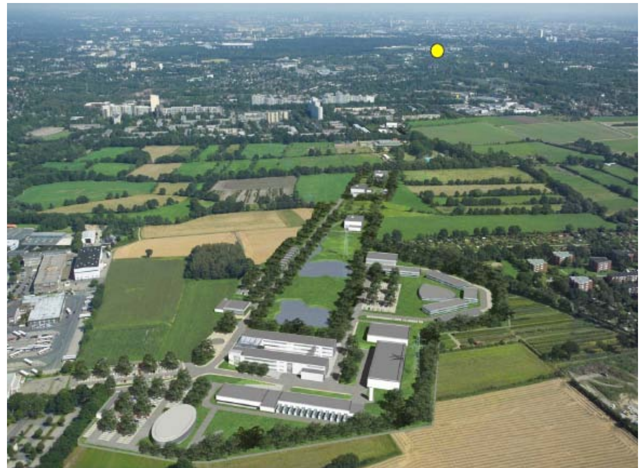

- European XFEL. Germany ($\lambda\sim$ 0.1-1.6 nm)
- FLASH @ DESY, Germany ($\lambda\sim$0.1-7 nm)
- SPARC, Italy ($\lambda\sim$ 0.6-40 nm)
- FERMI @ Elettra, Italy ($\lambda\sim$ 1 0-100 nm)
- SwissFEL, Switzerland ($\lambda\sim$0.1-7 nm)

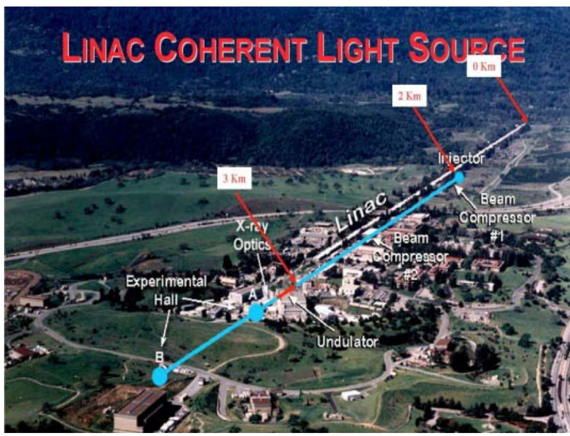

- LCLS FEL @ SLAC, USA
  ($\lambda\sim$ 0.15-1.5 nm)
- HGHG FEL @ NSLS, BNL, USA
  ($\lambda\sim$193 nm)

- SACLA XFEL @ Spring-8, Japan
  ($\lambda > 0.1$ nm)
- Shanghai FEL
- Pohang XFEL

Photocathode RF guns
(SACLA XFEL uses DC gun)

4^{th} Generation Light Sources (IR-FELs)

Fritz Haber Institute THz FEL
Max Planck Institute
Berlin, Germany

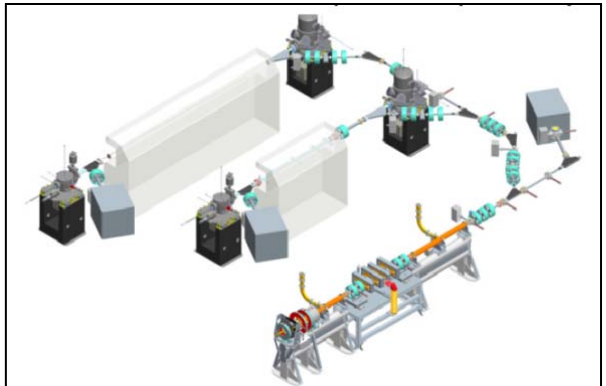

ELBE @ HZDR
Germany

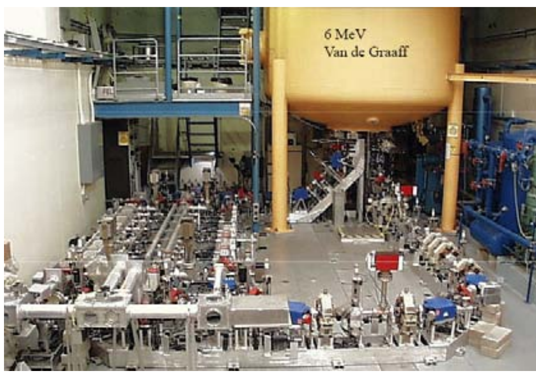

UCSB FEL, Santa Barbara, USA

KU-FEL, Kyoto University, Japan

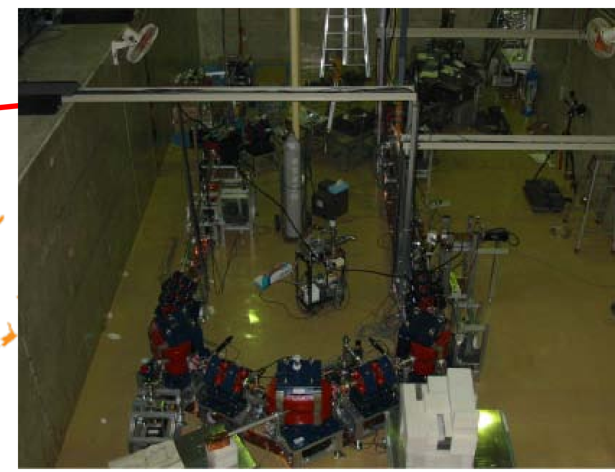

Thermionic DC guns
Thermionic RF guns
Photocathode RF guns

Lecture No. 3

- **Operation of RF Electron Gun**
  - Cathode preparation
  - Operation conditions
  - Measurements of electron beam properties
- **RF Gun Applications**
  - Electron sources for high energy physics accelerator
  - Electron sources for direct applications
  - Electron sources for light sources
- **Generation and Applications of Ultra Short Electron Bunches Produced by RF Gun**
  - Generation and applications of ultra short electron bunches at Chiang Mai University

Applications of Ultra Short Electron Bunches

➢ Direct Applications:

- Ultrafast time-resolved electron diffraction for studying dynamic of chemical reaction (A. Zeweil Noble Price Winner 2002)
- Ultrafast electron pulse radiolysis (K. Ka et al., Rev. of Sci. Instr., 2012)

➢ Production of short (femtosecond) photon pulses:

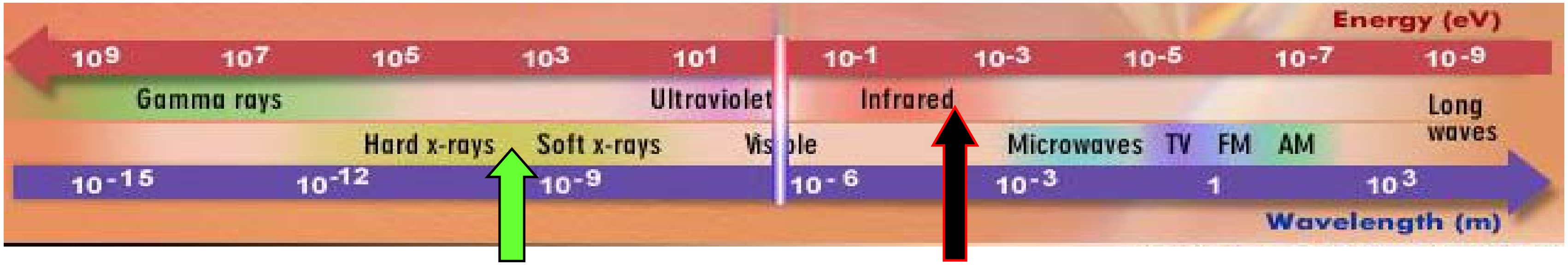

Femtosecond X-ray pulses for dynamic study at atomic scale

Intense far-infrared/THz radiation at frequencies of 100 GHz - 10 THz (λ: 3 – 0.03 mm) via, e.g.,
- Transition radiation
- Undulator radiation
- Free-electron lasers (FELs)

Generation of Short Electron Bunches (1)

Short electron bunches in the order of femtosecond scale can be generated by using an **RF gun** and a **magnetic bunch compressor**.

➢ High energy electron bunches with inversely linear correlation between energy-time distribution are normally compressed with **chicane**.

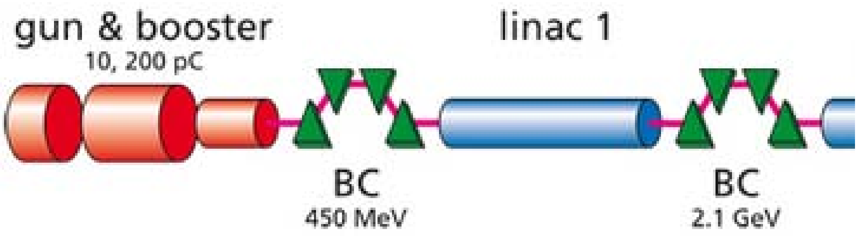

http:// www.psi.ch/swissfel/swissfel-accelerator

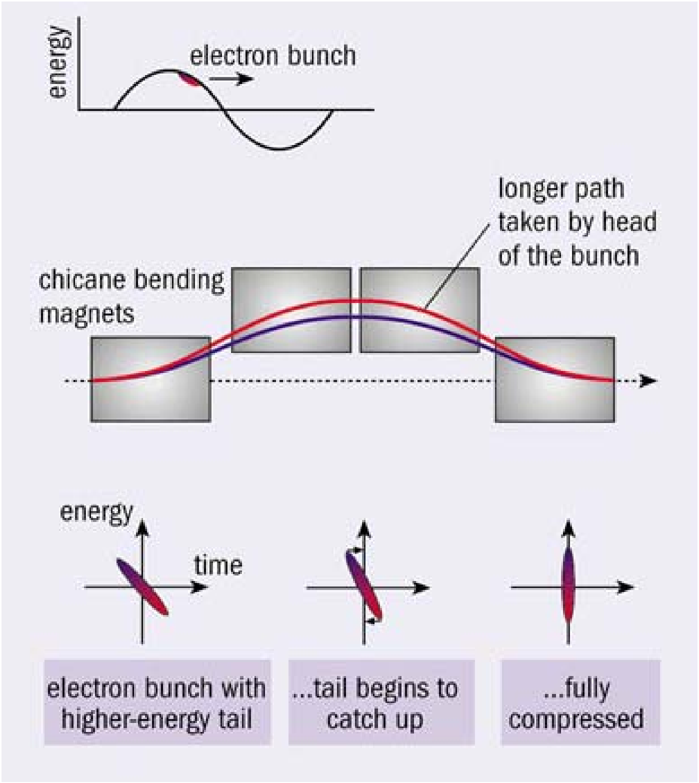

http://cerncourier.com/cws/article/cern/28925

Generation of Short Electron Bunches (2)

- Low energy electron bunches with linear correlation between energy-time distribution can be compressed with **α-magnet**.

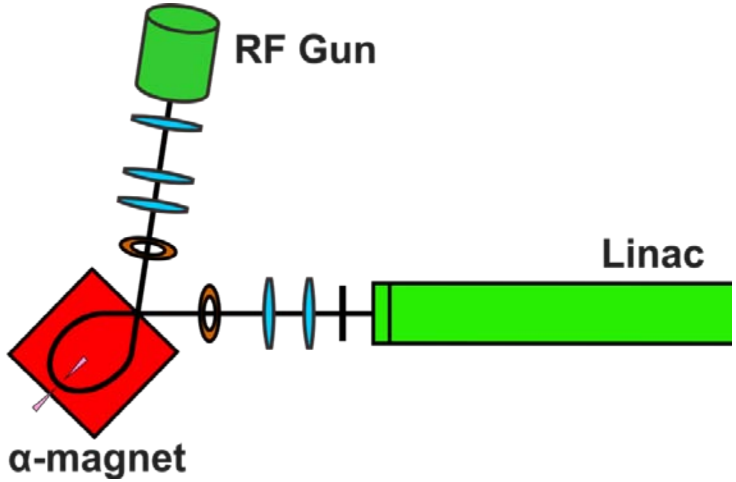

- Electrons with different momenta have different path lengths inside the α-magnet field.
- Energy slits are placed in a magnetic vacuum chamber to select only the core of the beam.

→ Emittance and energy spread are reduced.

→ The peak current is increased.

Linac System @ CMU

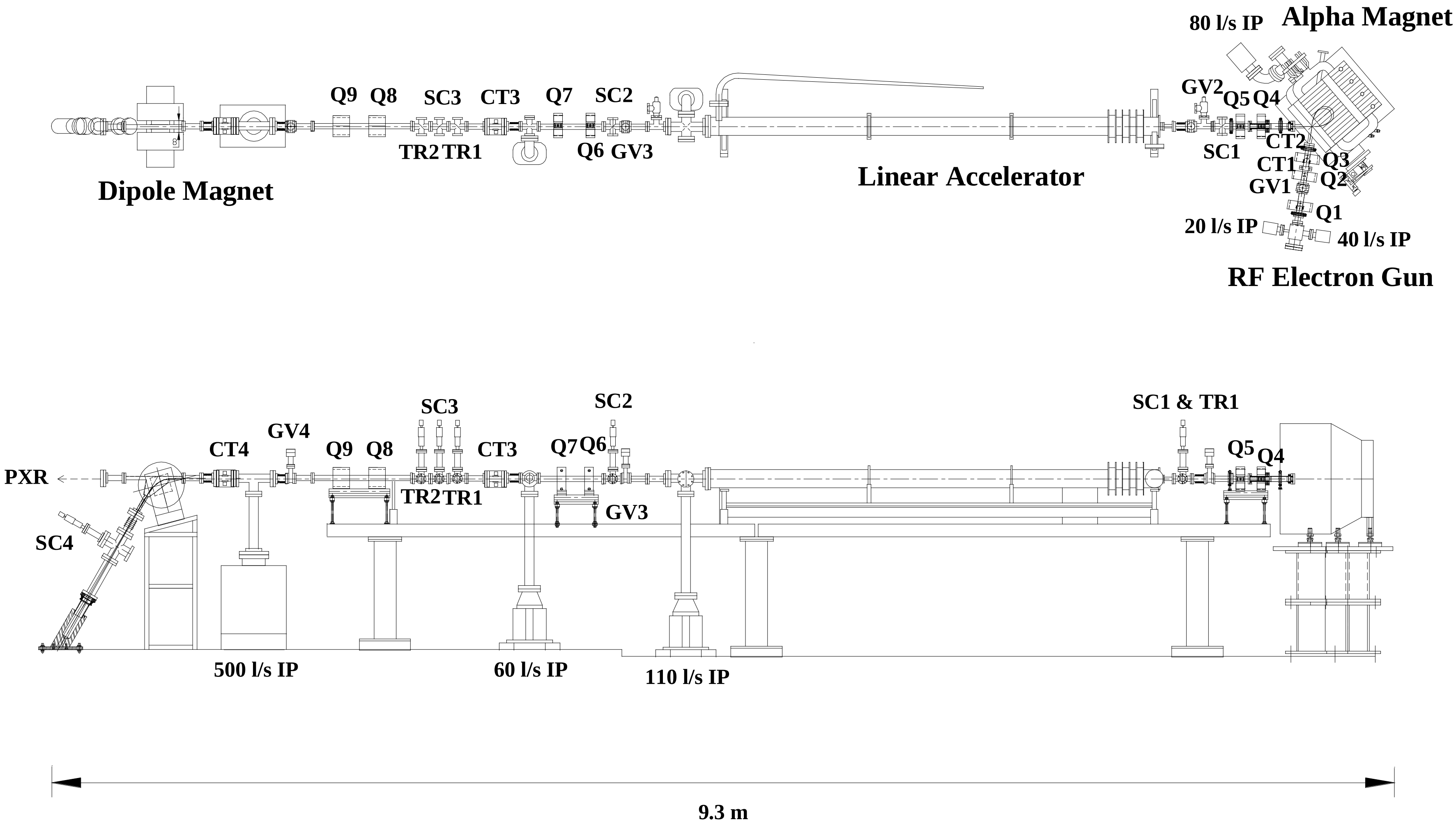

Generation of Short Electron Source at CMU

Alpha magnet
(bunch compressor)

S-band thermionic RF-gun (2-2.5 MeV (30 MV/m @ cathode)

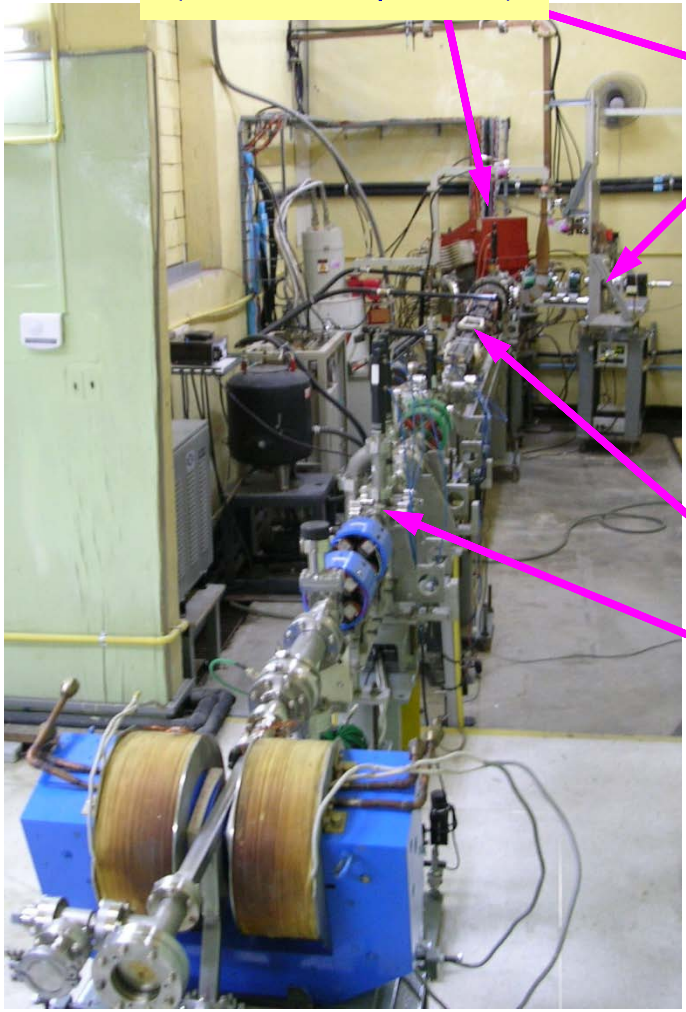

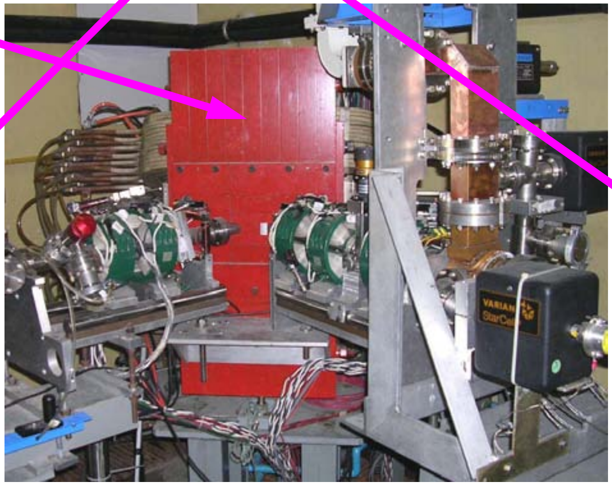

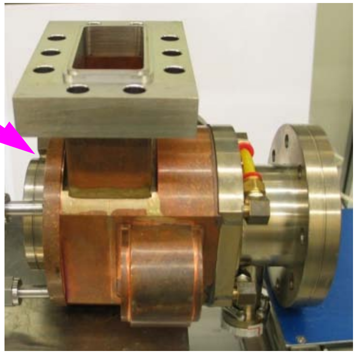

Linac (10-15 MeV (up to 30 MeV with higher RF power)

Transition radiation stations (0.23 nC/bunch, $\leq$ 200 fs)

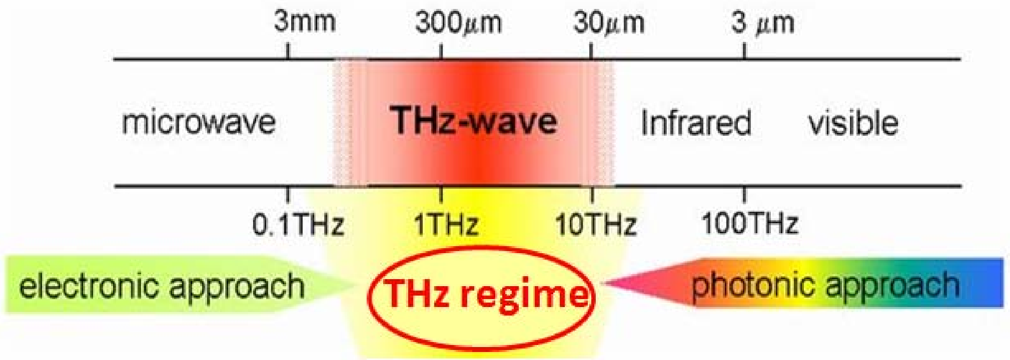

Generation of Short Electron Bunches (3)

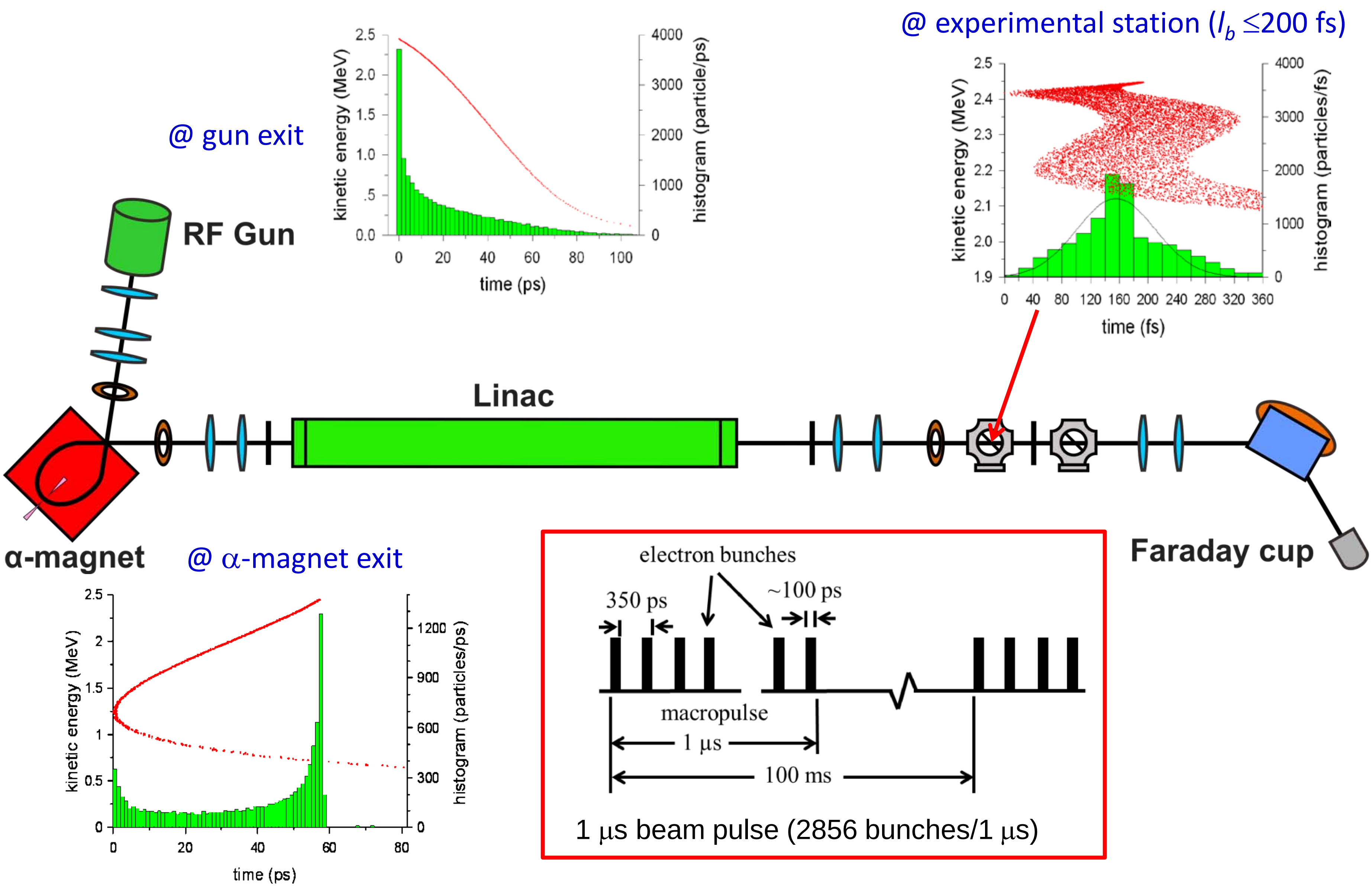

Generation of Transition Radiation

E_{kin} ~2-2.5 MeV (E_Z~30 MV/m @ cathode)

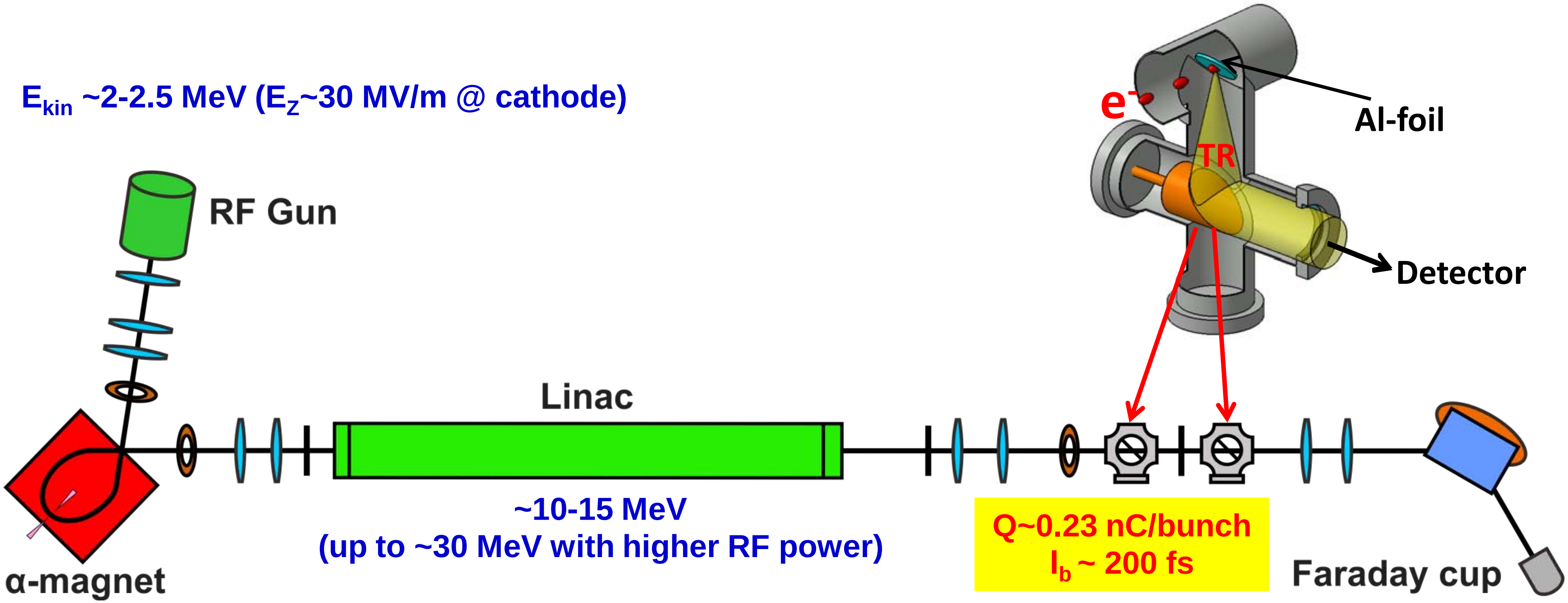

~1.8-2.5 MeV, l_b ~ 10-20 ps

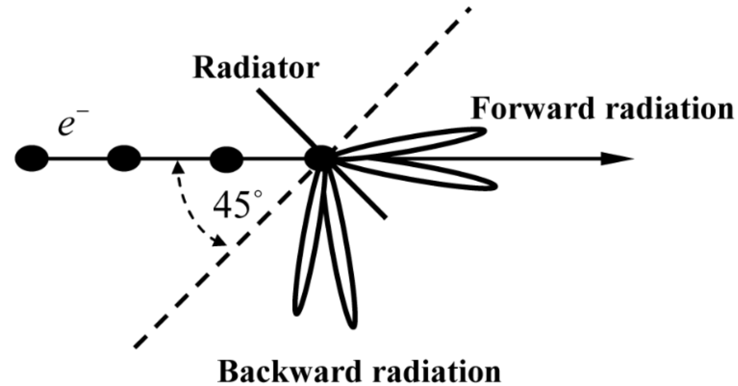

Coherent Transition Radiation

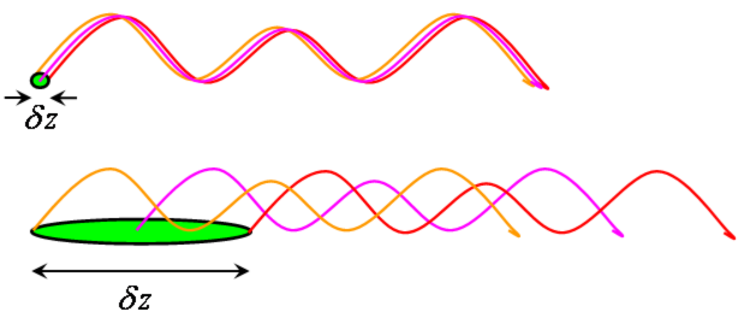

At wavelengths about or longer than the bunch length

↓

Radiation field add up coherently

↓

Electron short bunches is desired to produce coherent radiation

↓

Radiation intensity α N^2

ISR CSR

$$\frac{d^2 I}{d\omega\, d\Omega} = [N[1 - f(\omega)] + N^2 f(\omega)]$$

Detector signal of coherent transition radiation intensity vs. number of electrons.

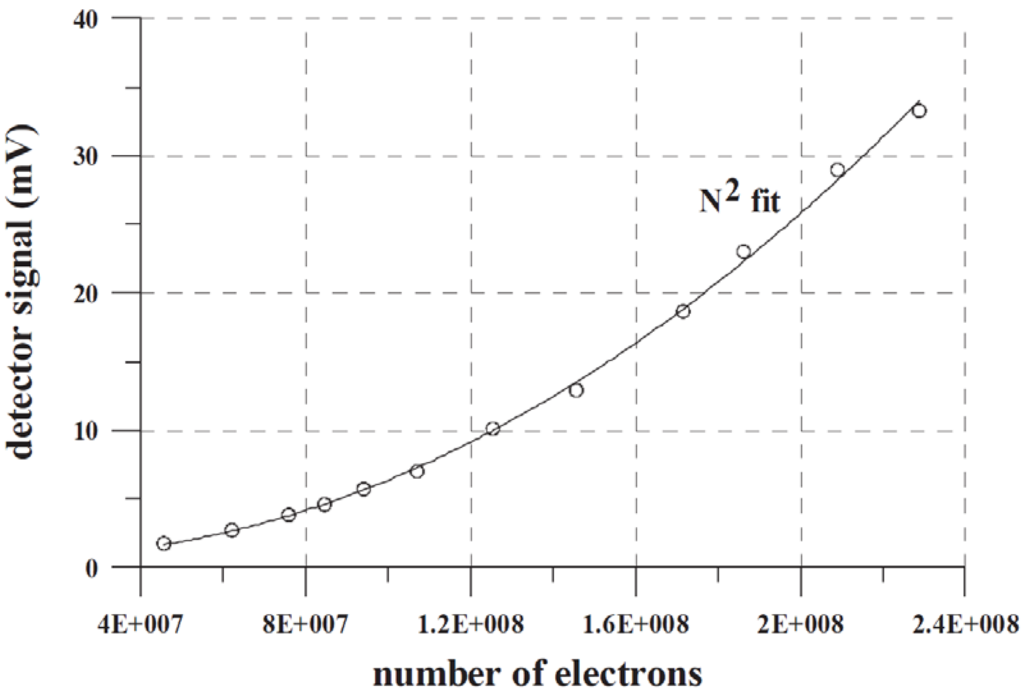

Bunch Length Measurement

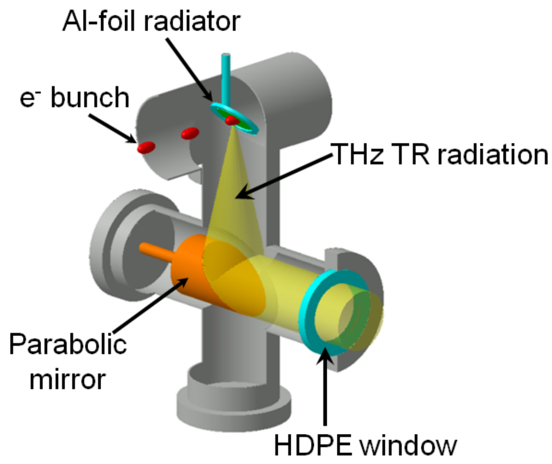

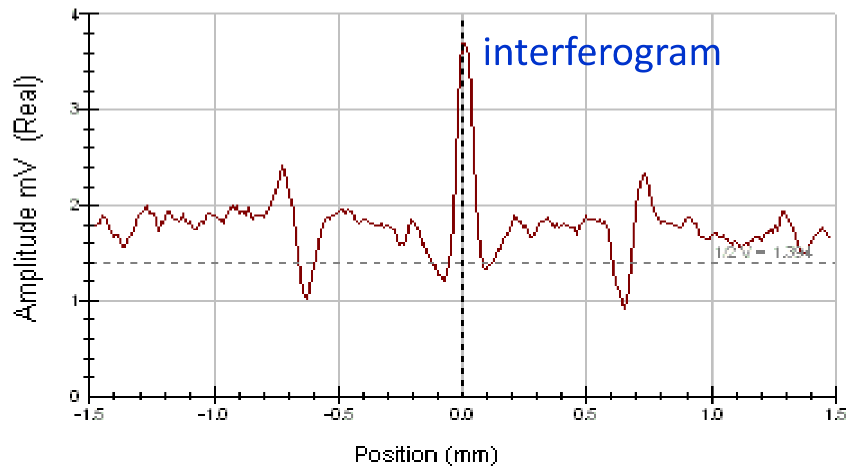

Measured electron bunch ~ 200 fs (120 μm)

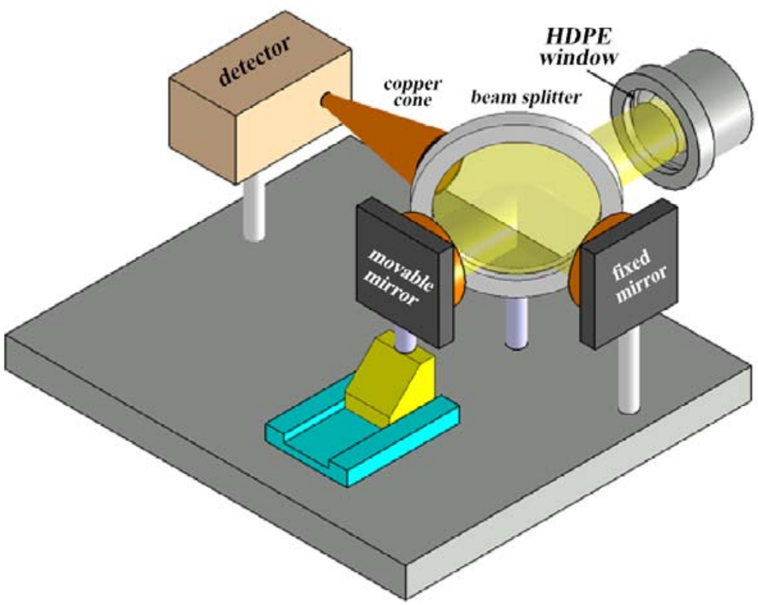

Michelson Interferometer

High Brightness THz Radiation with Broad Spectrum

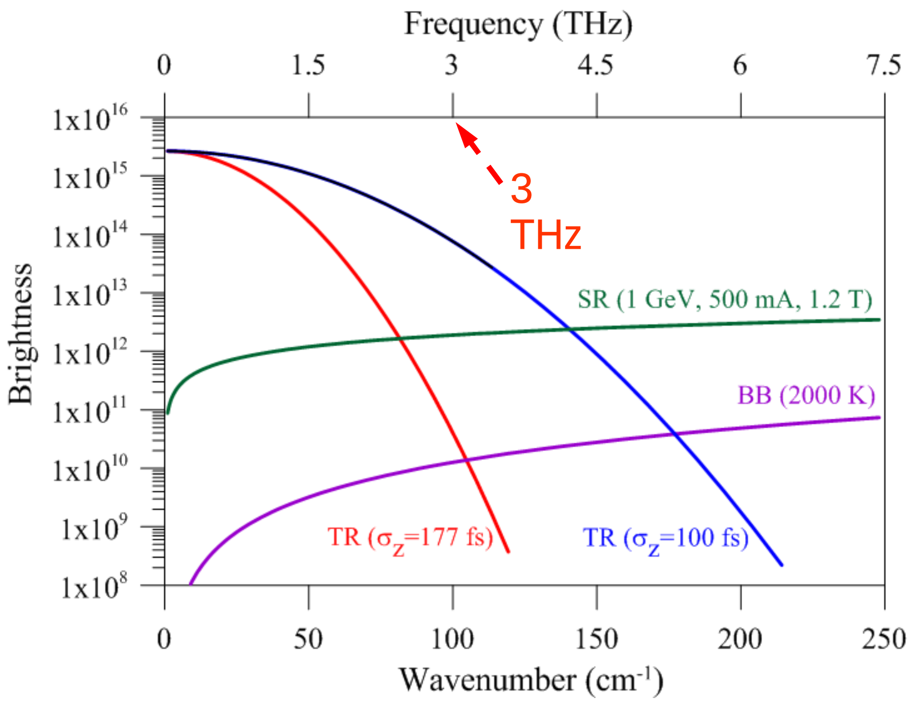

Calculated radiation brightness B(ph/s/mm^2/100%BW) vs. wave number for CTR, SR and black body radiation.

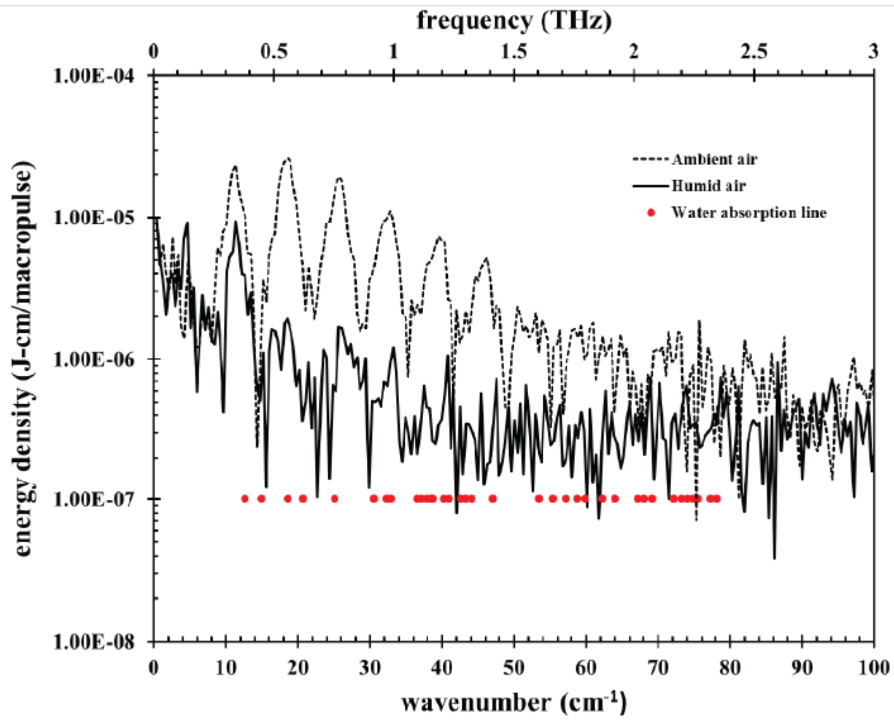

Measured THz radiation covers wave number of 5-80 cm^{-1} (frequency range of 0.3 – 2.4 THz)

Examples of THz Spectroscopy & Imaging @ CMU (120)

Water vapor spectrum & absorption lines

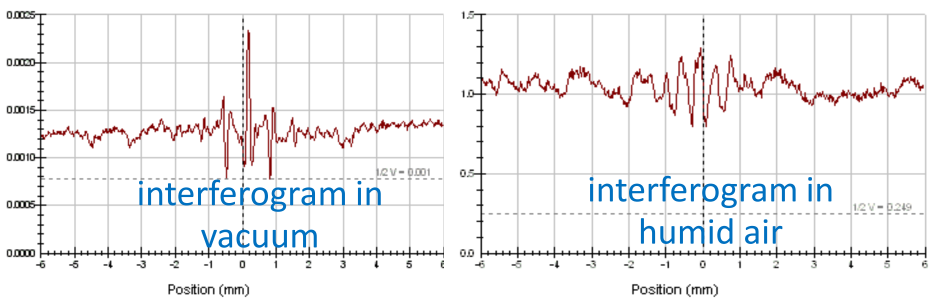

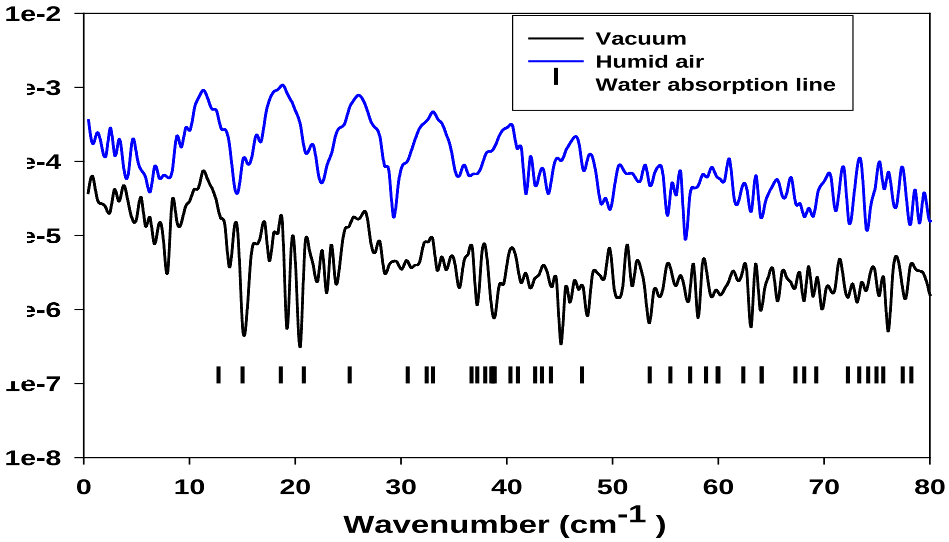

THz image of live leaves with 180x180 µm copper mesh filter (20–40 cm^{-1} transmission band)

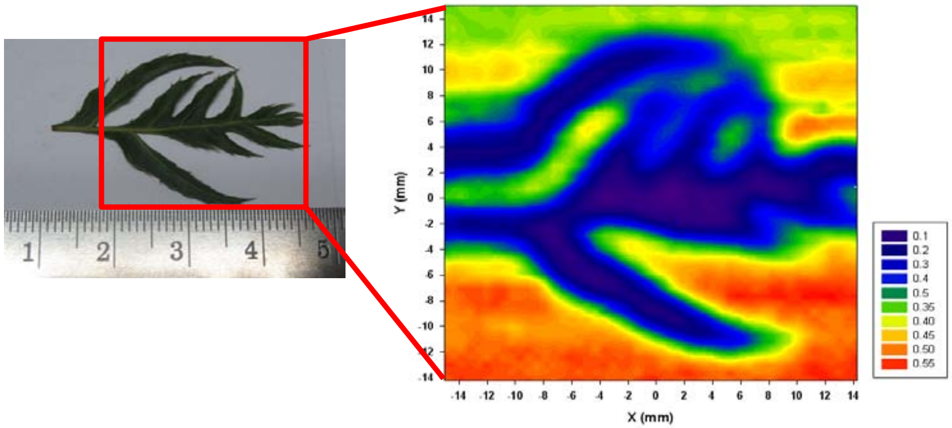

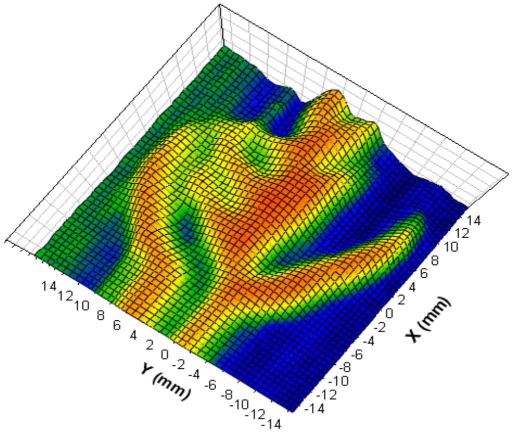

Properties of Coherent THz Radiation @ CMU

Parameters	Value	Unit
Spectral range	5 - 80	cm^{-1},
Energy per macropulse	8.8	μJ
(21.5% collection effeciency)		
Polarization	radial	
Macropulse power	11	W
Microbunch power	19	kW
Average power (at 10 Hz rep. rate)	88	μW
Micropulse duration (σ_z)	200	fs
Micropulse separation	350	ps
Macropulse duration	0.8	μs
Number of radiation pulses/macropulse	2300	pulse

Electron beam parameters	
Resonant frequency	2856 MHz
Beam energy	10 MeV
Electron bunch length	200 fs
Bunch charge	230 pC
Macropulse length	1 μs
Repetition rate	10 Hz

How to obtain brighter radiation?

How to obtain brighter radiation?

The greater the brightness, the more photons that can be concentrated on a spot.

Improvement of electron beam	
Resonant frequency	2856 MHz
Beam energy	10 MeV
Electron bunch length	**100 fs**
Bunch charge	**~100-200 pC**
Macropulse length	1 μs
Repetition rate	10 Hz

Brightness: number of photons produced per second, angular divergence of photons, cross-sectional area of beam, photons falling within a bandwidth (BW) of 0.1% of central wavelength.

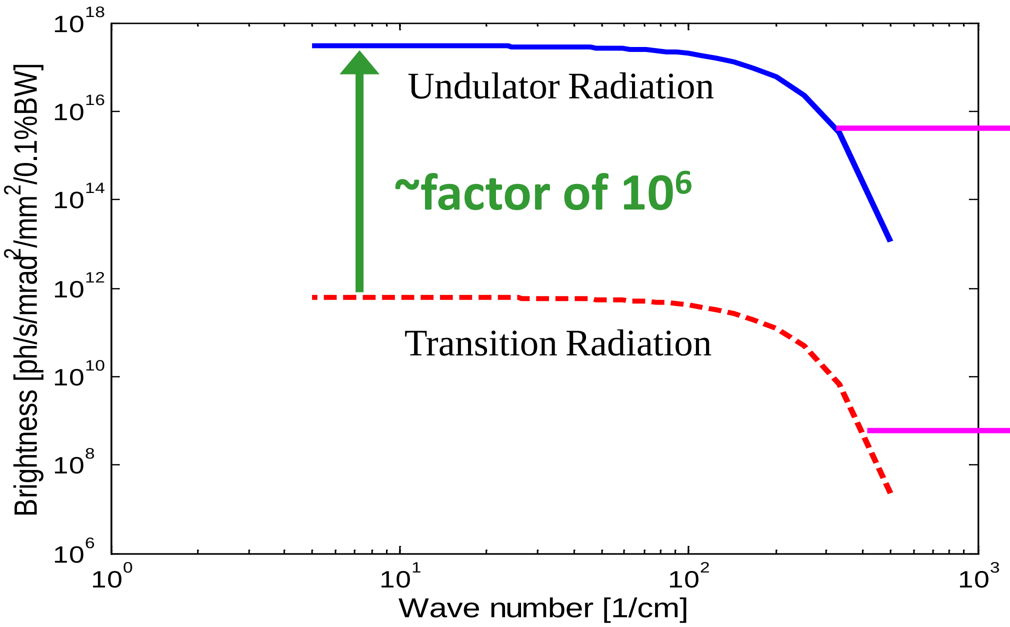

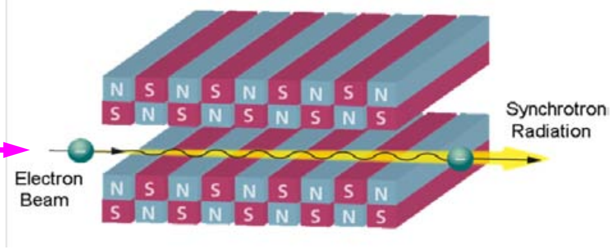

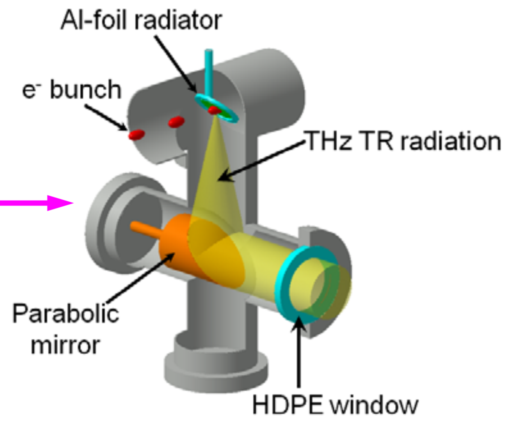

Coherent THz Undulator Radiation @ CMU

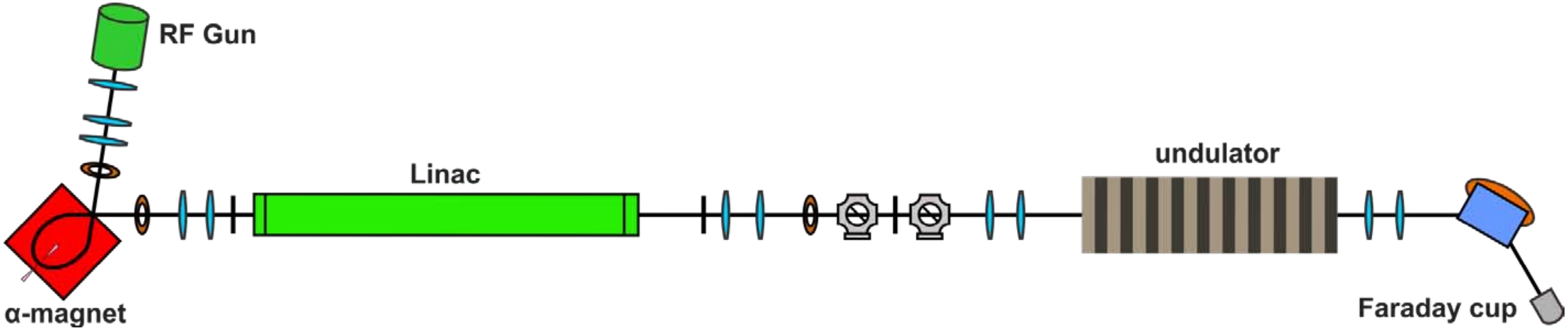

Planar Electromagnet Undulator (EMU)

- Economical & simple choice
- Based on some experience of electromagnet dipoles and quadrupoles development in house
- Magnetic field strength is adjusted by varying the applied current

→ To avoid difficulty of mechanics for adjusting the gap

Preliminary parameters for CMU EMU	
K-parameter	1- 1.2
Max. on-axis peak magnetic field	~0.2 T
Period length	55 mm
Undulator gap	10 mm
Number of periods	40
Radiation wavelength	~100 um

Final Remarks

Characteristics of particle beams and reliability in operation of an accelerator facility strongly depend on properties of the source.

- Development of high-brightness electron beams is a key and a critical issue in the success of most electron accelerator projects.
- RF electron guns are the powerful source with specifications depending on types of accelerators and applications.
- RF gun technology is one of main streams in the development of particle accelerators.

End of Lecture No. 3

Questions
&
Discussion